AD

USAAMRDL TECHNICAL REPORT 71-66

COMPARISON OF UH-1C FLIGHT TEST DATA WITH MOSTAB-C SMALL PERTURBATION MATH MODEL

By

Arthur J. Welch
Edward L. Warren

December 1971

EUSTIS DIRECTORATE
U. S. ARMY AIR MOBILITY RESEARCH AND DEVELOPMENT LABORATORY
FORT EUSTIS, VIRGINIA

CONTRACT DAAJ02-71-C-0023
AMERICAN NUCLEONICS CORPORATION
WOODLAND HILLS, CALIFORNIA

DISCLAIMERS

The findings in this report are not to be construed as an official Department of the Army position unless so designated by other authorized documents.

When Government drawings, specifications, or other data are used for any purpose other than in connection with a definitely related Government procurement operation, the United States Government thereby incurs no responsibility nor any obligation whatsoever; and the fact that the Government may have formulated, furnished, or in any way supplied the said drawings, specifications, or other data is not to be regarded by implication or otherwise as in any manner licensing the holder or any other person or corporation, or conveying any rights or permission, to manufacture, use, or sell any patented invention that may in any way be related thereto.

Trade names cited in this report do not constitute an official endorsement or approval of the use of such commercial hardware or software.

DISPOSITION INSTRUCTIONS

Destroy this report when no longer needed. Do not return it to the originator.

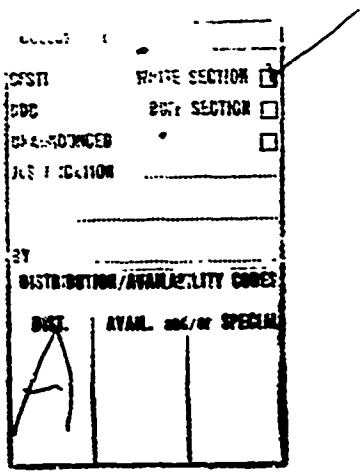

Unclassified

Security Classification

DOCUMENT CONTROL DATA - R & D

(Security classification of title, body of abstract and indexing annotation must be entered when the overall report is classified)

1. ORIGINATING ACTIVITY *(Corporate author)*
American Nucleonics Corporation
Woodland Hills, California

2a. REPORT SECURITY CLASSIFICATION
Unclassified

2b. GROUP

3. REPORT TITLE
COMPARISON OF UH-1C FLIGHT TEST DATA WITH MOSTAB-C SMALL PERTURBATION MATH MODEL

4. DESCRIPTIVE NOTES *(Type of report and inclusive dates)*
Final Report

5. AUTHOR(S) *(First name, middle initial, last name)*
Arthur J. Welch
Edward L. Warren

6. REPORT DATE	7a. TOTAL NO. OF PAGES	7b. NO. OF REFS
December 1971	114	5

8a. CONTRACT OR GRANT NO.	9a. ORIGINATOR'S REPORT NUMBER(S)
DAAJ02-71-C-0023	USAAMRDL Technical Report 71-66
b. PROJECT NO.	
c. Task 1F162204AA4401	9b. OTHER REPORT NO(S) *(Any other numbers that may be assigned this report)*
d.	ANC 95R-1

10. DISTRIBUTION STATEMENT
Approved for public release; distribution unlimited.

11. SUPPLEMENTARY NOTES	12. SPONSORING MILITARY ACTIVITY
	Eustis Directorate U.S. Army Air Mobility R&D Laboratory Fort Eustis, Virginia

13. ABSTRACT

The purpose of the work performed under this contract was to conduct a UH-1C model validation analysis. The model was obtained from Government-furnished MOSTAB-C computer data that defined the UH-1C stability and control derivatives at selected flight conditions. The reference data consisted of Government-furnished UH-1C helicopter flight test data.

Overall, the MOSTAB-C data represented a fair first approximation to the actual vehicle dynamics. The MOSTAB-C data that was least representative of the actual vehicle response dynamics was the cross-coupling responses.

Some of the results of the validation effort are as follows:

1. Digital (IBM/CSMP and CDC/MIMIC) and analog vehicle simulation models were generated. A lumped coefficient vehicle representation was used for the analog and digital simulations.
2. Simulation responses essentially duplicated Government-furnished time responses to ensure the validity of the simulation models.
3. Flight test traces were selected and replotted for ease of comparison of vehicle time responses with simulation data.
4. Root loci were made for each of the stability derivatives. These plots show the effect in the frequency domain of changing each derivative from its "normal" value.

DD FORM 1 NOV 68 1473 ... TO DD FORM 1473, 1 JAN 64, WHICH IS ... FOR ARMY USE.

Unclassified

Security Classification

14. KEY WORDS	LINK A		LINK B		LINK C	
	ROLE	WT	ROLE	WT	ROLE	WT
UH-1C Helicopter Analytical Investigation Digital Computer Simulation						

DEPARTMENT OF THE ARMY
U. S. ARMY AIR MOBILITY RESEARCH & DEVELOPMENT LABORATORY
EUSTIS DIRECTORATE
FORT EUSTIS, VIRGINIA 23604

This report has been reviewed by the Eustis Directorate, U.S. Army Air Mobility Research and Development Laboratory and is considered to be technically sound. The purpose of the program was to conduct a UH-1C model validation analysis. The stability and control derivatives were computer by MOSTAB-C computer program and defined a predicted vehicle model ac specific flight conditions. The time responses provided a means for checking the simulation of this model. UH-1C flight test data were used to compare the predicted vehicle model. The report is published for the exchange of information and appropriate application. The technical monitor for this contract was Mr. Robert P. Smith, Aeromechanics Division.

Task 1F162204AA4401
Contract DAAJ02-71-C-0023
USAAMRDL Technical Report 71-66
December 1971

COMPARISON OF UH-1C FLIGHT TEST DATA WITH MOSTAB-C SMALL PERTURBATION MATH MODEL

ANC 95R-1

By

Arthur J. Welch
Edward L. Warren

Prepared by

American Nucleonics Corporation
Woodland Hills, California

for

EUSTIS DIRECTORATE
U.S. ARMY AIR MOBILITY RESEARCH AND DEVELOPMENT LABORATORY
FORT EUSTIS, VIRGINIA

SUMMARY

The purpose of the work performed under this contract was to conduct a UH-1C model validation analysis. The model was obtained from Government-furnished MOSTAB-C computer data that defined the UH-1C stability and control derivatives at selected flight conditions. The reference data consisted of Government-furnished UH-1C helicopter flight test data.

Overall, the MOSTAB-C data represented a fair first approximation to the actual vehicle dynamics. The MOSTAB-C data that was least representative of the actual vehicle response dynamics was the cross-coupling responses.

Some of the results of the validation effort are as follows:

1. Digital (IBM/CSMP and CDC/MIMIC) and analog vehicle simulation models were generated. A lumped coefficient vehicle representation (i.e., a model using MOSTAB-C "Modified Form Stability Derivative" * data) was used for the analog and digital simulations.

2. Simulation responses essentially duplicated Government-furnished time responses to ensure the validity of the simulation models.

3. Flight test traces were selected and replotted for ease of comparison of vehicle time responses with simulation data. Also, transparent overlays of the flight test data were generated (these were placed behind an oscilloscope mask). These overlays enable simultaneous comparison of the flight test data with analog simulation responses.

4. Root loci were made for each of the stability derivatives (i.e., except cross-coupling derivatives). These plots show the effect in the frequency domain of changing each derivative from its "normal" value. Root loci plots were made for the hover and 60 knots stability derivatives.

*Recomputed stability derivatives that do not contain right-hand side acceleration coefficients (i.e., the acceleration coefficients, which would normally give troublesome algebraic simulation loops, have been represented in a different form).

5. Stability derivatives were varied on the analog computer to arrive at a better match of flight test data. These results together with the root loci provide insight into finer tuning of the MOSTAB-C input data and/or model calculations.

6. A curve fit program was used to generate a vehicle model using the flight test data. Vehicle models were generated using one set of data, two sets of data (i.e., one set of data for each of two control inputs), and three sets of data (one set of data for each of three control inputs). These vehicle math models were then simulated and the responses compared with the original test data. It appears that with sufficient attention to testing techniques and test instrumentation, this approach can provide a very useful and accurate math model of the vehicle.

FOREWORD

This report represents the results of efforts expended by American Nucleonics Corporation (ANC) in performance of USAAMRDL Contract DAAJ02-71-C-0023 (Task 1F162204AA4401). The work was conducted from March 1971 through August 1971. Mr. Edward Warren was the ANC Program Manager and Mr. Arthur Welch was the ANC Project Engineer.

Mr. R. P. Smith was the USAAMRDL technical monitor on this program. His advice and technical coordination were instrumental in the efficient and effective conduct of this work.

TABLE OF CONTENTS

	Page
SUMMARY	iii
FOREWORD	v
LIST OF ILLUSTRATIONS	viii
LIST OF TABLES	xii
LIST OF SYMBOLS	xiii
INTRODUCTION	1
FLIGHT TEST DATA	2
VEHICLE MATH MODEL	5
SIMULATION MODELS	17
Digital Computer Model	21
Analog Computer Model	33
Root Loci	46
MODIFIED VEHICLE MODEL	70
CURVE FIT MODEL	80
Model of Single Data Set	81
Model of Two Data Sets	85
Model of Three Data Sets	91
CONCLUSIONS	96
RECOMMENDATION	97
LITERATURE CITED	98
DISTRIBUTION	99

LIST OF ILLUSTRATIONS

Figure		Page
1	Longitudinal Cyclic Pitch Position vs. Horizontal Tail Position.....	9
2	60-Knot Vehicle Model Longitudinal Cyclic Response (ANC Analog, CSMP & MRI).....	18
3	60-Knot Vehicle Model Lateral Cyclic Response (ANC Analog, CSMP & MRI).....	19
4	60-Knot Vehicle Model Pedal Response (ANC Analog, CSMP & MRI).....	20
5	Flight Test vs. CSMP Simulation (60 Knots at 3000 Feet, Pilot Pitch Input Response).....	24
6	Flight Test vs. CSMP Simulation (60 Knots at 3000 Feet, Pilot Roll Input Response).....	25
7	Flight Test vs. CSMP Simulation (60 Knots at 3000 Feet, Pilot Yaw Input Response).....	26
8	Flight Test vs. CSMP Simulation (110 Knots at 3000 Feet, Pilot Pitch Input Response).....	27
9	Flight Test vs. CSMP Simulation (110 Knots at 3000 Feet, Pilot Roll Input Response).....	28
10	Flight Test vs. CSMP Simulation (110 Knots at 3000 Feet, Pilot Yaw Input Response).....	29
11	Flight Test vs. CSMP Simulation (Hover at 3000 Feet, Pilot Pitch Input Response).....	30
12	Flight Test vs. CSMP Simulation (Hover at 3000 Feet, Pilot Roll Input Response).....	31
13	Flight Test vs. CSMP Simulation (Hover at 3000 Feet, Pilot Yaw Input Response).....	32
14	Close-Up View of the R-123 Simulator.....	34
15	Flight Test vs. CSMP Simulation (60 Knots at 3000 Feet, Pitch Step Response).....	37

LIST OF ILLUSTRATIONS (Cont'd)

Figure		Page
16	Flight Test vs. CSMP Simulation (60 Knots at 3000 Feet, Roll Step Response).....	38
17	Flight Test vs. CSMP Simulation (60 Knots at 3000 Feet, Yaw Step Response).....	39
18	Flight Test vs. CSMP Simulation (110 Knots at 3000 Feet, Pitch Step Response).....	40
19	Flight Test vs. CSMP Simulation (110 Knots at 3000 Feet, Roll Step Response).....	41
20	Flight Test vs. CSMP Simulation (110 Knots at 3000 Feet, Yaw Step Response).....	42
21	Flight Test vs. CSMP Simulation (Hover at 3000 Feet, Pitch Step Response).....	43
22	Flight Test vs. CSMP Simulation (Hover at 3000 Feet, Roll Step Response).....	44
23	Flight Test vs. CSMP Simulation (Hover at 3000 Feet, Yaw Step Response).....	45
24	Hover Longitudinal M_w and M_q Root Loci.....	50
25	Hover Longitudinal M_u and Z_w Root Loci.....	51
26	Hover Longitudinal Z_u and Z_q Root Loci.....	52
27	Hover Longitudinal X_u and X_w Root Loci.....	53
28	Hover Longitudinal X_q Root Locus.....	54
29	Hover Lateral N_v and N_p Root Loci.....	55
30	Hover Lateral N_r and L_p Root Loci.....	56
31	Hover Lateral L_v and L_r Root Loci.....	57
32	Hover Lateral Y_v and Y_r Root Loci.....	58
33	60 Knots Longitudinal M_q and M_w Root Loci.....	59
34	60 Knots Longitudinal M_u and Z_w Root Loci.....	60

LIST OF ILLUSTRATIONS (Cont'd)

Figure		Page
35	60 Knots Longitudinal Z_u and Z_q Root Loci.....	61
36	60 Knots Longitudinal X_u and X_w Root Loci.....	62
37	60 Knots Longitudinal X_q Root Locus.....	63
38	60 Knots Lateral N_p and N_v Root Loci.....	64
39	60 Knots Lateral N_r and L_p Root Loci.....	65
40	60 Knots Lateral L_v and L_r Root Loci.....	66
41	60 Knots Lateral Y_v and Y_p Root Loci.....	67
42	60 Knots Lateral Y_r Root Locus.....	68
43	M_w Root Locus Hover 6 Degrees of Freedom and N_v^w Root Locus 60 Knots 6 Degrees of Freedom...	69
44	Flight Test vs. CSMP Simulation (60 Knots at 3000 Feet, Modified MOSTAB Pitch Step Response)	71
45	Flight Test vs. CSMP Simulation (60 Knots at 3000 Feet, Modified MOSTAB Roll Step Response).	72
46	Flight Test vs. CSMP Simulation (60 Knots at 3000 Feet, Modified MOSTAB Yaw Step Response)..	73
47	Flight Test vs. CSMP Simulation (110 Knots at 3000 Feet, Modified MOSTAB Pitch Step Response)	74
48	Flight Test vs. CSMP Simulation (110 Knots at 3000 Feet, Modified MOSTAB Roll Step Response).	75
49	Flight Test vs. CSMP Simulation (110 Knots at 3000 Feet, Modified MOSTAB Yaw Step Response)..	76
50	Flight Test vs. CSMP Simulation (Hover at 3000 Feet, Modified MOSTAB Pitch Step Response).....	77
51	Flight Test vs. CSMP Simulation (Hover at 3000 Feet, Modified MOSTAB Roll Step Response).....	78
52	Flight Test vs. CSMP Simulation (Hover at 3000 Feet, Modified MOSTAB Yaw Step Response).....	79

LIST OF ILLUSTRATIONS (Cont'd)

Figure		Page
53	Pitch Response of a Single Data Set Model...	82
54	Pitch Response of Two-Data-Set Model.....	86
55	Roll Response of Two-Data-Set Model.....	87
56	Pitch Response of Three-Data-Set Model.....	92
57	Roll Response of Three-Data-Set Model.....	93
58	Yaw Response of Three-Data-Set Model.....	94

LIST OF TABLES

Table		Page
I	UH-1C Instrumentation Characteristics.....	3
II	Modified Form Stability Derivative Matrices for Hover at 3000 Feet.....	11
III	Modified Form Stability Derivative Matrices for 60 Knots at Sea Level.....	12
IV	Modified Form Stability Derivative Matrices for 60 Knots at 10,000 Feet.....	13
V	Modified Form Stability Derivative Matrices for 90 Knots at 3000 Feet.....	14
VI	Modified Form Stability Derivative Matrices for 110 Knots at 3000 Feet.....	15
VII	Modified Form Stability Derivative Matrices for 120 Knots at 3000 Feet.....	16
VIII	Analog Computer Potentiometer Settings.....	35
IX	Longitudinal 3-DOF Root Locus Matrix.....	47
X	Lateral 3-DOF Root Locus Matrix.....	48
XI	6-DOF Root Locus Matrix.....	49

LIST OF SYMBOLS

Al	roll control (lateral stick deflection) (rad) positive for right stick
Bl	pitch control (longitudinal stick deflection) (rad) positive for forward stick
CO	height control (collective stick deflection) (rad) positive for up collective
D-HT	horizontal tail deflection (rad) positive for leading edge up
DLR	yaw control (pedal deflection) (rad) positive for right pedal
$\bar{F}_s$	stability derivative matrix
$\bar{F}_c$	control derivative matrix
g	acceleration due to gravity $\left(\frac{ft}{sec^2}\right)$
$\bar{h}$	squared roll angle matrix
I_{xx}, I_{yy}, I_{zz}	moments of inertia about x, y, and z axes (slug-ft^2)
I_{xz}	product of inertia (slug-ft^2)
j	$\sqrt{-1}$
$\bar{k}$	inertial attitude matrix
L	rolling moment (ft-lb)
L_p	rolling moment due to roll rate (1/sec)
L_q	rolling moment due to pitch rate (1/sec)
L_r	rolling moment due to yaw rate (1/sec)
L_v	rolling moment due to side velocity (1/ft-sec)
m	mass of the aircraft $\left(\frac{lb\text{-}sec^2}{ft}\right)$
M	pitching moment (ft-lb)

LIST OF SYMBOLS - Continued

M_p	pitching moment due to roll rate (1/sec)
M_q	pitching moment due to pitch rate (1/set)
M_u	pitching moment due to forward velocity (1/ft-sec)
M_w	pitching moment due to z velocity (1/ft-sec)
N	yawing moment (ft-lb)
N_p	yawing moment due to roll rate (1/sec)
N_r	yawing moment due to yaw rate (1/sec)
N_v	yawing moment due to side velocity (1/ft-sec)
p	roll rate (rad/sec) positive for right roll rate
q	pitch rate (rad/sec) positive for up pitch rate
r	yaw rate (rad/sec) positive for right yaw rate
s	Laplace operator, $s = \sigma + j\omega$
t	time (sec)
u	perturbation velocity along x-axis (ft/sec) positive for increasing forward speed
U_o	steady-state velocity along x-axis (ft/sec)
v	perturbation velocity along y-axis (ft/sec) positive for velocity to the right
w	perturbation velocity along z-axis (ft/sec) positive for downward velocity
W	gross weight (lb)
x	horizontal displacement in direction of x-axis (ft)
X	force in x-direction (lb)
X_q	forward force due to pitch rate (ft/sec)

LIST OF SYMBOLS - Continued

X_u	forward force due to forward velocity (1/sec)
X_w	forward force due to z velocity (1/sec)
y	side displacement in direction of y-axis (ft)
y	force in y-direction (lb)
Y_p	side force due to roll rate (ft/sec)
Y_r	side force due to yaw rate (ft/sec)
Y_v	side force due to side velocity (1/sec)
Z	force in z-direction (lb)
Z_q	z force due to pitch rate (ft/sec)
Z_u	z force due to forward velocity (1/sec)
Z_w	z force due to z velocity (1/sec)
ζ	damping ratio
θ	pitch angle (rad)
σ	real part of s
τ	time delay (sec)
φ	roll angle (rad)
ψ	yaw angle (rad)
ω	imaginary part of s
ω_n	natural frequency (rad/sec)
Ω	rotational speed (rad/sec)

INTRODUCTION

In March 1971, work was initiated by ANC to compare a small perturbation simulation of the UH-1C with flight test data on the UH-1C. Stability and control derivatives and vehicle model time responses were provided by USAAMRDL to ANC. The stability and control derivatives, which were generated by the MOSTAB-C program described in References 1 through 3, defined a predicted vehicle model at specific flight conditions. The time responses provided a means for checking the simulation of this model. Also provided by USAAMRDL was flight test data that was generated during the flight test program of Reference 4. This flight test data provided the reference against which to compare the predicted vehicle model. It also defined the flight conditions for which the predicted model data was generated.

The purpose of the work done to date was to perform the vehicle model validation work that was recommended in Reference 5. It was felt that this work was necessary to provide a better analytical base for conducting a Pilot Assist System test program.

FLIGHT TEST DATA

The flight test data that was used for this program was obtained during the flight test program of Reference 4. The flight conditions for which data was taken (i.e., the data that was used here) had the following common characteristics:

1. The test vehicle was a UH-1C (SN 14101) with stabilizer bar removed.

2. The weight of the vehicle was considered to be 7100 pounds. Each flight had a takeoff gross weight of 7425 pounds (includes 1000 pounds of fuel, instrumentation and a crew of three) and a landing weight of approximately 6800 pounds.

3. The center of gravity was within 0.25 inch of mast center line (fuselage station 131.5).

4. Six control responses were recorded for each test condition. The control inputs were fore and aft longitudinal cyclic, left and right lateral cyclic, and left and right pedal.

Six straight and level conditions were investigated; namely,

1. hover, 3000 feet

2. 60 knots, 3000 feet

3. 60 knots, 10,000 feet

4. 90 knots, 3000 feet

5. 110 knots, 3000 feet

6. 120 knots, 3000 feet

Table I is a tabulation of the pertinent instrumentation that was used on the test vehicle. Sensor and instrumentation dynamics occurred at high enough frequencies that they were considered straight gains.

The flight test data provided good first-cut responses. In subsequent test programs of this nature, however, the following changes might be considered:

TABLE I. UH-1C INSTRUMENTATION CHARACTERISTICS

Item	Channel: Oscillograph[1]	Channel: Strip Chart[3]	Sensor	Sensitivity: Oscillograph	Sensitivity: Strip Chart	Instrumentation Filter
Yaw Attitude	1		Sperry Compass Gyro, 2K pot.	90 deg/in.		NI[2]
Pedal Position	3	2	Helipot, Model G, 1KΩ	1 in/in.	.0.059 in/mm	NI
Yaw Rate	5	1	Honeywell, Model GG79, pot., ω_n 66rps, $\zeta \approx 0.7$			
Lateral Accelerometer	6		Systron Donner, Model 4310 (±5g), $\omega_n \approx 90$ rps	1g/in.		$\omega_n > 7$rps
Pitch Attitude	7	5	Honeywell, Model JG7044A56	10 deg/in.	1.18 deg/mm	NI
Longitudinal Cyclic Stick	9	4	Helipot, Model G, 1KΩ	1 in/in.	0.059 in/mm	NI
Pitch Rate	11	3	Honeywell, Model GG79, pot., $\omega_n \approx$ 25rps, $\zeta \approx 0.7$	10 deg/sec/in.	0.59 deg/sec/mm	NI
Vertical Accelerometer	12		Systron Donner, Model 4310 (±5g), $\omega_n \approx$ 90rps $\zeta \approx 0.7$	1g/in.		$\omega_n > 7$rps
Roll Attitude	13	6	Honeywell, Model JG7044A56	20 deg/in.	1.18 deg/mm	NI
Lateral Cyclic Stick	15	7	Helipot, Model G, 1KΩ	1 in/in.	0.059 in/mm	NI
Roll Rate	17	8	Honeywell, Model GG79, pot., $\omega_n \approx$ 40 rps, $\zeta \approx 0.7$	10 deg/sec/in.	0.59 deg/sec/mm	NI
Collective Stick	18		Helipot, Model G, 1KΩ	4 in/in.		NI
Longitudinal Accelerometer	21		Systron Donner, Model 4310 (±5g), $\omega_n \approx$ 90 rps $\zeta \approx 0.7$	1g/in.		$\omega_n > 7$rps

[1] Honeywell Oscillograph Model No. 1108, Kodak 1855 paper, 6-second (≈4 in.) timing markers.

[2] None indicated (NI)

[3] Timing ≈ 0.25 in/sec

1. Make sufficient duplicate responses to establish a "typical" response at any given flight condition.

2. Keep multi-input responses to a minimum.

3. Include collective responses.

4. Increase, if possible, the sensitivities of the lateral and longitudinal accelerometers and put as many significant traces on the strip chart recorder (as opposed to the oscillograph) as possible.

5. Apply several input levels at each condition to establish a "typical small perturbation response".

6. Trim aircraft for zero body rates before applying input disturbances.

VEHICLE MATH MODEL

The basic derivatives that are generated by the MOSTAB-C program are used in the equations of motion defined by equations (1) through (9) below. In equations (1) through (6), the X, Y, Z, L, M, and N terms contain the aerodynamic stability and control derivatives that are generated by the MOSTAB program.

$$X - mg\theta = m\ (\dot{u} + qw_o - rv_o) \tag{1}$$

$$Y + mg\varphi = m\ (\dot{v} + ru_o - pw_o) \tag{2}$$

$$Z - 0.5\ mg\varphi^2 - mg\varphi_o\varphi = m\ (\dot{w} + pv_o - qu_o) \tag{3}$$

$$L = I_{xx}\dot{p} - I_{xz}\dot{r} \tag{4}$$

$$M = I_{yy}\dot{q} \tag{5}$$

$$N = I_{zz}\dot{r} - I_{zx}\dot{p} \tag{6}$$

$$\dot{\theta} = q\ (1 - 0.5\varphi^2) - r\varphi \tag{7}$$

$$\dot{\varphi} = p \tag{8}$$

$$\dot{\Psi} = q\varphi + r\ (1 - 0.5\varphi^2) \tag{9}$$

Rearranging equations (1) through (6), we have

$$\dot{u} = X/m - g\theta - qw_o + rv_o \tag{10}$$

$$\dot{v} = Y/m + g\varphi - ru_o + pw_o \tag{11}$$

$$\dot{w} = Z/m - 0.5\ g\varphi^2 - g\varphi_o\varphi - pv_o + qu_o \tag{12}$$

$$\dot{p} = L/I_{xx} + (I_{xz}/I_{xx})\dot{r} \tag{13}$$

$$\dot{q} = M/I_{yy} \tag{14}$$

$$\dot{r} = N/I_{zz} + (I_{zx}/I_{zz})\dot{p} \tag{15}$$

Coefficients in equations (10) through (15) are determined by the MOSTAB-C program.

A converted MOSTAB-C output is called the "modified form" output. The modified form MOSTAB-C output* is defined as

$$\dot{S} = \bar{F}_S S + \bar{F}_C C - \bar{K}\alpha - \bar{h}\varphi^2 \tag{16}$$

where

$$S = \begin{bmatrix} u \\ v \\ w \\ p \\ q \\ r \end{bmatrix}$$

$$\alpha = \begin{bmatrix} \theta \\ \varphi \end{bmatrix} \tag{17}$$

$$C = \begin{bmatrix} \theta_o \\ A_{1S} \\ B_{1S} \\ D\text{-}HT \\ \theta_{DTR} \end{bmatrix}$$

and where θ and φ are determined by equations (7) and (8).

The modified form printout contains the $\bar{F}_S$, $\bar{F}_C$, + $\bar{K}$ and + $\bar{h}$ matrices for use in equation (16).

The modified form stability axis equations for the UH-1C (written to correspond with the MOSTAB-C computer printout) is as follows:

---

* Derived by J. Hoffman in Reference 1.

$$\begin{bmatrix} \dot{u} \\ \dot{v} \\ \dot{w} \\ \dot{p} \\ \dot{q} \\ \dot{r} \end{bmatrix} = \begin{bmatrix} X_u & X_v & X_w & X_p & X_q & X_r \\ Y_u & Y_v & Y_w & Y_p & Y_q & Y_r \\ Z_u & Z_v & Z_w & Z_p & Z_q & Z_r \\ L_u & L_v & L_w & L_p & L_q & L_r \\ M_u & M_v & M_w & M_p & M_q & M_r \\ N_u & N_v & N_w & N_p & N_q & N_r \end{bmatrix} \begin{bmatrix} u \\ v \\ w \\ p \\ q \\ r \end{bmatrix} \tag{18}$$

$$+ \begin{bmatrix} X_{\theta o} & X_{AlS} & X_{BlS} & X_{D\text{-}HT} & X_{\theta_{DTR}} \\ Y_{\theta o} & Y_{AlS} & Y_{BlS} & Y_{D\text{-}HT} & Y_{\theta_{DTR}} \\ Z_{\theta o} & Z_{AlS} & Z_{BlS} & Z_{D\text{-}HT} & Z_{\theta_{DTR}} \\ L_{\theta o} & L_{AlS} & L_{BlS} & L_{D\text{-}HT} & L_{\theta_{DTR}} \\ M_{\theta o} & M_{AlS} & M_{BlS} & M_{D\text{-}HT} & M_{\theta_{DTR}} \\ N_{\theta o} & N_{AlS} & N_{BlS} & N_{D\text{-}HT} & N_{\theta_{DTR}} \end{bmatrix} \begin{bmatrix} \theta_o \\ AlS \\ BlS \\ D\text{-}HT \\ \theta_{DTR} \end{bmatrix}$$

$$- \begin{bmatrix} X_\theta & X_\varphi \\ Y_\theta & Y_\varphi \\ Z_\theta & Z_\varphi \\ L_\theta & L_\varphi \\ M_\theta & M_\varphi \\ N_\theta & N_\varphi \end{bmatrix} \begin{bmatrix} \theta \\ \varphi \end{bmatrix} - \begin{bmatrix} X_{\varphi^2} \\ Y_{\varphi^2} \\ Z_{\varphi^2} \\ L_{\varphi^2} \\ M_{\varphi^2} \\ N_{\varphi^2} \end{bmatrix} \begin{bmatrix} \varphi^2 \end{bmatrix}$$

The control input portion of equation (18) that was used by ANC is as follows:

$$\bar{F}_C C = \begin{bmatrix} X_{CO} & X_{A1} & X_{B1} & X_{DLR} \\ Y_{CO} & Y_{A1} & Y_{B1} & Y_{DLR} \\ Z_{CO} & Z_{A1} & Z_{B1} & Z_{DLR} \\ L_{CO} & L_{A1} & L_{B1} & L_{DLR} \\ M_{CO} & M_{A1} & M_{B1} & M_{DLR} \\ N_{CO} & N_{A1} & N_{B1} & N_{DLR} \end{bmatrix} \begin{bmatrix} CO \\ A1 \\ B1 \\ DLR \end{bmatrix} \qquad (19)$$

Where comparing (18) and (19),

$$\theta_o \triangleq CO \qquad (20)$$

$$A1S \triangleq A1 \qquad (21)$$

$$B1S \triangleq B1 \qquad (22)$$

$$D\text{-}HT \triangleq 0 \qquad (23)$$

$$\theta_{DTR} = DLR \qquad (24)$$

The horizontal tail deflection, D-HT, is related to the pitch control, B1, by the relationship shown in Figure 1. At speeds below 60 knots, the D-HT derivatives are small compared to the B1 derivatives and essentially D-HT=0. Above 60 knots it was assumed that D-HT could also be set to 0 without significantly affecting the results (there is some control effectiveness change in the pitching moment equation).

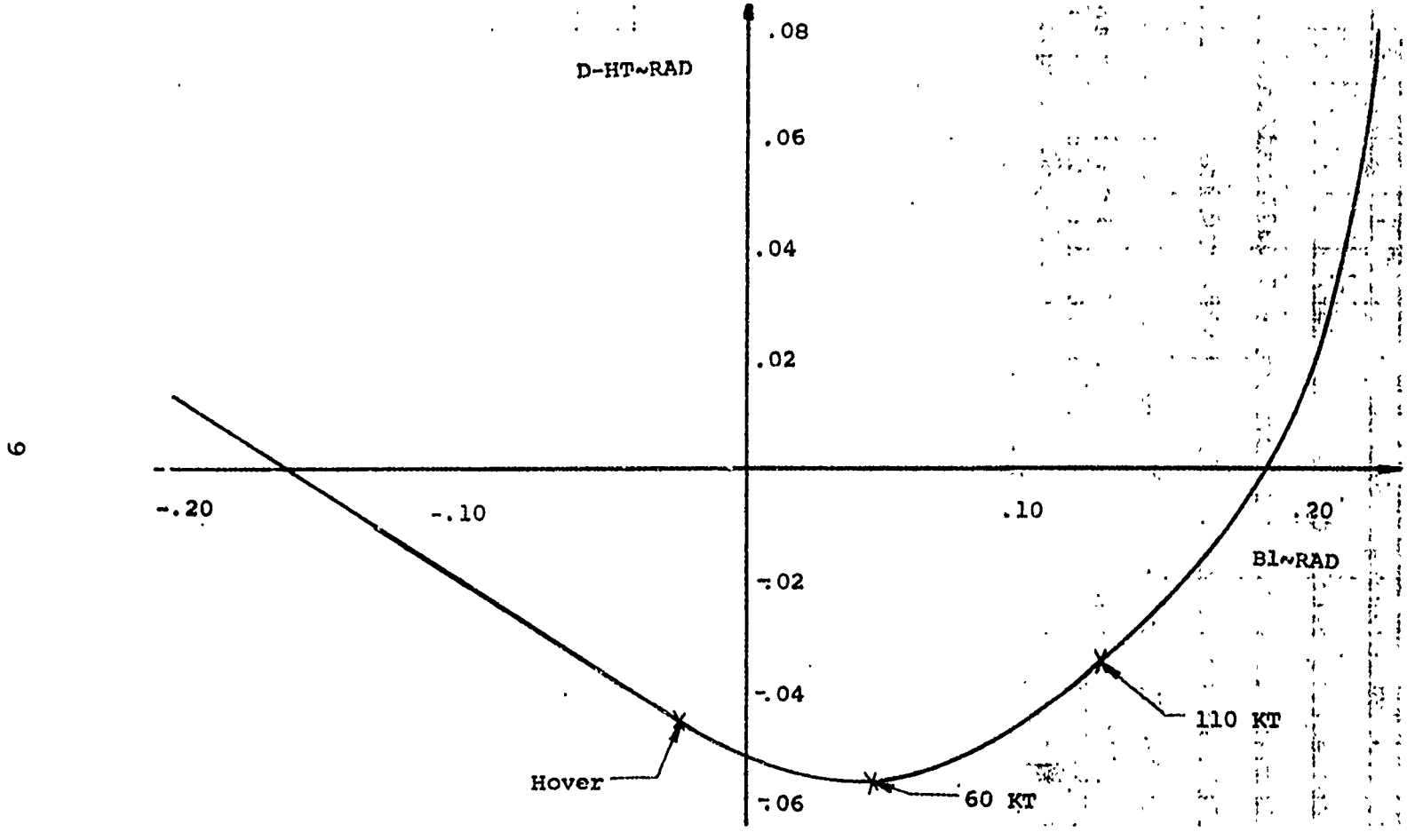

Figure 1. Longitudinal Cyclic Pitch Position vs. Horizontal Tail Position.

The mechanical relationships between pilot inputs at the sticks and pedals and motions at the swash plate and tail rotor for the UH-1C are as follows:

1. Collective pitch (CO) - 0.057 rad/in.

2. Longitudinal cyclic pitch (B1) - 0.0377 rad/in.

3. Lateral cyclic pitch (A1) - 0.0281 rad/in.

4. Pedal (DLR) - 0.065 rad/in.

The modified form stability derivatives for six straight and level flight conditions from hover to 120 knots are given in Tables II through VII. These derivatives are used in equations (18) and (19) to model the vehicle.

TABLE II. MODIFIED FORM STABILITY DERIVATIVE MATRICES FOR HOVER AT 3000 FEET

	U	V	W	P	Q	R
U DOT	-.9961-02	.4436-03	.1013-01	-.1335+01	.1460+01	-.1670-00
V DOT	.5551-03	-.3512+01	-.1123-01	-.1562+01	-.1455+01	.5570-00
W DOT	.7280-02	-.1157+01	-.3443-00	-.8713-01	-.5326-01	.2090+01
P DOT	.1056-02	-.1441-01	-.7039-02	-.7479-00	-.1044+01	.1814-00
Q DOT	.1074-02	.1491-03	-.9246-03	.3063-00	-.2723-00	.7084-01
R DOT	.1212-03	.1538-01	.9990-03	-.4917-00	.8474-01	-.5183-00

	THETA 0	A1S	B1S	D HT	THETA DTR
U DOT	.1064+02	-.9927-00	.3282+02	.5166-00	-.2182-01
V DOT	-.1191+02	.3300+02	.7471-00	-.3392-04	-.1851+02
W DOT	-.3354+03	-.5328-00	.1326+01	.1193-01	.1407-00
P DOT	-.7128+01	.1619+02	-.1402+01	-.1639-04	-.6287+01
Q DOT	.1455-00	-.3704-00	-.5356+01	.1720-02	-.1002+00
R DOT	.1571+02	.9549-00	-.8757-01	-.1174-04	.1424+02

	THETA	PHI
U DOT	.3220+02	.1599-03
V DOT	.1026-03	-.3219+02
W DOT	-.2195-03	-.5558-00
P DOT	.2001-03	.2437-02
Q DOT	-.2219-03	-.9363-04
R DOT	.5846-04	-.5326-02

	PHI SQUARED
U DOT	-.2027-03
V DOT	-.5133-03
W DOT	.1610+02
P DOT	-.1755-02
Q DOT	.2629-03
R DOT	-.5965-03

TRIM CONDITIONS

THETA	.3158-01	PHI	-.1725-01		
U0	.0000	V0	.0000	W0	.0000
X0	.2242+03	Y0	.1225+03	Z0	-.7095+04
THETA D	.2992-00	A1S	-.3400-01	B1S	-.2088-01
THETA DTR	-.1311-00	D HT	-.4695-01	Q0	.1069+05

TABLE III. MODIFIED FORM STABILITY DERIVATIVE MATRICES FOR 60 KNOTS AT SEA LEVEL

	U	V	W	P	Q	R
U DOT	-.3304-01	.4198-02	.3872-01	-.1164+01	-.1315+01	-.2499-00
V DOT	.6036-02	-.1075+00	-.1727-01	.9763-00	-.1367+01	-.1004+03
W DOT	-.1953-01	-.1830-01	-.9073-00	-.1579+01	.1008+03	.1835+01
P DOT	.1280-02	-.2221-01	-.1020-01	-.1287+01	-.8757-00	.4132-00
Q DOT	.5146-02	-.9491-03	-.8031-02	.2487-00	-.6739-00	.5159-01
R DOT	-.4693-02	.3177-01	-.1111-01	-.1894-00	-.1240-00	-.1119+01

	THETA 0	A1S	B1S	D HT	THETA DTR
U DOT	.1760+02	-.1345+01	.2621+02	.5656-01	-.2953+01
V DOT	-.7127+01	.3294+02	.2348+01	.5361-01	-.1482+02
W DOT	-.4177+03	.2301-00	.8696+02	-.4139+01	.4207+01
P DOT	-.4220+01	.1793+02	.2386-00	.2835-01	-.6232+01
Q DOT	.1015+01	-.8755-01	-.5007+01	-.1662+01	.2695+01
R DOT	.8470+01	.9958-00	.9676-00	.8007-02	.1180+02

	THETA	PHI
U DOT	.3220+02	.1529-02
V DOT	-.1212-02	-.3219+02
W DOT	-.4578-03	-.3972-00
P DOT	-.5401-03	.2119-02
Q DOT	-.1028-03	-.1273-02
R DOT	.1436-04	-.4393-02

	PHI SQUARED
U DOT	-.2629-03
V DOT	-.1092-03
W DOT	.1610+02
P DOT	-.6199-03
Q DOT	-.1965-03
R DOT	-.5091-03

TRIM CONDITIONS

THETA	.3453-01	PHI	-.1228-01		
UO	.1017+03	VO	.3703-09	WO	.3515+01
XO	.2452+03	YO	.8719+02	ZO	-.7095+04
THETA 0	.2169-00	A1S	-.2021-01	B1S	.4511-01
THETA DTR	-.5771-01	D HT	-.5529-01	QO	.6165+04

TABLE IV. MODIFIED FORM STABILITY DERIVATIVE MATRICES FOR 60 KNOTS AT 10,000 FEET

	U	V	W	P	Q	R
U DOT	-.2706-01	.1893-02	.1793-01	-.1156+01	-.1176+01	-.2222-00
V DOT	.1576-02	-.8196-01	-.1040-01	.6875-00	-.1261+01	-.1008+03
W DOT	-.3695-01	-.1194-01	-.6664-00	-.1145+01	.1015+03	.1900+01
P DOT	.6492-03	-.1873-01	-.7177-02	-.1713+01	-.9024-00	.2741-00
Q DOT	.2547-02	.5099-03	-.3253-02	.2282-00	-.6436-00	.5895-01
R DOT	-.2386-02	.2153-01	-.1311-01	-.2466-00	.4842-01	-.8823-00

	THETA 0	A1S	B1S	D HT	THETA DTR
U DOT	.3973+01	-.1728+01	.2857+02	-.8231-02	.1499+01
V DOT	-.6149+01	.3309+02	.2139+01	.5611-01	-.1491+02
W DOT	-.3103+03	.3587-00	.6478+02	-.3072+01	-.7549-00
P DOT	-.3233+01	.1912+02	.4470-01	.3001-01	-.5126+01
Q DOT	.1256+01	-.2978-01	-.5177+01	-.1233+01	-.6673-00
R DOT	.9585+01	.9052-00	.9644-00	.6260-02	.1152+02

	THETA	PHI
U DOT	.3220+02	-.2761-04
V DOT	-.2914-03	-.3219+02
W DOT	-.4658-03	-.3826-00
P DOT	-.3246-04	.1890-02
Q DOT	-.7952-04	.1051-03
R DOT	-.6232-05	-.4212-02

	PHI SQUARED
U DOT	-.1122-02
V DOT	.1297-02
W DOT	.1610+02
P DOT	-.9279-04
Q DOT	-.2351-04
R DOT	-.9111-03

TRIM CONDITIONS

THETA	.3959-01	PHI	-.1189-01		
U0	.1017+03	V0	.3703-09	W0	.4030+01
X0	.2811+03	Y0	.8442+02	Z0	-.7094+04
THETA 0	.2434-00	A1S	-.2054-01	B1S	.4872-01
THETA DTR	-.7748-01	D HT	-.5493-01	Q0	.6129+04

TABLE V. MODIFIED FORM STABILITY DERIVATIVE MATRICES FOR 90 KNOTS AT 3000 FEET

	U	V	W	P	Q	R
U DOT	-.4644-01	.6164-02	.5602-01	-.1020+01	-.1265+01	-.3492-00
V DOT	.0778-02	-.1340-00	-.1853-01	.8898-00	-.1293+01	-.1504+03
W DOT	.4092-01	-.2032-01	-.9254-00	-.2312+01	.1506+03	.1952+01
P DOT	.1695-02	-.2486-01	-.1002-01	-.1288+01	-.8825-00	.4841-00
Q DOT	.3968-02	-.1409-02	-.1354-01	.2381-00	-.7761-00	.8484-01
R DOT	-.2421-02	.3542-01	-.1031-01	-.1257-00	-.3270-00	-.1326+01

	THETA 0	A1S	B1S	D HT	THETA DTR
U DOT	.2276+02	-.1715+01	.2052+02	.2434-00	-.1048+01
V DOT	-.7175+01	.3307+02	.3200+01	.1068+00	-.1553+02
W DOT	-.4271+03	.4572-00	.1288+03	-.8434+01	.2731+01
P DOT	-.4350+01	.1807+02	.4366-00	.5541-01	-.6359+01
Q DOT	-.2482-00	-.7994-01	-.4310+01	-.3389+01	.1646+01
R DOT	.5617+01	.1088+01	.1350+01	.1684-01	.1230+02

	THETA	PHI
U DOT	.3220+02	.1669-03
V DOT	-.0777-03	-.3219+02
W DOT	-.4192-03	-.6581-00
P DOT	-.3972-03	.2268-02
Q DOT	-.2657-04	-.3773-03
R DOT	.2667-04	-.4456-02

	PHI SQUARED
U DOT	-.1557-02
V DOT	.2692-02
W DOT	.1610+02
P DOT	.6500-03
Q DOT	-.3207-03
R DOT	-.5239-03

TRIM CONDITIONS

THETA	.2312-01	PHI	-.2041-01		
U0	.1519+03	V0	-.0000	W0	.3512+01
X0	.1642+03	Y0	.1449+03	Z0	-.7097+04
THETA 0	.2373-00	A1S	-.2201-01	B1S	.9276-01
THETA DTR	-.6314-01	D HT	-.4575-01	Q0	.7176+04

TABLE VI. MODIFIED FORM STABILITY DERIVATIVE MATRICES FOR 110 KNOTS AT 3000 FEET

	U	V	W	P	Q	R
U DOT	-.5712-01	.8243-02	.6607-01	-.9039-00	.1030+01	-.4024-00
V DOT	.8348-02	-.1577-00	-.2361-01	-.1364+01	-.1293+01	-.1842+03
W DOT	.6782-01	-.2632-01	-.9675-00	-.2879+01	.1845+03	.2105+01
P DOT	.2334-02	-.2778-01	-.1270-01	-.1041+01	-.9406-00	.5791-00
Q DOT	.6694-02	-.1622-02	-.1766-01	.2442-00	-.8202-00	.9858-01
R DOT	-.2071-02	.3927-01	-.5148-02	-.7953-01	-.4869-00	-.1534+01

	THETA 0	A1S	B1S	D HT	THETA OTR
U DOT	.2828+02	-.1931+01	.1576+02	.2804-00	-.3914-00
V DOT	-.9695+01	.3336+02	.4486+01	.1255-00	-.1605+02
W DOT	-.4514+03	.7330-00	.1613+03	-.1270+02	.2878+01
P DOT	-.5926+01	.1830+02	.7715-00	.6146-01	-.6593+01
Q DOT	-.1164+01	-.1534-00	-.3736+01	-.5102+01	.1664+01
R DOT	.1083+02	.1136-01	.7350-00	.2882-01	.1272+02

	THETA	PHI
U DOT	.3220+02	.4188-03
V DOT	.6374-03	-.3219+02
W DOT	-.2887-03	-.9649-00
P DOT	.4469-03	.2943-02
Q DOT	-.8049-04	-.9476-03
R DOT	.9187-04	-.4462-02

	PHI SQUARED
U DOT	-.1689-02
V DOT	.2111-02
W DOT	.1610+02
P DOT	.1589-03
Q DOT	-.5687-03
R DOT	-.6436-03

TRIM CONDITIONS

THETA	.4838-02	PHI	-.2991-01		
UO	.1860+03	VO	-.3383-09	WO	.9003-00
XO	.3435+02	YO	.2124+03	ZO	-.7097+04
THETA 0	.2579-00	A1S	-.2786-01	B1S	.1267-00
THETA OTR	-.7770-01	D HT	-.3330-01	GO	.9300+04

TABLE VII. MODIFIED FORM STABILITY DERIVATIVE MATRICES FOR 120 KNOTS AT 3000 FEET

	U	V	W	P	Q	R
U DOT	-.6311-01	.9853-02	.6909-01	-.8659-00	.3233+01	-.4397-00
V DOT	.9568-02	-.1698-00	-.2750-01	-.3560+01	-.1276+01	-.2010+03
W DOT	.7702-01	-.3034-01	-.9856-00	-.3100+01	.2015+03	.2272+01
P DOT	.2922-02	-.2944-01	-.1498-01	-.8669-00	-.9728-00	.6310-00
Q DOT	.7099-02	-.1743-02	-.1956-01	.2498-00	-.8316-00	.1099+00
R DOT	-.2298-02	.4129-01	-.1384-02	-.8063-01	-.5670-00	-.1645+01

	THETA 0	A1S	B1S	D HT	THETA DTR
U DOT	.3045+02	-.2094+01	.1330+02	.2270-00	-.3978-01
V DOT	-.1192+02	.3365+02	.5560+01	.1152+00	-.1613+02
W DOT	-.4631+03	.9520-00	.1774+03	-.1518+02	.3170+01
P DOT	-.7338+01	.1850+02	.1127+01	.5210-01	-.6657+01
Q DOT	-.1480+01	-.2052-00	-.3445+01	-.6094+01	.1798+01
R DOT	.1303+02	.1101+01	.3836-01	.3756-01	.1279+02

	THETA	PHI
U DOT	.3220+02	-.1070-03
V DOT	-.2562-02	-.3219+02
W DOT	-.1783-03	-.1159+01
P DOT	-.1281-02	.2308-02
Q DOT	-.2691-03	-.4888-03
R DOT	-.1790-04	-.4454-02

	PHI SQUARED
U DOT	-.2627-03
V DOT	.2721-02
W DOT	.1610+02
P DOT	.2898-03
Q DOT	-.9167-03
R DOT	-.7131-03

TRIM CONDITIONS

THETA	-.7626-02	PHI	-.3596-01		
UO	.2030+03	VC	.7385-09	WO	-.1549+01
XO	-.5414+02	YO	.2553+03	ZO	-.7095+04
THETA 0	.2716-00	A1S	-.3205-01	B1S	.1435-00
THETA DTR	-.8929-01	D HT	-.2557-01	QO	.1082+05

SIMULATION MODELS

Digital and analog simulations were used during the study. The digital simulation work was done primarily using the IBM System 360, Continuous System Modelling Program (CSMP). The vehicle math model was also run using the IBM 1130 CSMP and the Control Data Corporation MIMIC programs. The analog simulation work was done on ANC's Aircraft Analog Simulator. The analog and digital simulations were used interactively with ANC's root locus program to augment and check the results of each program.

Figures 2, 3, and 4 show a comparison between ANC's analog and digital simulations and the comparable Mechanics Research Corporation (MRI) time response outputs. The comparable traces are sufficiently close (i.e., considering possible scaling and roundoff differences) to ensure that the simulation models are giving the proper solutions.

Comparisons between the simulation model responses and flight test data showed a fair agreement. However, the cross-coupling simulation responses were almost mirror images of the flight test responses. Several possible causes* of the inaccurate cross-coupling modelling are as follows:

1. The model of rotor inflow may be inaccurate.

2. The tethering representation of the rotor as two unconnected blades may be inaccurate.

3. The model of the interference velocities may be incorrect.

4. The representation of blade dynamics may be inadequate.

Item 3 above seems to be the most probable cause of the modelling inaccuracy.

---

* Per MRI analysis of the MOSTAB-C program.

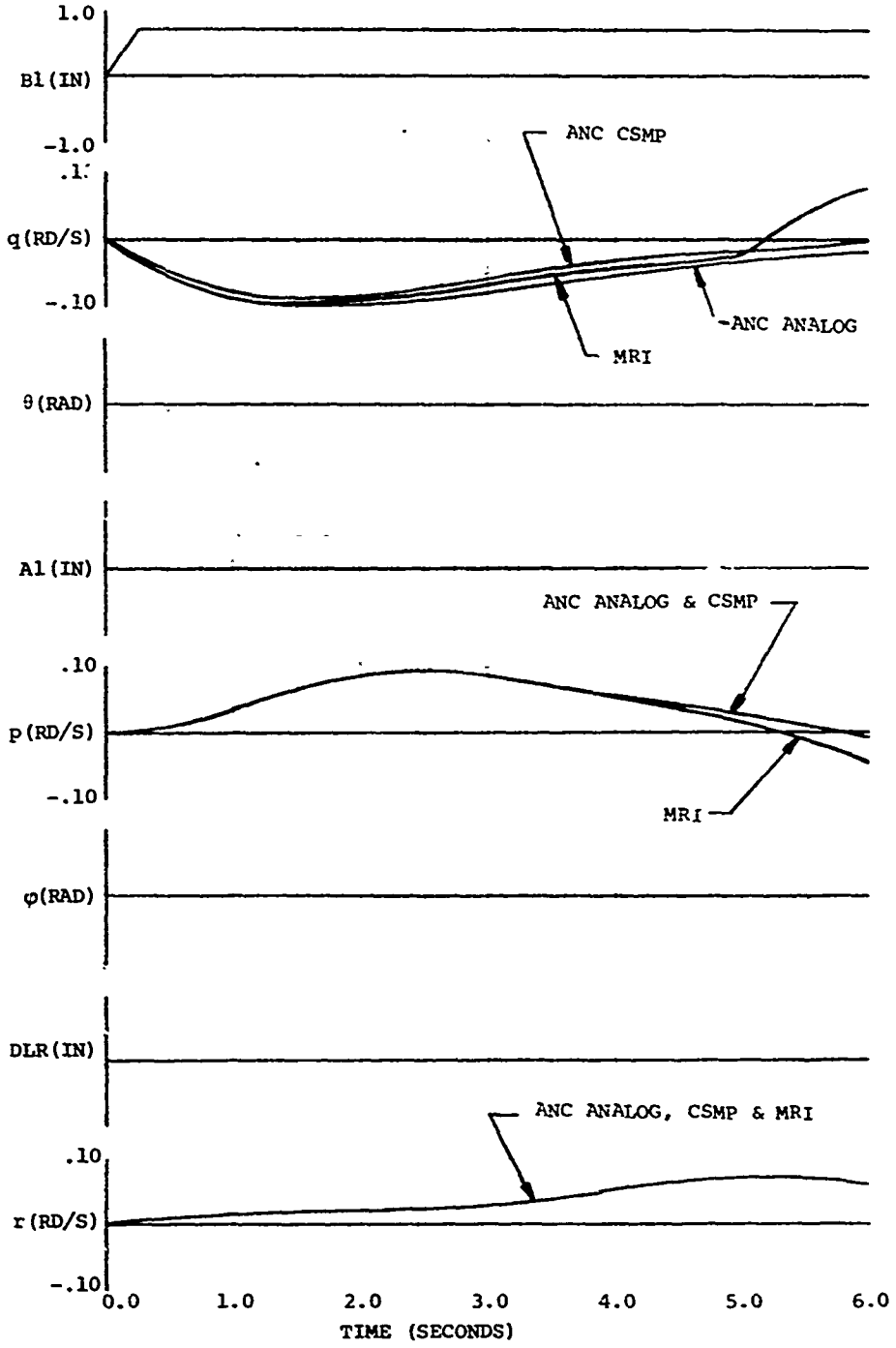

Figure 2. 60-Knot Vehicle Model Longitudinal Cyclic Response (ANC Analog, CSMP & MRI).

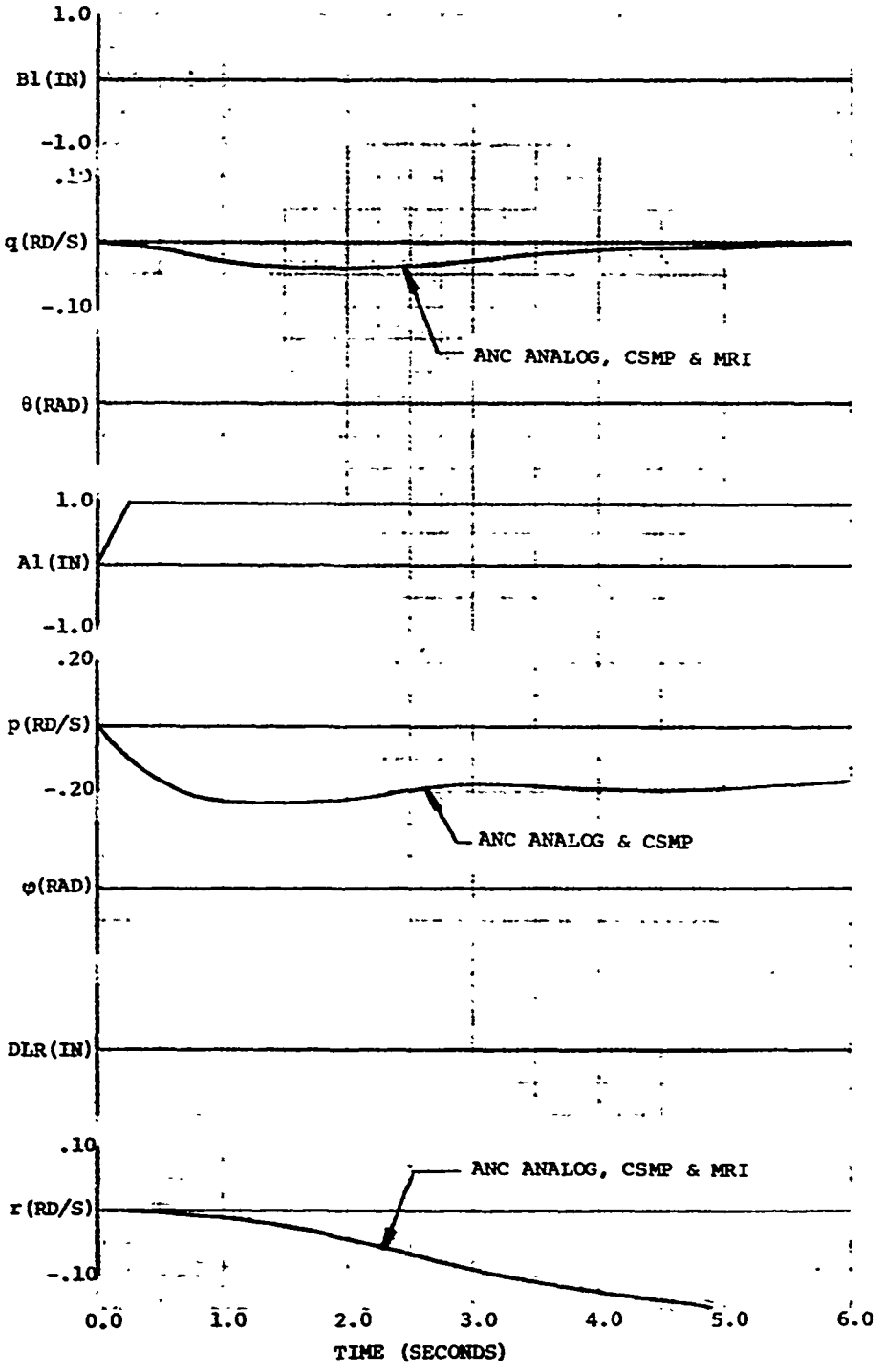

Figure 3. 60-Knot Vehicle Model Lateral Cyclic Response (ANC Analog, CSMP & MRI).

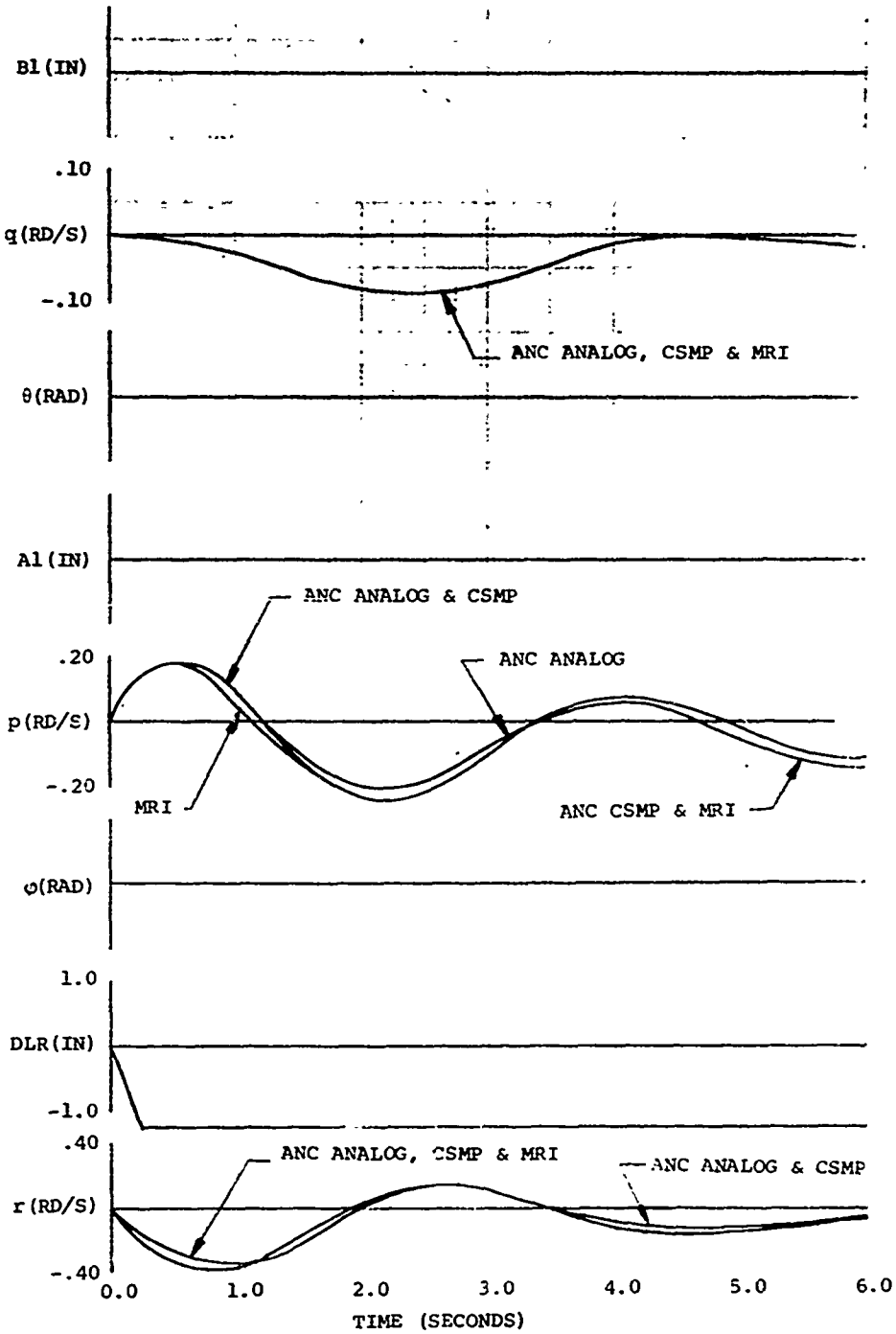

Figure 4. 60-Knot Vehicle Model Pedal Response (ANC Analog, CSMP & MRI).

DIGITAL COMPUTER MODEL

The CSMP simulation of the vehicle math model is given by:

SYSTEM INPUTS

```
B12=AFGEN(CURVE1,TIME)
A12=AFGEN(CURVE2,TIME)
DLR2=AFGEN(CURVE3,TIME)
B1=.03775*B12
CO=.05725*CO2
A1=.02812*A12
DLR=.0650*DLR2
```

AIRCRAFT EQUATIONS

```
UDT=  XU*U+ XV*V+ XW*W+ XP*P+ XQ*Q+ XR*R- XT*THETA- XPH*PHI  ...
     - XPH2*PH2+ XCO*CO+ XA1*A1+ XB1*B1+ XDLR*DLR

AVDT=YU*U+ YV*V- YW*W+ YP*P+ YQ*Q+ YR*R- YT*THETA- YPH*PHI   ...
    - YPH2*PH2+ YCO*CO+ YA1*A1+ YB1*B1+ YDLR*DLR

WDT= ZU*U+ ZV*V+ ZW*W+ ZP*P+ ZQ*Q+ ZR*R- ZT*THETA- ZPH*PHI   ...
    - ZPH2*PH2+ ZCO*CO+ ZA1*A1+ ZB1*B1+ ZDLR*DLR

PDT=ALU*U+ALV*V+ALW*W+ALP*P+ALQ*Q+ALR*R-ALT*THETA-ALPH*PHI   ...
    -ALPH2*PH2+ALCO*CO+ALA1*A1+ALB1*B1+ALDLR*DLR

QDT=AMU*U+AMV*V+AMW*W+AMP*P+AMQ*Q+AMR*R-AMT*THETA-AMPH*PHI   ...
    -AMPH2*PH2+AMCO*CO+AMA1*A1+AMB1*B1+AMDLR*DLR

RDT=ANU*U+ANV*V+ANW*W+ANP*P+ANQ*Q+ANR*R-ANT*THETA-ANPH*PHI   ...
    -ANPH2*PH2+ANCO*CO+ANA1*A1+ANB1*B1+ANDLR*DLR


U         =INTGRL(0.0,UDT)

V         =INTGRL(0.0,AVDT)

W         =INTGRL(0.0,WDT)

P         =INTGRL(PIC,PDT)

Q         =INTGRL(QIC,QDT)

R         =INTGRL(RIC,RDT)
```

```
      PHI=INTGRL(0.0,P)

      PH2=PHI*PHI

      THEDT= Q*(1.0-.5*PH2)-R*PHI

      THETA=INTGRL(0.0,THEDT)

      AIRCRAFT PARAMETERS

TITLE          MOSTAB RESPONSES FOR FC-60-0-F-DS
FUNCTION    CURVE1=(0.0,0.0),(0.25,0.7),(10.0,0.7)
FUNCTION    CURVE2=(0.0,0.0),(10.0,0.0)
FUNCTION    CURVE3=(0.0,0.0),(1.25,0.0),(1.50,.06),(3.25,.06),(3.5,.12)   ...
            ,(10.0,.12)
PARAMETER       XU=-.033, XV=.0042, XW=.0387, XP=-1.18, XQ=-1.32, XR=-.2499
PARAMETER       YU=.0060, YV=-.108, YW=-.017, YP=.9763, YQ=-1.37, YR=-100.4
PARAMETER       ZU=-.019, ZV=-.018, ZW=-.907, ZP=-1.58, ZQ=100.8, ZR=1.835
PARAMETER      ALU=.0013,ALV=-.022,ALW=-.010,ALP=-1.29,ALQ=-.876,ALR=.4132
PARAMETER      AMU=.0051,AMV=-.001,AMW=-.008,AMP=.2487,AMQ=-.674,AMR=.05159
PARAMETER      ANU=-.005,ANV=.0318,ANW=-.011,ANP=-.189,ANQ=-.128,ANR=-1.119
PARAMETER      XCO=17.6, XA1=-1.3, XB1=26.21,          XDLR=-2.953
PARAMETER      YCO=-7.1, YA1=32.9, YB1=2.348,          YDLR=-14.82
PARAMETER      ZCO=-418.0,ZA1=.230, ZB1=86.96,          ZDLR=4.207
PARAMETER     ALCO=-4.2,ALA1=17,9,ALP1=.2786,         ALDLR=-6.232

PARAMETER   AMCO=1.02,AMA1=-.09,AMB1=5.01,            AMDLR=2.695
PARAMETER   ANCO=8.47,ANA1=.996,ANB1=.9676,           ANDLR=11.80
PARAMETER     XT=32.2, XPH=.001529        ,            XPH2=-.00026
PARAMETER     YT=-.002,YPH=-32.19         ,            YPH2=-.0001
PARAMETER     ZT=-.00, ZPH=-.3972         ,            ZPH2=16.10
PARAMETER    ALT=-.00,ALPH=.002119        ,           ALPH2=-.0008
PARAMETER    AMT=-.00,AMPH=-.00127        ,           AMPH2=-.0002
PARAMETER    ANT=-.00,ANPH=-.00439        ,           ANPH2=-.0005
PARAMETER     QIC=+0.0     , PIC=+0.024    ,   RIC=+0.014
```

Figures 5 through 13 show comparisons between flight test data and the CSMP results. Figures 5 through 10 (forward flight) show a fair agreement (i.e., considering that a "typical" flight test trace was not well defined) except for the cross-coupling responses. Figures 12 and 13 (lateral responses in a hover) are not close. However, it appears (by having assessed the results of varying Y_v) that possibly the flight test data might have been taken at some small forward speed.

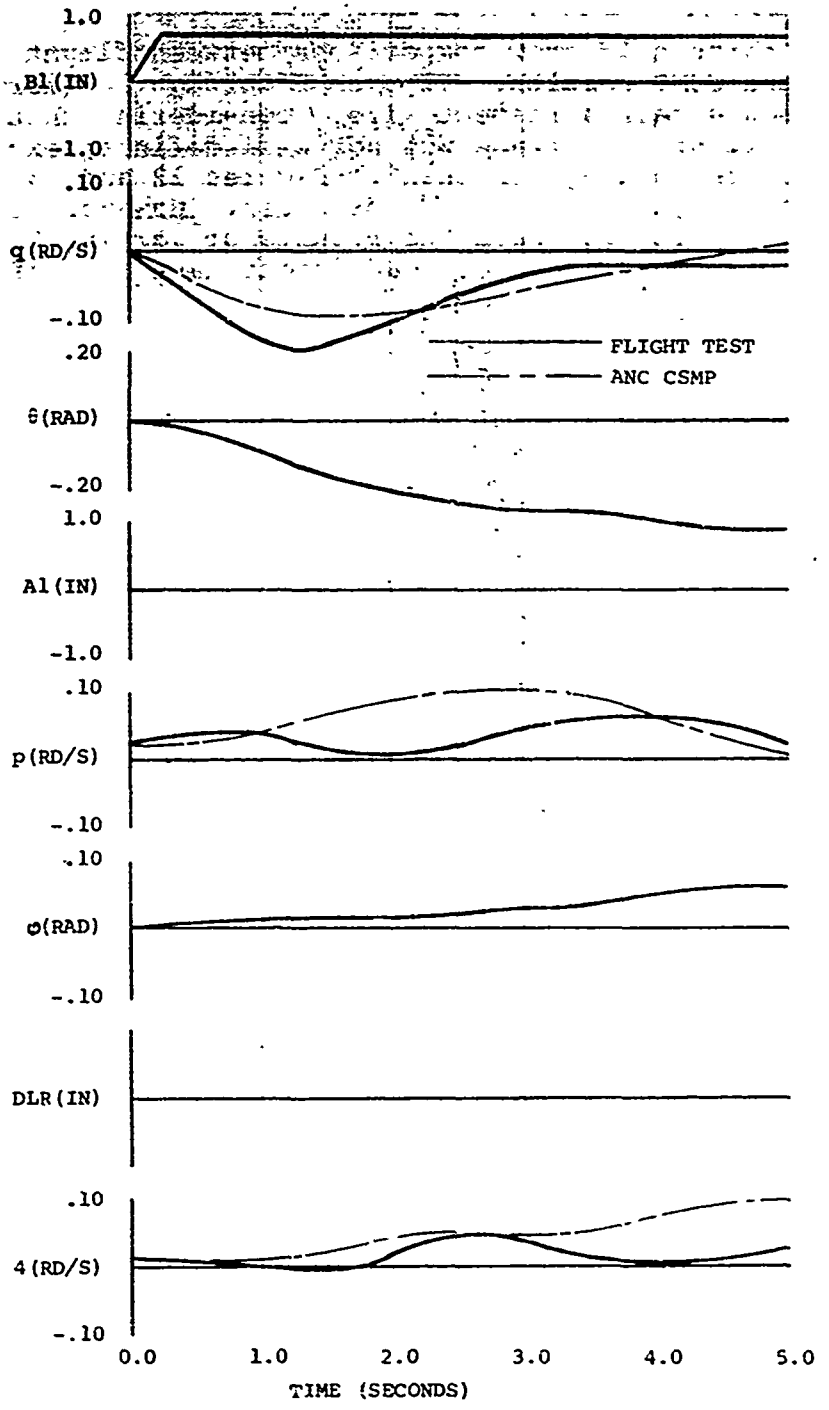

Figure 5. Flight Test vs. CSMP Simulation (60 Knots at 3000 Feet, Pilot Pitch Input Response).

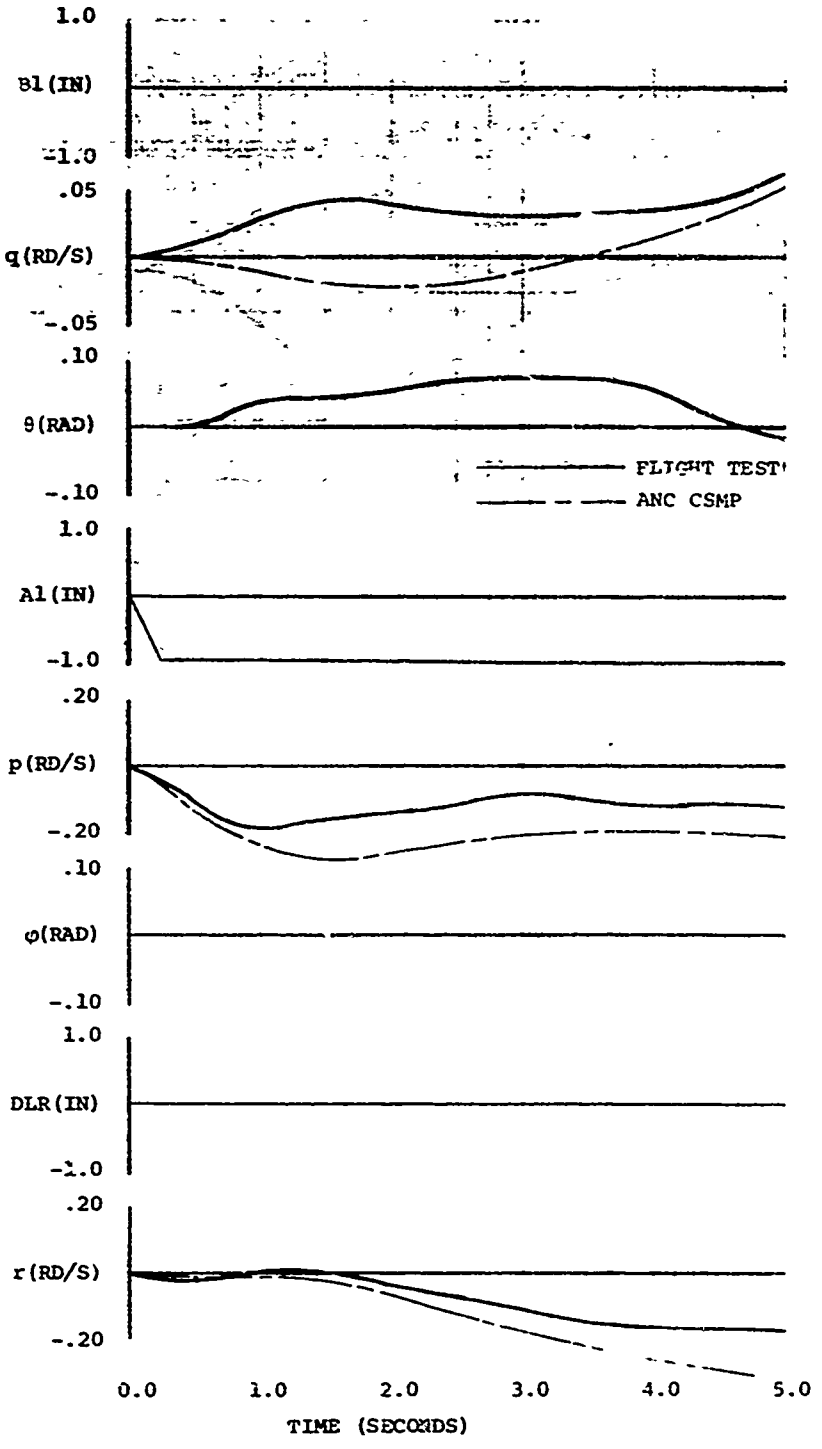

Figure 6. Flight Test vs. CSMP Simulation (60 Knots at 3000 Feet, Pilot Roll Input Response).

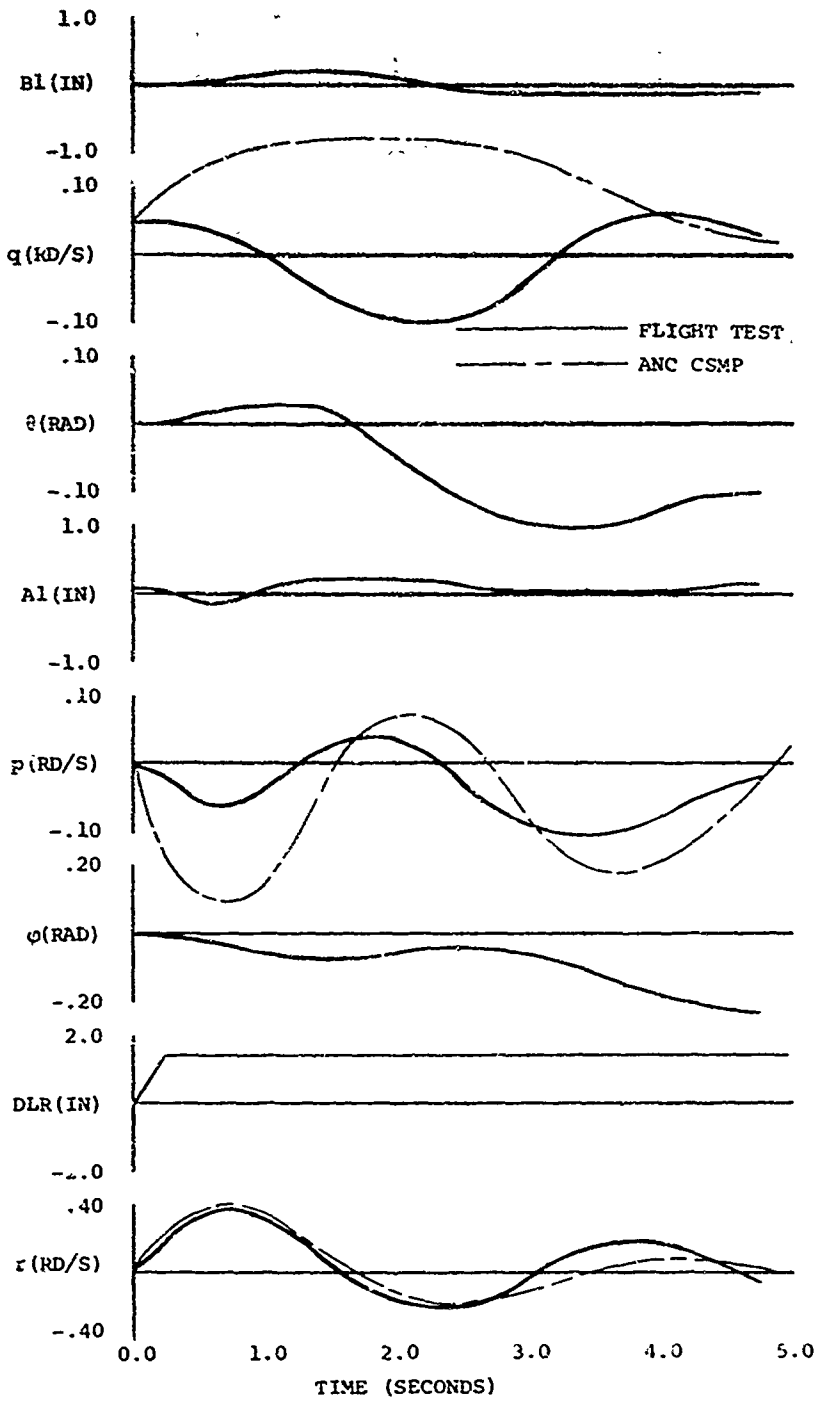

Figure 7. Flight Test vs. CSMP Simulation (60 Knots at 3000 Feet, Pilot Yaw Input Response).

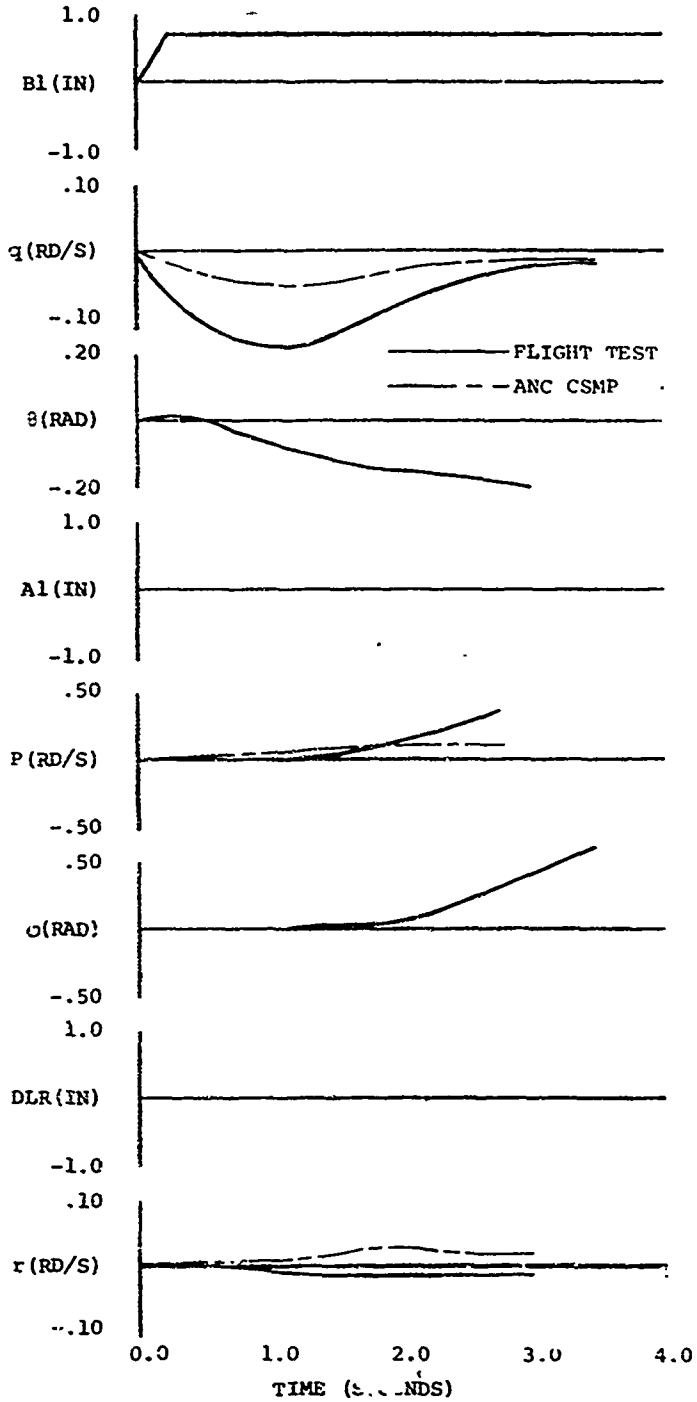

Figure 8. Flight Test vs. CSMP Simulation (110 Knots at 3000 Feet, Pilot Pitch Input Response).

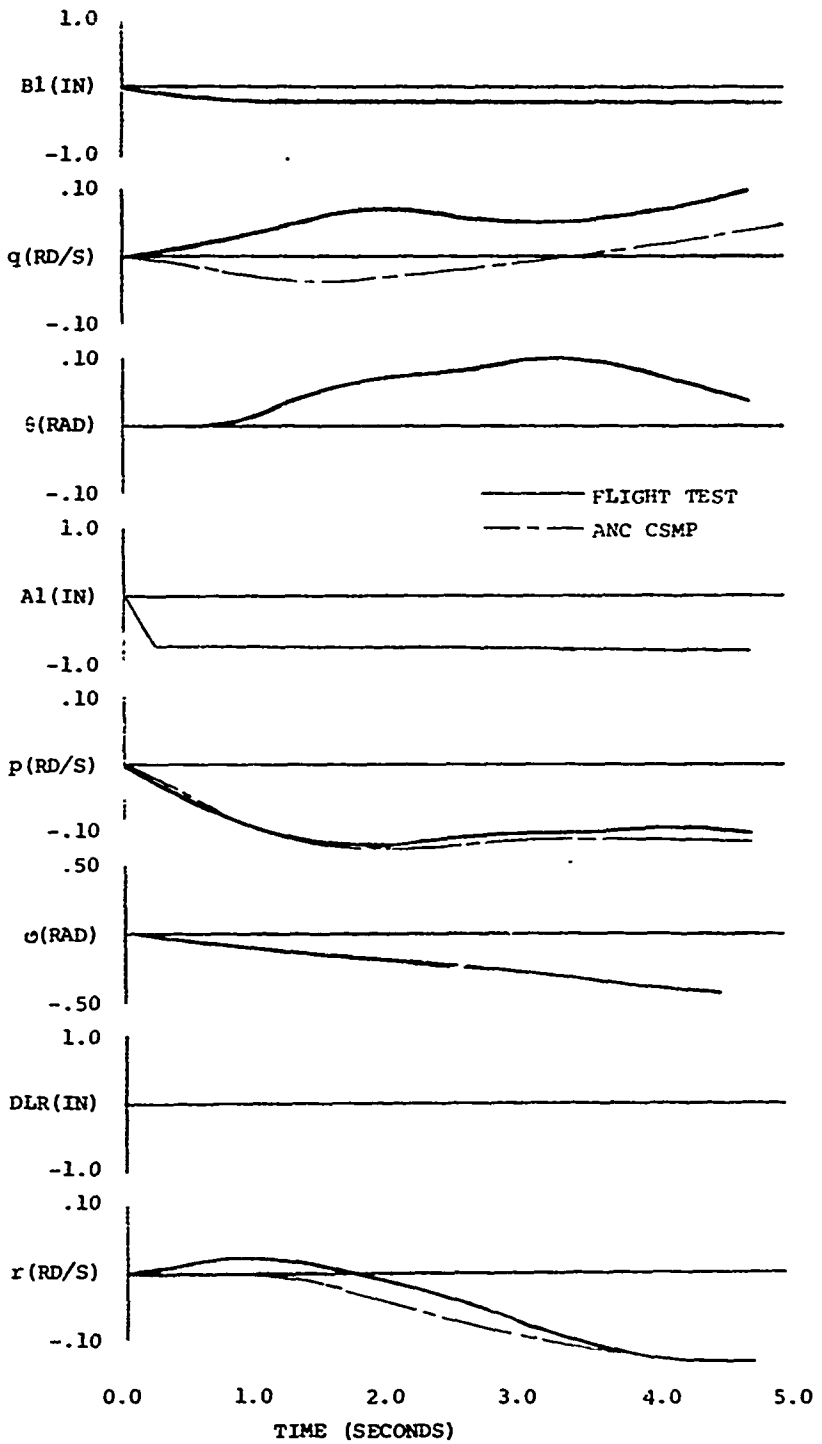

Figure 9. Flight Test vs. CSMP Simulation (110 Knots at 3000 Feet, Pilot Roll Input Response).

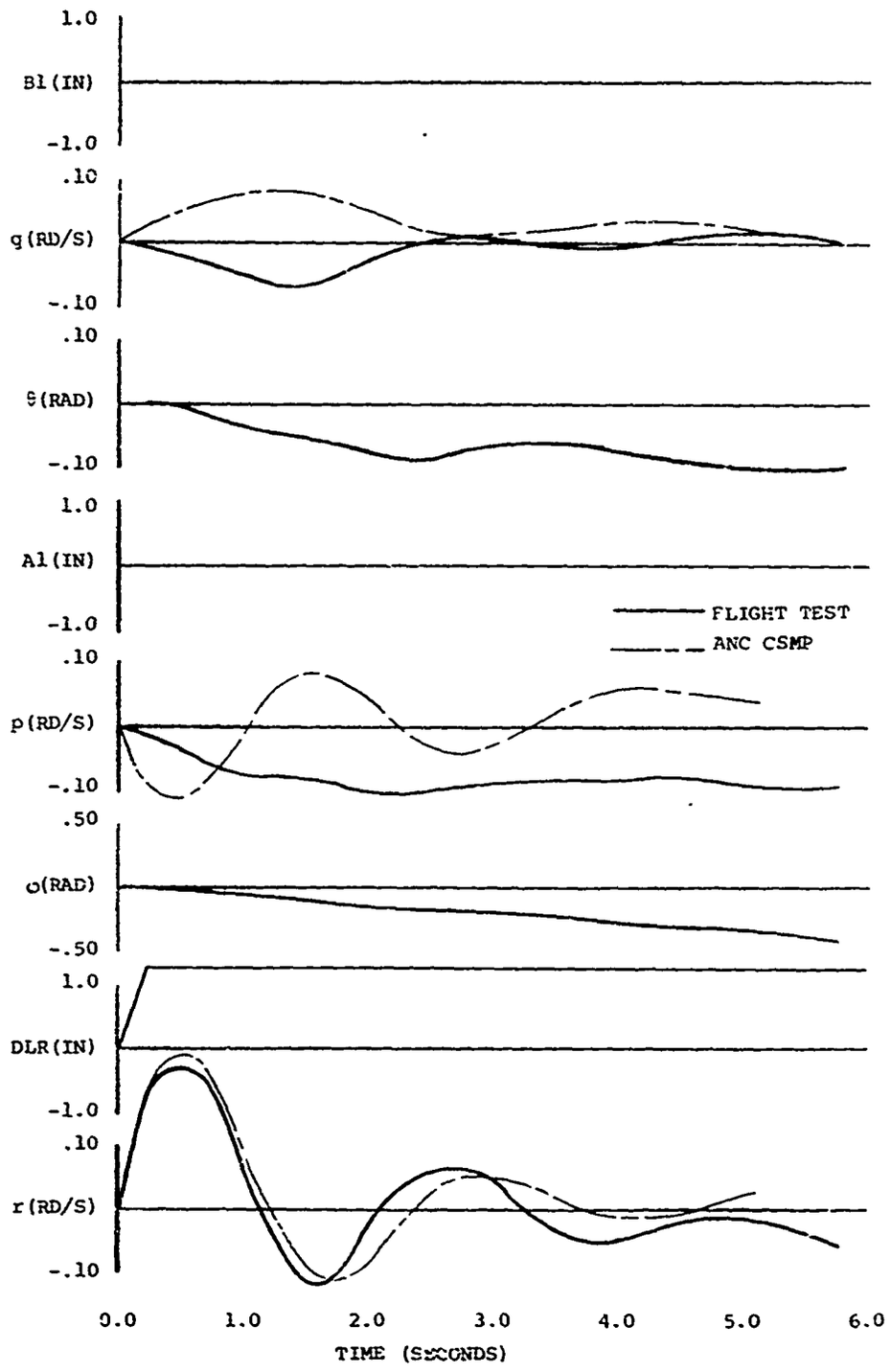

Figure 10. Flight Test vs. CSMP Simulation (110 Knots at 3000 Feet, Pilot Yaw Input Response).

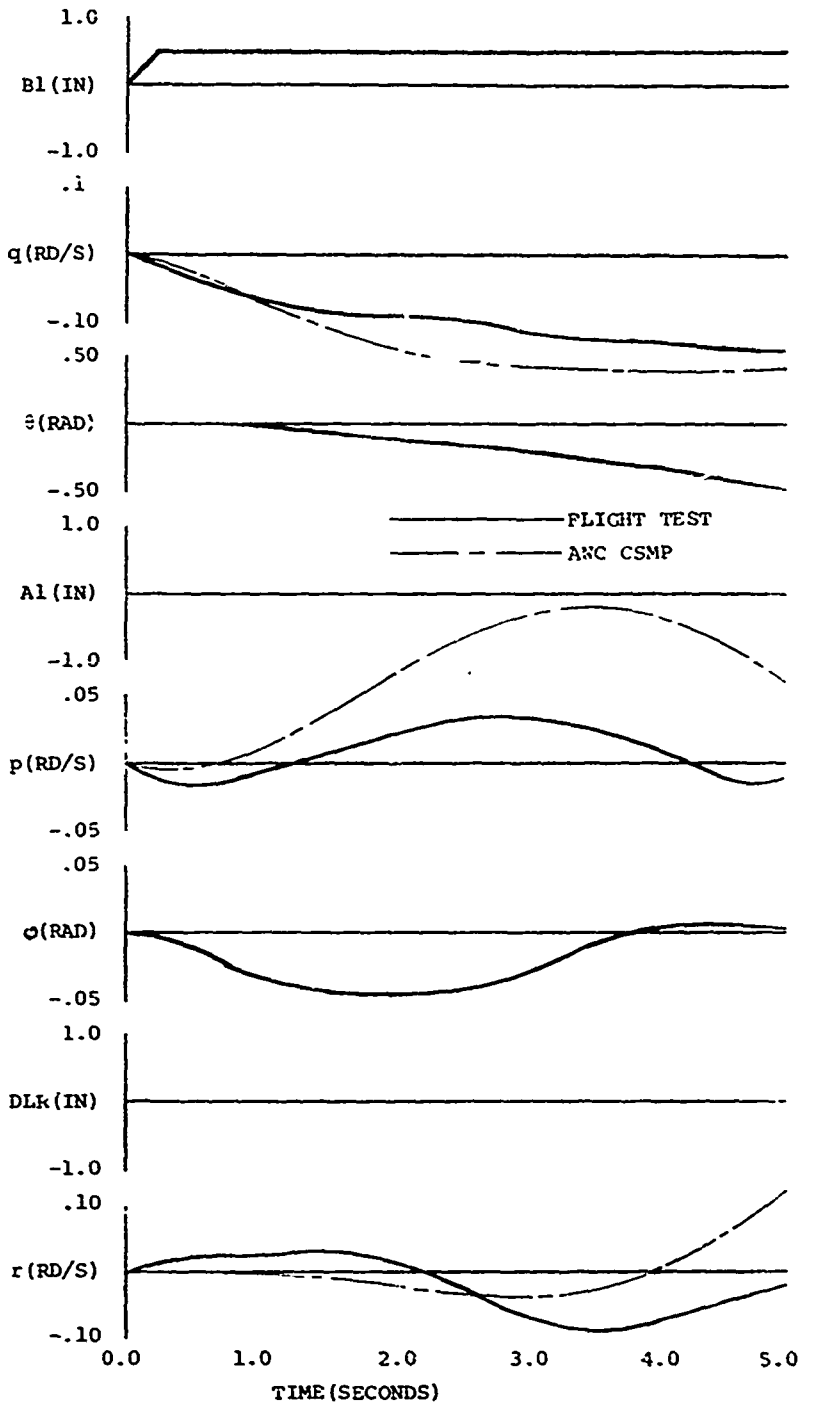

Figure 11. Flight Test vs. CSMP Simulation (Hover at 3000 Feet, Pilot Pitch Input Response).

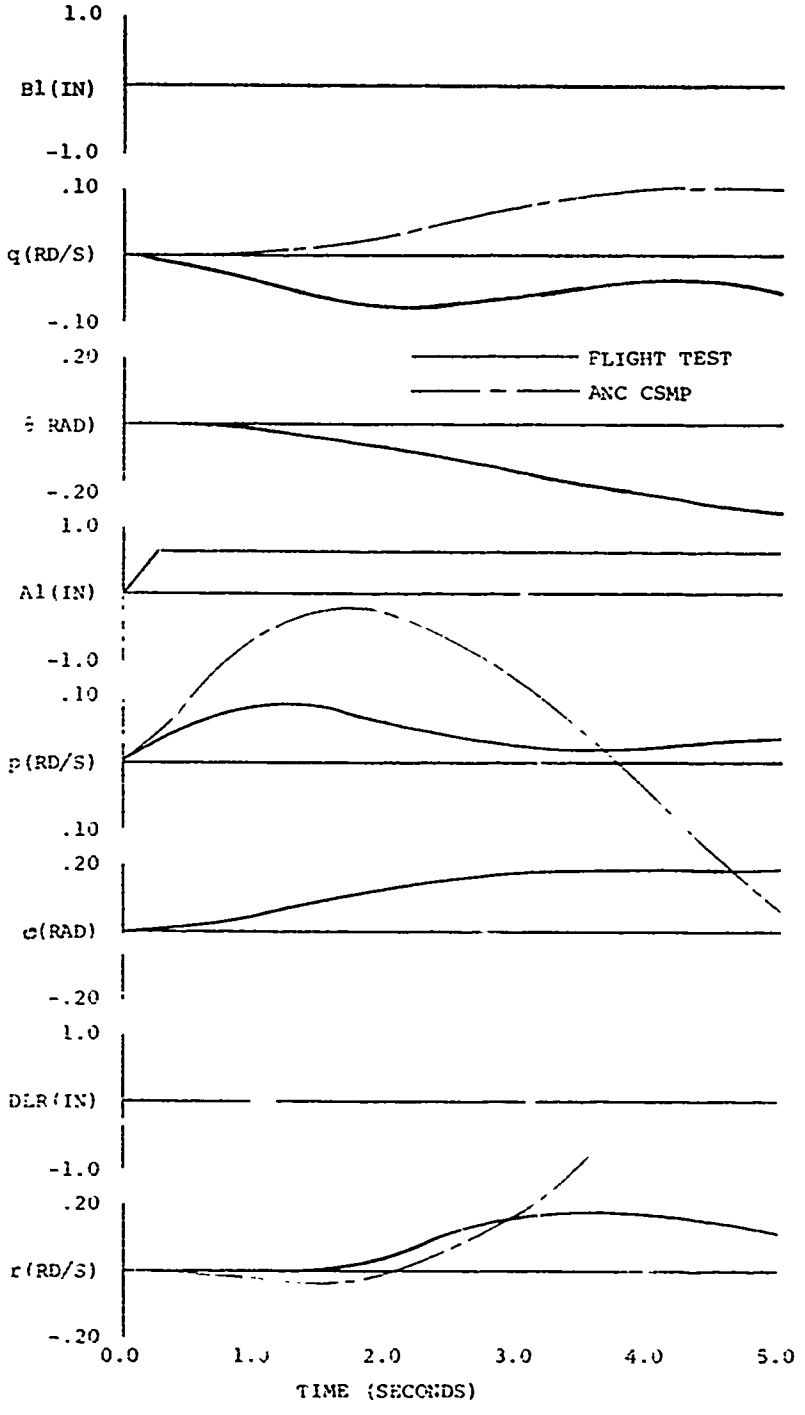

Figure 12. Flight Test vs. CSMP Simulation (Hover at 3000 Feet, Pilot Roll Input Response).

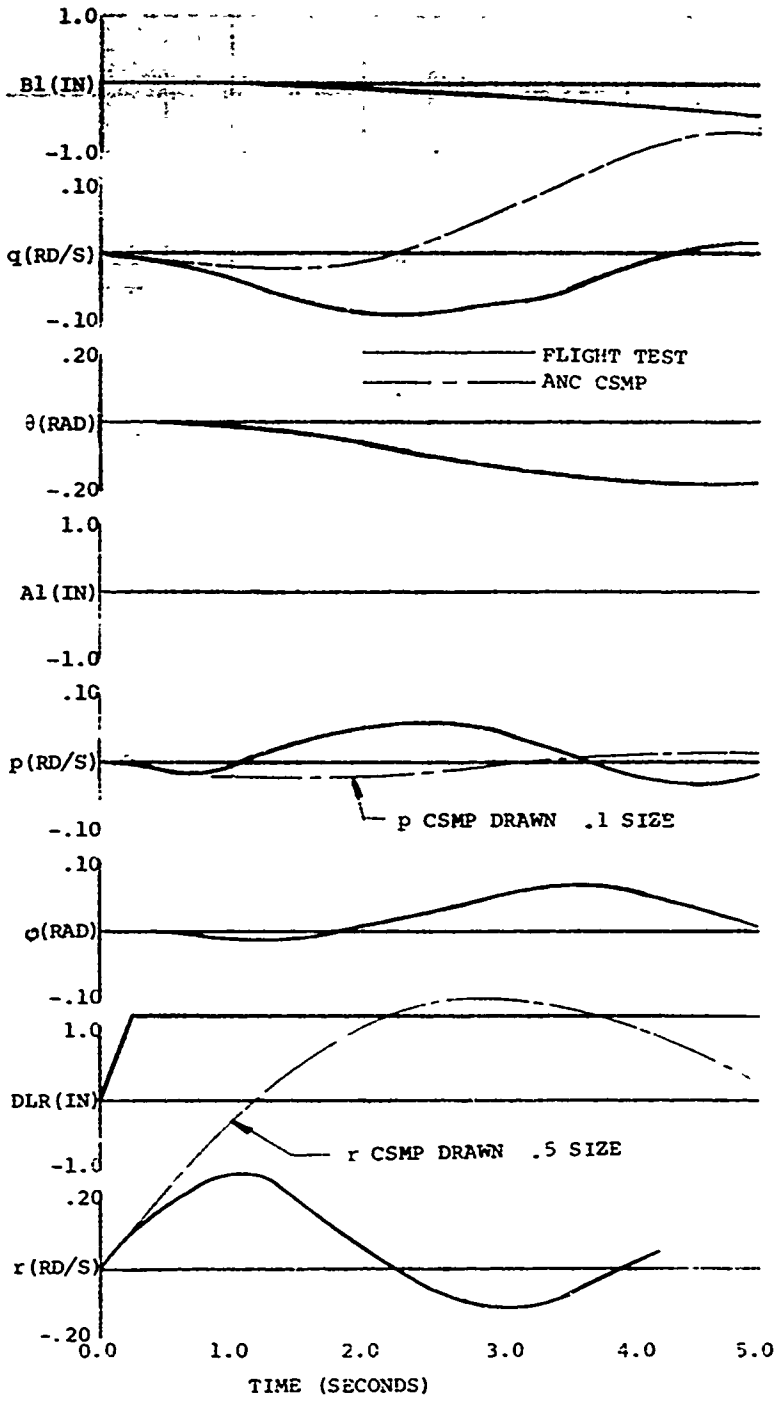

Figure 13. Flight Test vs. CSMP Simulation (Hover at 3000 Feet, Pilot Yaw Input Response).

ANALOG COMPUTER MODEL

Figure 14 is a close-up view of the simulator that was used in performing the analog simulation. Potentiometer settings for hover, 60 knots, and 110 knots are shown in Table III. Figures 15 through 23 compare flight test data with CSMP simulation responses. The CSMP responses were with step inputs (as opposed to the actual pilot input waveshape) to serve as a reference for the analog simulator responses. Also, these CSMP responses had zero initial conditions whereas the flight test data had rate initial conditions in some instances. Figures 15 through 23 are very close to those shown in Figures 5 through 13, respectively. Therefore, the difference between the actual pilot waveshape and a step input was relatively insignificant.

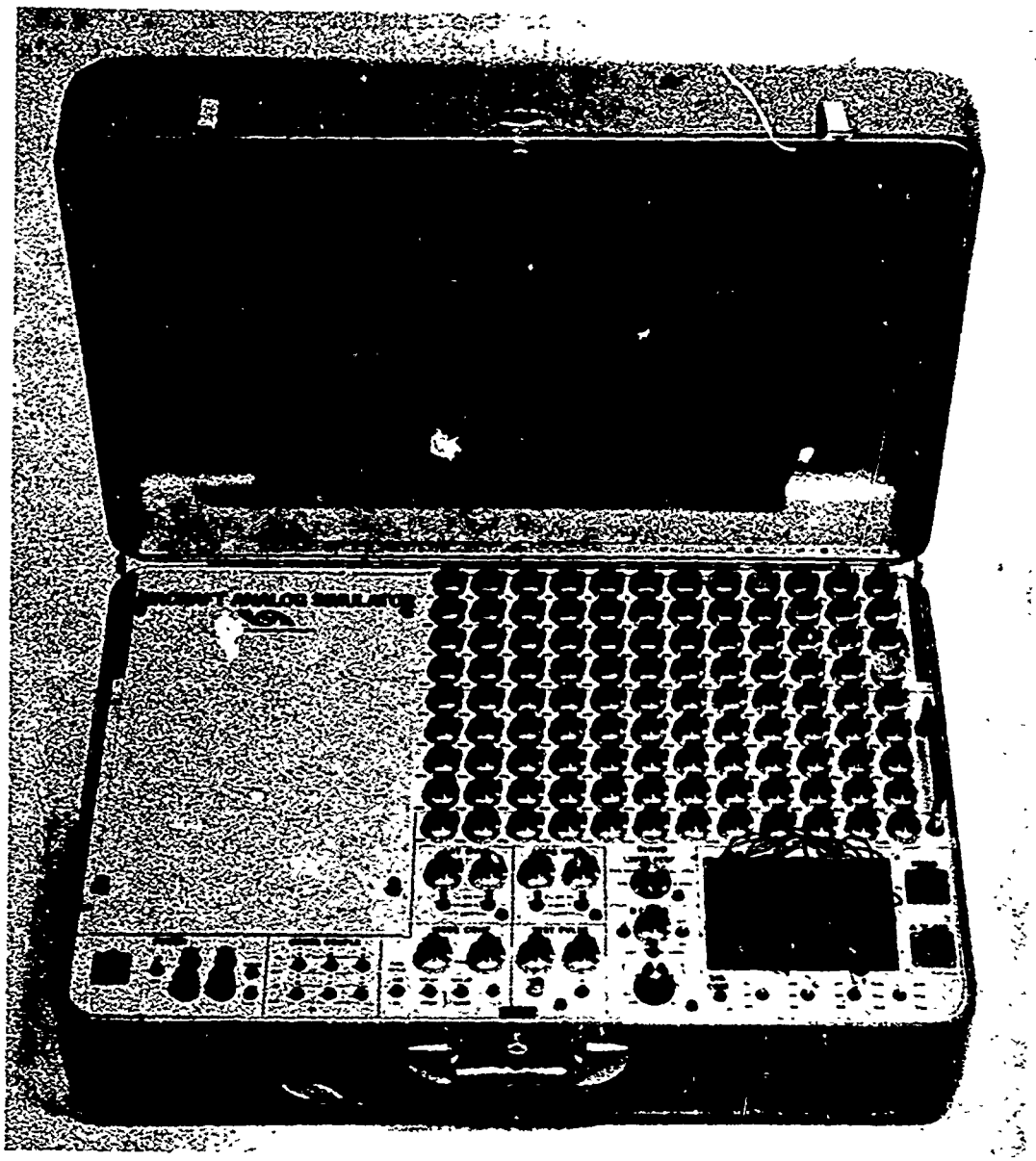

Figure 14. Close-Up View of the R-123 Simulator

TABLE VIII. ANALOG COMPUTER POTENTIOMETER SETTINGS			
Flight Condition	Weight (Pounds)	Altitude (10^3 Feet)	Airspeed (Knots)
FC-0-3	7100	3	0
FC-60-0	7100	0	60
FC-110-3	7100	3	110

Pot.	Parameter	FC-0-3	FC-60-0	FC-110-3
R1	$+ X_{B1}/80$	0.015	0.012	0.007
R2	$\pm X_q/40$	0.037	0.033	0.026
R3	$+X_w/2$	0.005	0.019	0.033
R4	$-X_u$	0.010	0.033	0.057
R5	$\pm X_{co}/4$	0.152	0.251	0.403
R6	$-X_v/10$	0.0004	0.004	0.008
R7	$-X_p/10$	0.1335	0.118	0.090
R8	$-X_r/10$	0.0167	0.025	0.040
R9	$-X_{A1}/10$	0.003	0.004	0.006
R10	$\pm X_{DLR}/4$	0.0003	0.048	0.006
R13	$-Z_w/10$	0.0344	0.091	0.097
R14	$(U_o + Z_q)/400$	0.0001	0.252	0.461
R15	$\pm 2 Z_u$	0.015	0.039	0.136
R17	$+Z_{B1}/4$	0.0001	0.820	1.520
R18	$-Z_{co}/20$	0	1.190	1.286
R19	$-2Z_v$	0.023	0.037	0.053
R20	$-Z_p/5$	0.017	0.316	0.576
R21	$+Z_r/5$	0.418	0.367	0.421
R22	$-Z_{A1}/5$	0.003	0.001	0.004
R23	$\pm Z_{DLR}/4$	0.004	0.137	0.094
R25	$-M_q/10$	0.027	0.067	0.082
R26	$\pm 2M_w$	0.002	0.016	0.035
R27	$\pm 40M_u$	0.043	0.206	0.268
R28	$-2M_w$	0.000	0.000	0.000
R29	$-M_{B1}/2$	0.101	0.094	0.070
R30	$\pm M_{co}$	0.008	0.058	0.066

R27	$\pm 40M_u$	0.023	0.206	0.268
R28	$-2M_w$	0.000	0.000	0.000
R29	$-M_{B1}/2$	0.101	0.094	0.070
R30	$\pm M_{co}$	0.008	0.058	0.066
R31	$\pm 40M_v$	0.006	0.038	0.065
R32	$+4\ M_p/10$	0.126	0.099	0.098
R33	$+4M_r$	0.243	0.206	0.394
R34	$-4\ M_{A1}/10$	0.004	0.0003	0.002
R35	$\pm 10M_{DLR}$	0.065	1.752	1.082
R49	$\pm Y_p/10$	0.156	0.098	0.136
R50	$-Y_v$	0.035	0.108	0.158
R51	$\pm (U_o - Y_r)/200$	$\approx$0.000	0.502	0.921
R52	$+Y_{A1}/100$	0.009	0.009	0.009
R53	$-Y_{DLR}/4$	0.301	0.241	0.261
R54	$-Y_u$	$\approx$0.000	$\approx$0.000	$\approx$0.000
R55	$-Y_w/2$	0.006	0.009	0.012
R56	$-Y_u/40$	0.036	0.034	0.032
R57	$Y_{A1}/8$	0.004	0.011	0.021
R61	$+5N_v$	0.077	0.159	0.196
R62	$-N_r/10$	0.052	0.112	0.153
R63	$\pm N_{A1}$	0.027	0.028	0.032
R64	$+N_{DLR}/4$	0.231	0.192	0.207
R65	$\pm N_p$	0.492	0.189	0.080
R66	$-10N_u$	$\approx$0.000	0.047	0.021
R67	$\pm 5N_w$	$\approx$0.000	0.056	0.026
R68	$\pm N_q/4$	0.021	0.032	0.122
R69	$\pm 1.25N_{B1}$	$\approx$0.000	0.046	0.035
R70	$+2.5N_{co}$	2.239	1.207	1.543
R73	$-L_p/10$	0.075	0.129	0.104
R74	$-5L_v$	0.072	0.111	0.139
R75	$\pm L_v/10$	0.018	0.041	0.058
R76	$+L_{A1}/10$	0.051	0.050	0.051
R77	$-L_{DLR}/4$	0.102	0.101	0.107
R78	$\pm 10L_u$	0.011	0.013	0.023
R79	$-5L_w$	0.0351	0.051	0.064
R80	$-L_q/4$	0.261	0.219	0.235
R81	$\pm 1.25L_{B1}$	0.066	0.011	0.036
R82	$-2.5L_{co}$	1.016	0.601	0.844

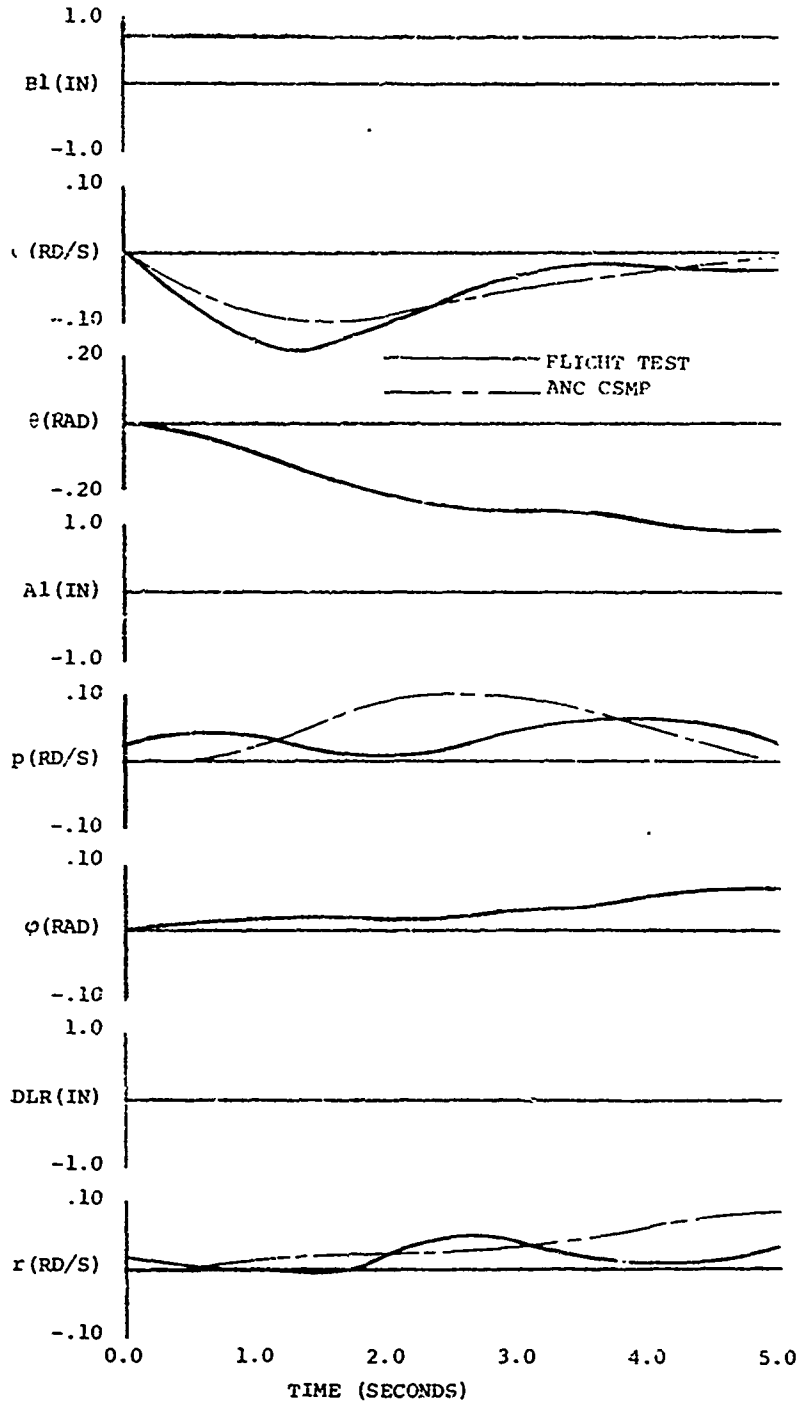

Figure 15. Flight Test vs. CSMP Simulation (60 Knots at 3000 Feet, Pitch Step Response).

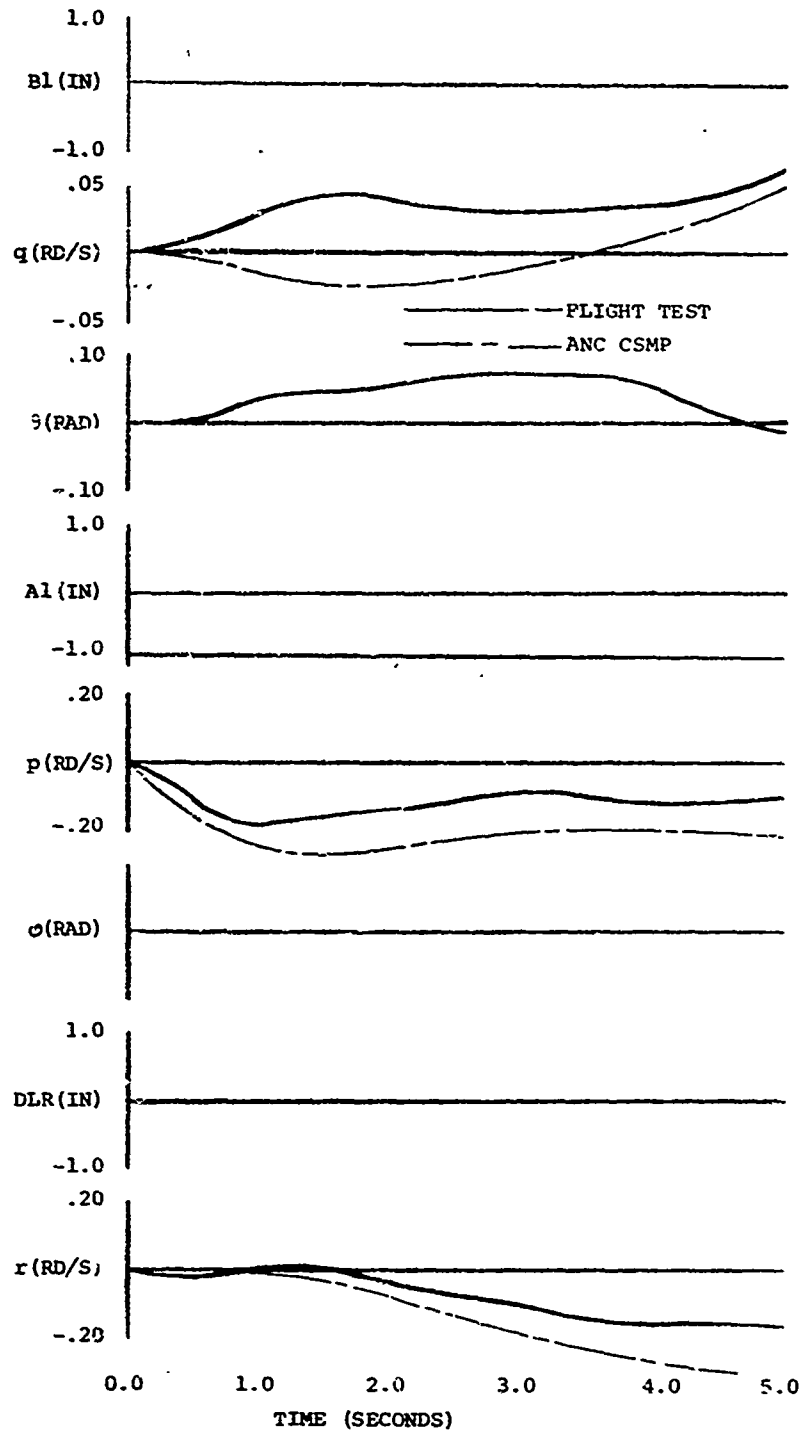

Figure 16. Flight Test vs. CSMP Simulation (60 Knots at 3000 Feet, Roll Step Response).

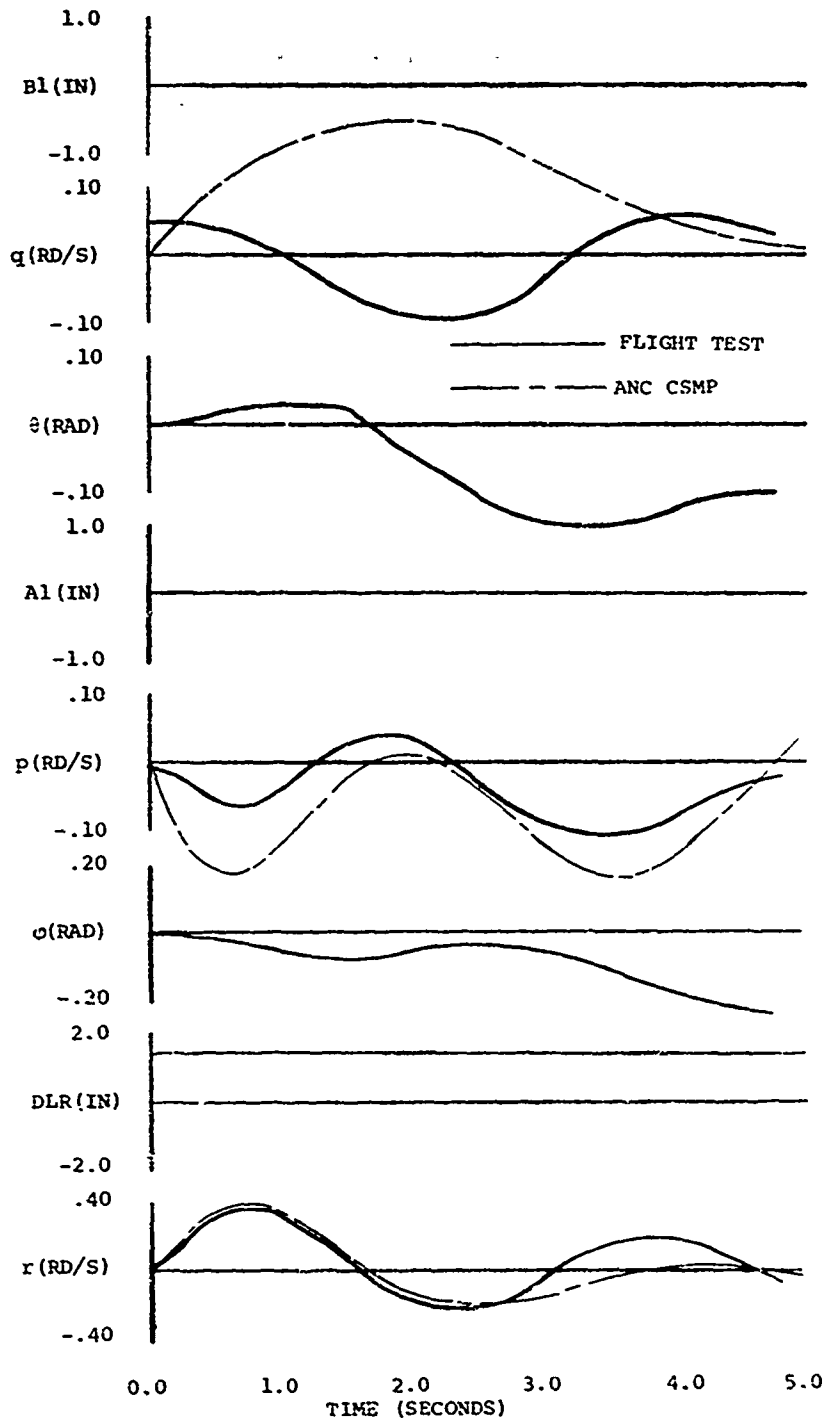

Figure 17. Flight Test vs. CSMP Simulation (60 Knots at 3000 Feet, Yaw Step Response).

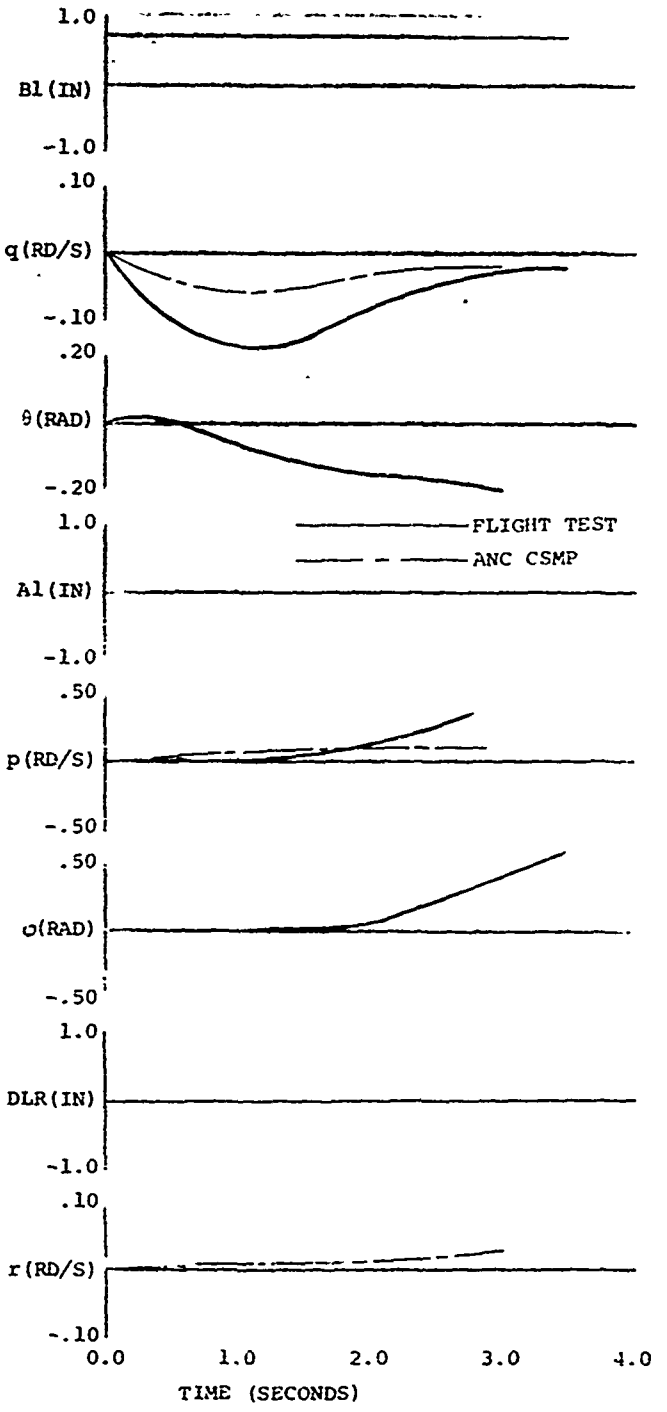

Figure 18. Flight Test vs. CSMP Simulation (110 Knots at 3000 Feet, Pitch Step Response).

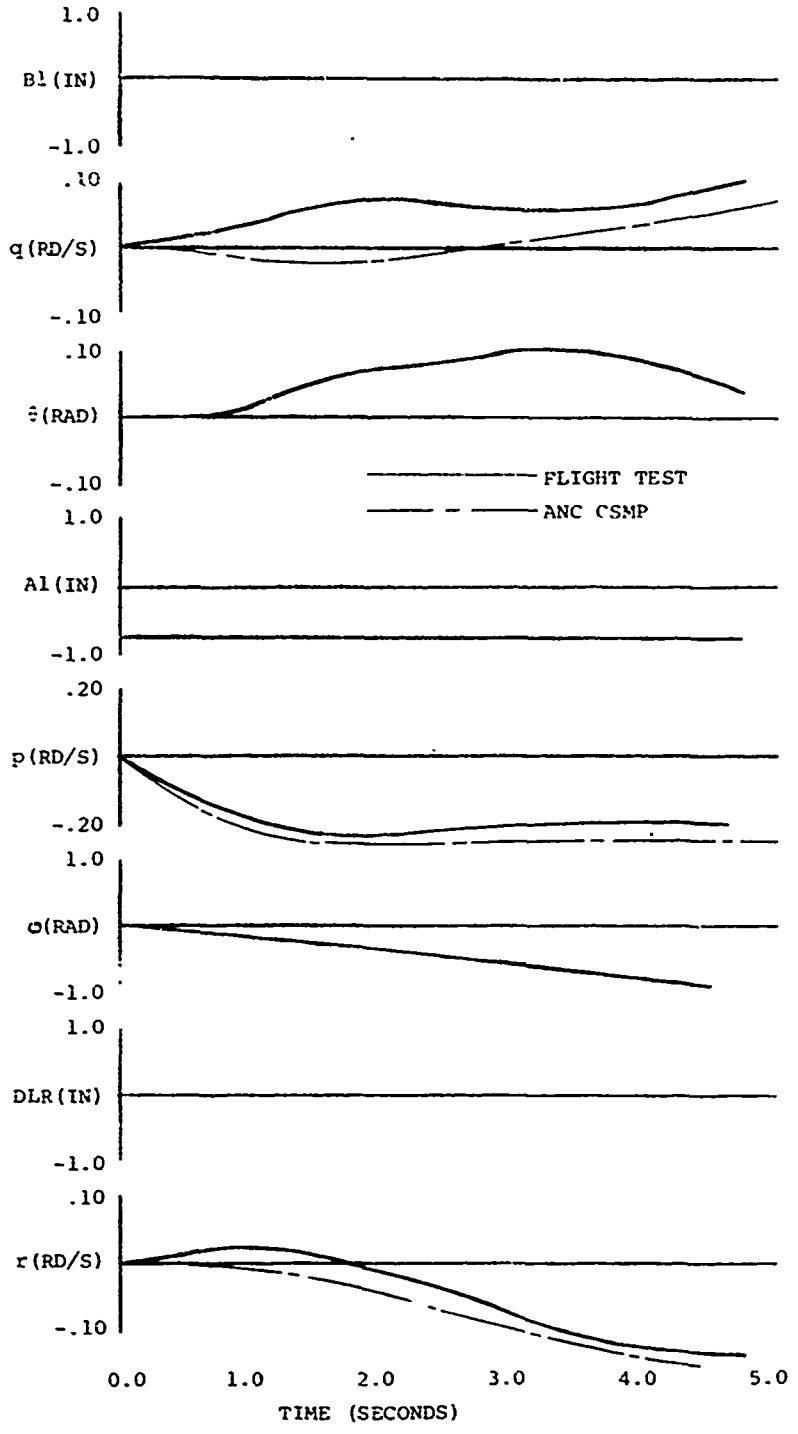

Figure 19. Flight Test vs. CSMP Simulation (110 Knots at 3000 Feet, Roll Step Response).

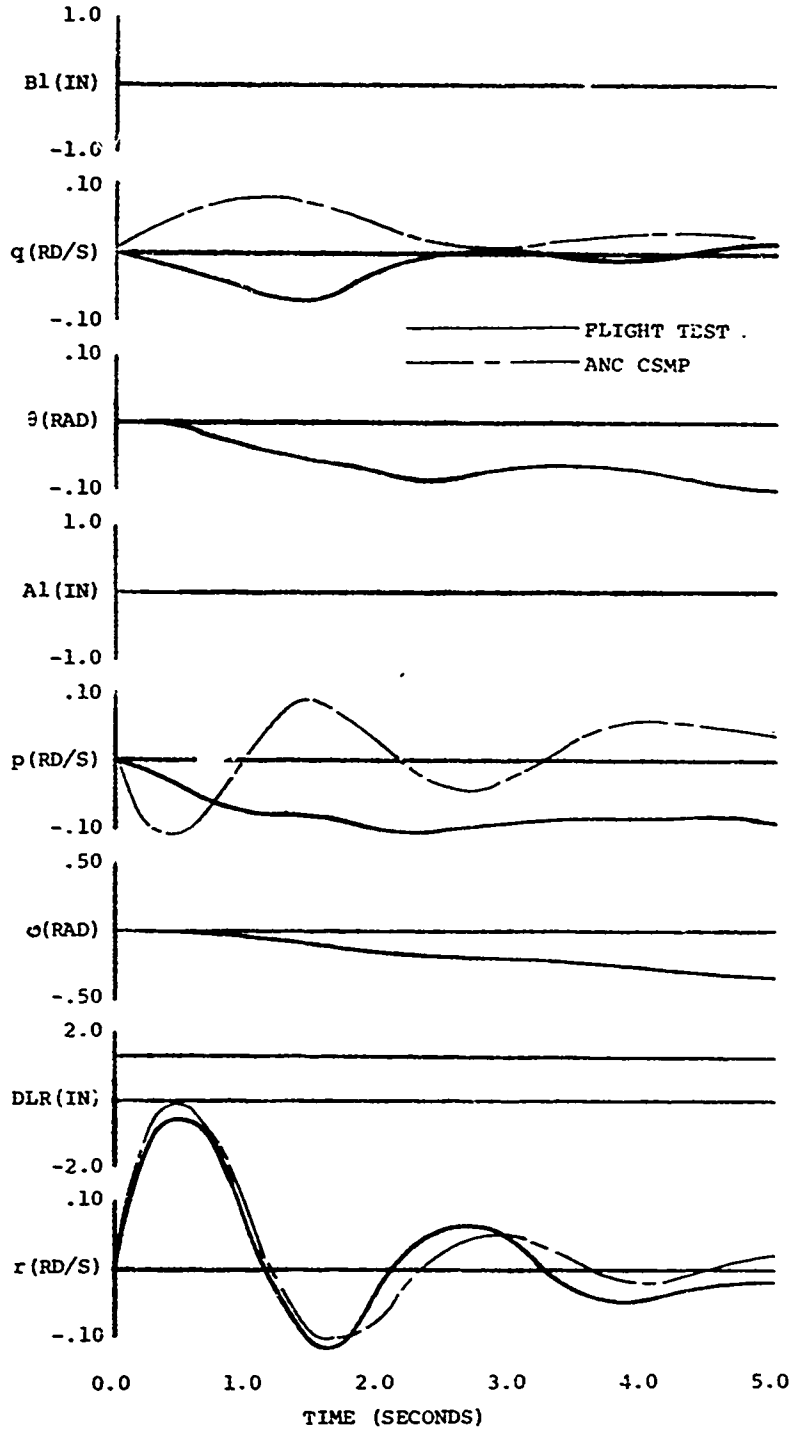

Figure 20. Flight Test vs. CSMP Simulation (110 Knots at 3000 Feet, Yaw Step Response).

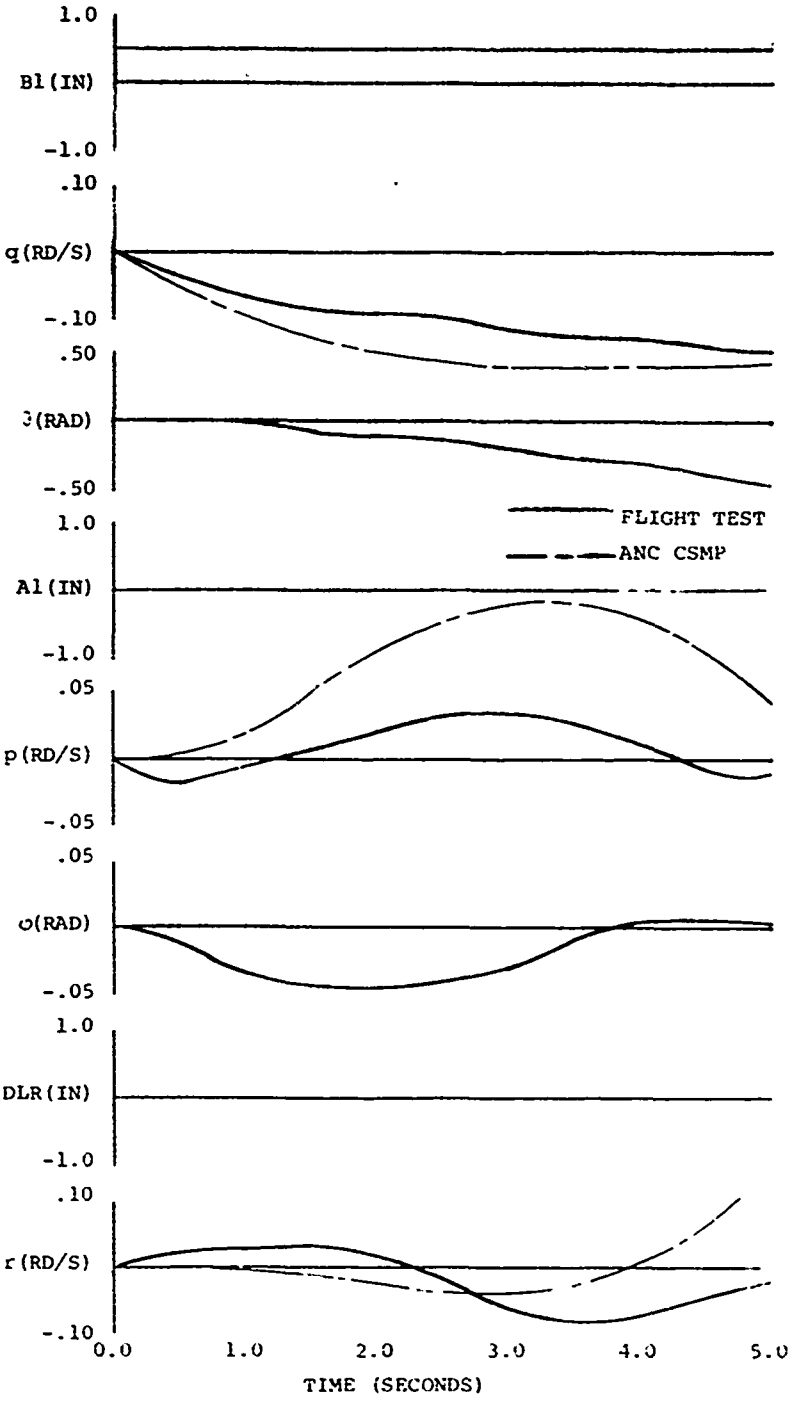

Figure 21. Flight Test vs. CSMP Simulation (Hover at 3000 Feet, Pitch Step Response).

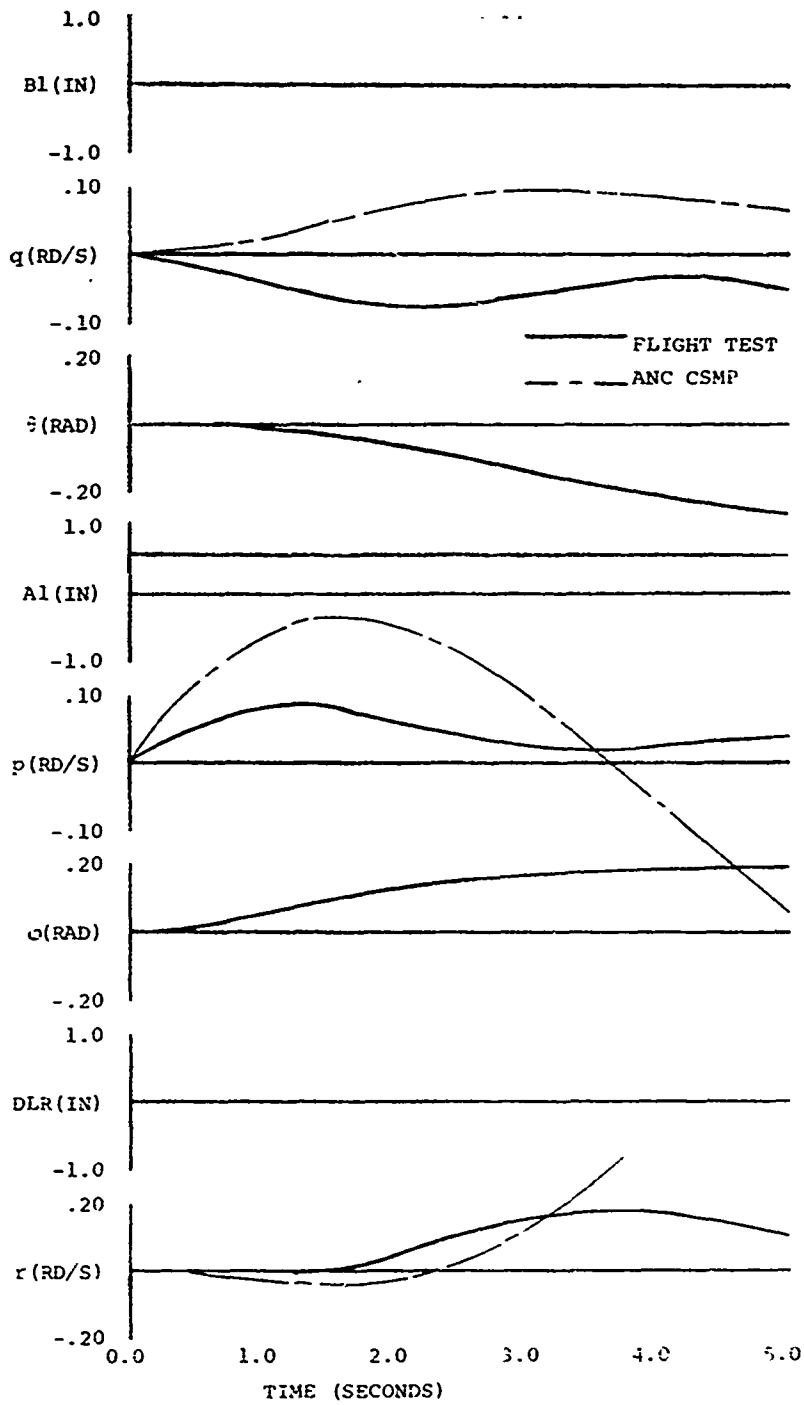

Figure 22. Flight Test vs. CSMP Simulation (Hover at 3000 Feet, Roll Step Response).

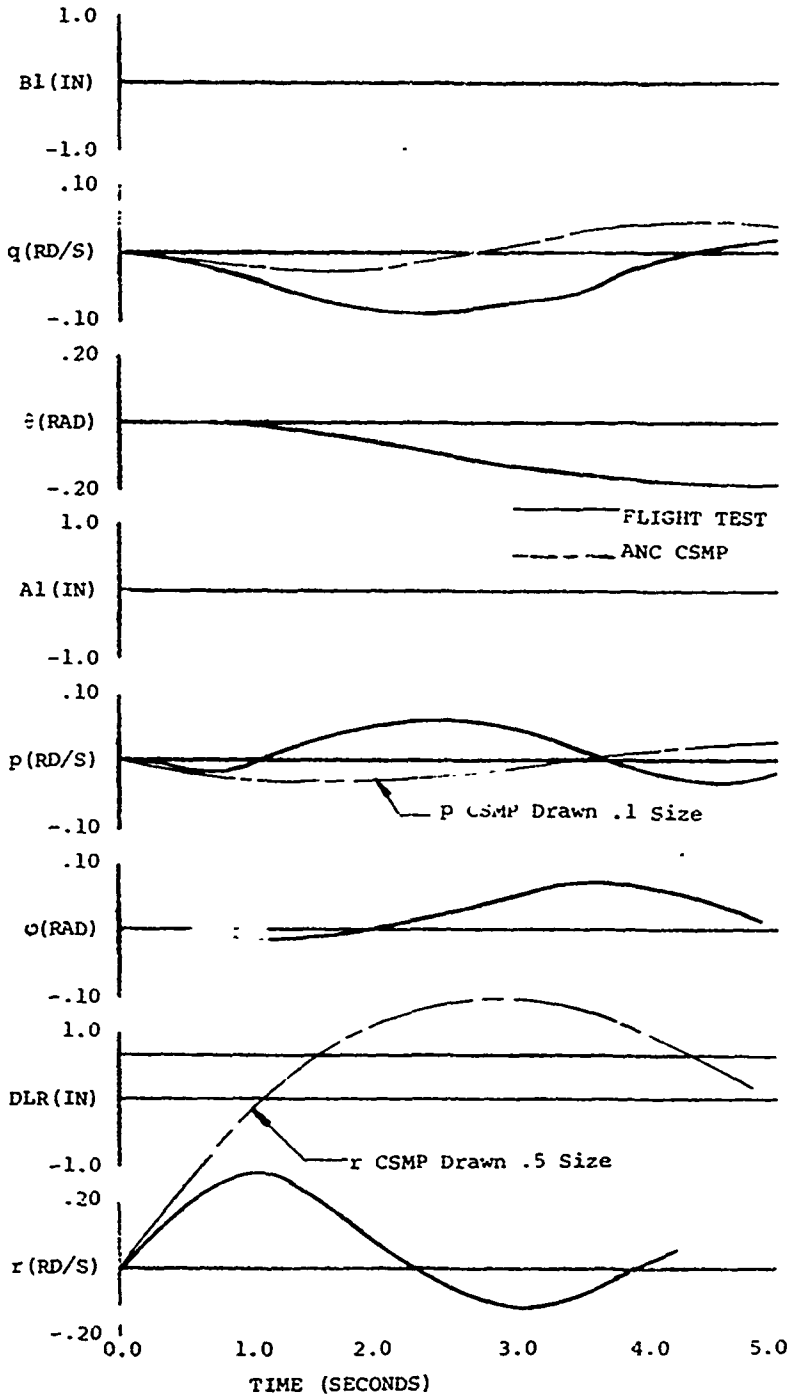

Figure 23. Flight Test vs. CSMP Simulation (Hover at 3000 Feet, Yaw Step Response).

ROOT LOCI

Tables IX and X are matrices for the longitudinal and lateral three-degree-of-freedom (3-DOF) root locus equations of motion. Table XI is the matrix for the 6-DOF root locus. Figures 24 through 42 show the 3-DOF root loci as the individual stability derivatives were varied between 0.1 and 8 times their "nominal" gain. The effects of 6-DOF longitudinal and lateral parameter variations are shown in Figure 43. The root loci were used to check the effects of potentiometer changing for the analog and to assess what parameters might be changed to obtain flight test response frequencies and damping ratios.

TABLE IX. LONGITUDINAL 3-DOF ROOT LOCUS MATRIX

	u(ft/sec) 1	w(ft/sec) 2	θ (rad 3	4	B1(RAD) 5	CO(RAD) 6	7	8	9	10	11	12
1	$-X_u+S$	$-X_w$	$g-X_qS$		$-X_{B1}$	$-X_{CO}$						
2	$-Z_u$	$-Z_w+S$	$g \sin \varphi_o - (U_o+Z_q)S$		$-Z_{B1}$	$-Z_{CO}$						
3	$-M_u$	$-M_w-M_{\dot{w}}S$	$-M_qS+S^2$		$-M_{B1}$	$-M_{CO}$						
4				+1								
5					+1							
6						+1						
7												
8												
9												
10												
11												
12												

TABLE X. LATERAL 3-DOF ROOT LOCUS MATRIX

	v(ft/sec) 1	φ(rad) 2	r(rad/sec) 3	4	Al(RAD) 5	DLR(RAD) 6	7	8	9	10	11	12
1	$-Y_v+S$	$-g-Y_pS$	$-(-U_o+Y_r)$		$-Y_{Al}$	$-Y_{DLR}$						
2	$-L_v$	$-L_pS+S^2$	$-L_r$		$-L_{Al}$	$-L_{DLR}$						
3	$-N_v$	$-N_pS$	$-N_r+S$		$-N_{Al}$	$-N_{DLR}$						
4				+1								
5					+1							
6						+1						
7												
8												
9												
10												
11												
12												

TABLE XI. 6-DOF ROOT LOCUS MATRIX

	u(ft/sec) 1	w(ft/sec) 2	θ(rad) 3	4	B1(RAD) 5	CO(RAD) 6	v(ft/sec) 7	φ(rad) 8	r(rad/sec) 9	10	A1(RAD) 11	DLR(RAD) 12
1	$-X_u+S$	$-X_w$	$g-X_qS$		$-X_{B1}$	$-X_{CO}$	$-X_v$	$-X_pS$	$-X_r$		$-X_{A1}$	$-X_{DLR}$
2	$-Z_u$	$-Z_w+S$	$g \sin \theta_o - (U_o+Z_q)S$		$-Z_{B1}$	$-Z_{CO}$	$-Z_v$	$-Z_pS$	$-Z_r$		$-Z_{A1}$	$-Z_{DLR}$
3	$-M_u$	$-M_w-M_{\dot{w}}S$	$-M_wS+S^2$		$-M_{B1}$	$-M_{CO}$	$-M_v$	$-M_pS$	$-M_r$		$-M_{A1}$	$-M_{DLR}$
4				+1								
5					+1							
6						+1						
7	$-Y_u$	$-Y_w$	$-Y_qS$		$-Y_{B1}$	$-Y_{CO}$	$-Y_v+S$	$-g-Y_pS$	U_o-Y_r		$-Y_{A1}$	$-Y_{DLR}$
8	$-L_u$	$-L_w$	$-L_qS$		$-L_{B1}$	$-L_{CO}$	$-L_v$	$-L_pS+S^2$	$-L_r$		$-L_{A1}$	$-L_{DLR}$
9	$-N_u$	$-N_w$	$-N_qS$		$-N_{B1}$	$-N_{CO}$	$-N_v$	$-N_pS$	$-N_r+S$		$-N_{A1}$	$-N_{DLR}$
10										+1		
11											+1	
12												+1

M_w ROOT LOCUS LONG 1 (HOVER)

INSIGNIFICANT EFFECT WHEN GAIN VARIES FROM 0.1 TO 10 TIMES NOMINAL GAIN.

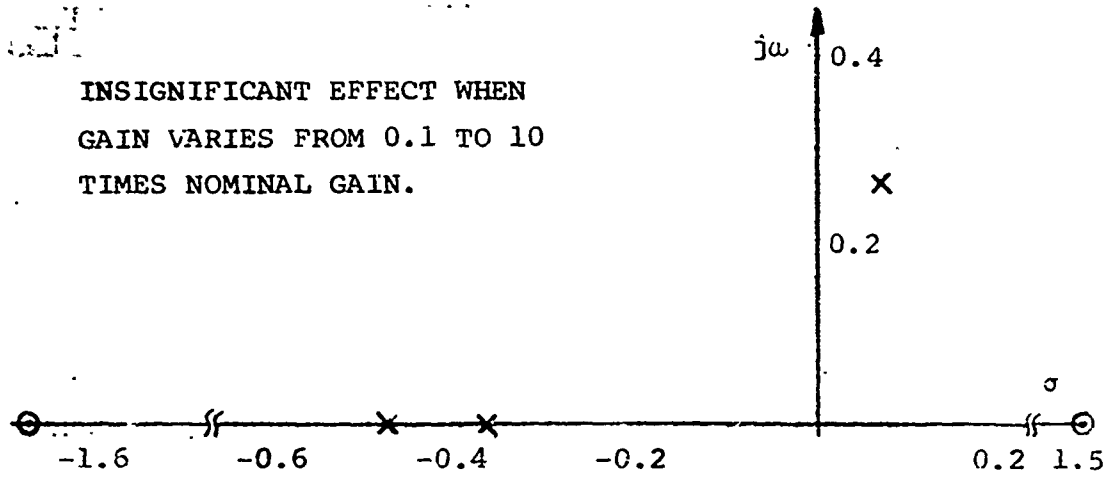

M_q ROOT LOCUS LONG 1 (HOVER)

0.1 → ~ 0.1 x Nominal Value
1.0 → ~ 1.0 x Nominal Value
8.0 → ~ 8.0 x Nominal Value

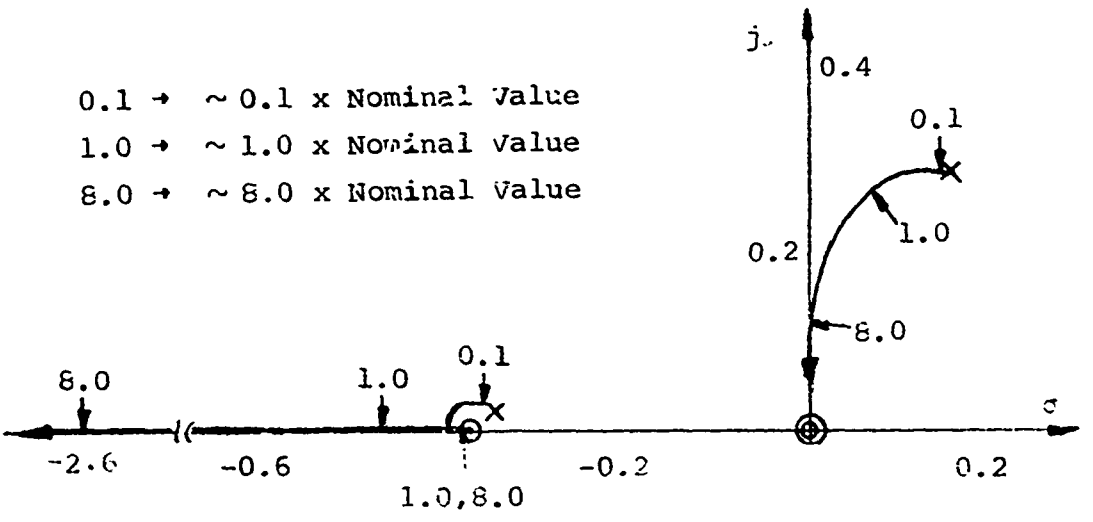

Figure 24. Hover Longitudinal M_w and M_q Root Loci.

M_u ROOT LOCUS LONG 1 (HOVER)

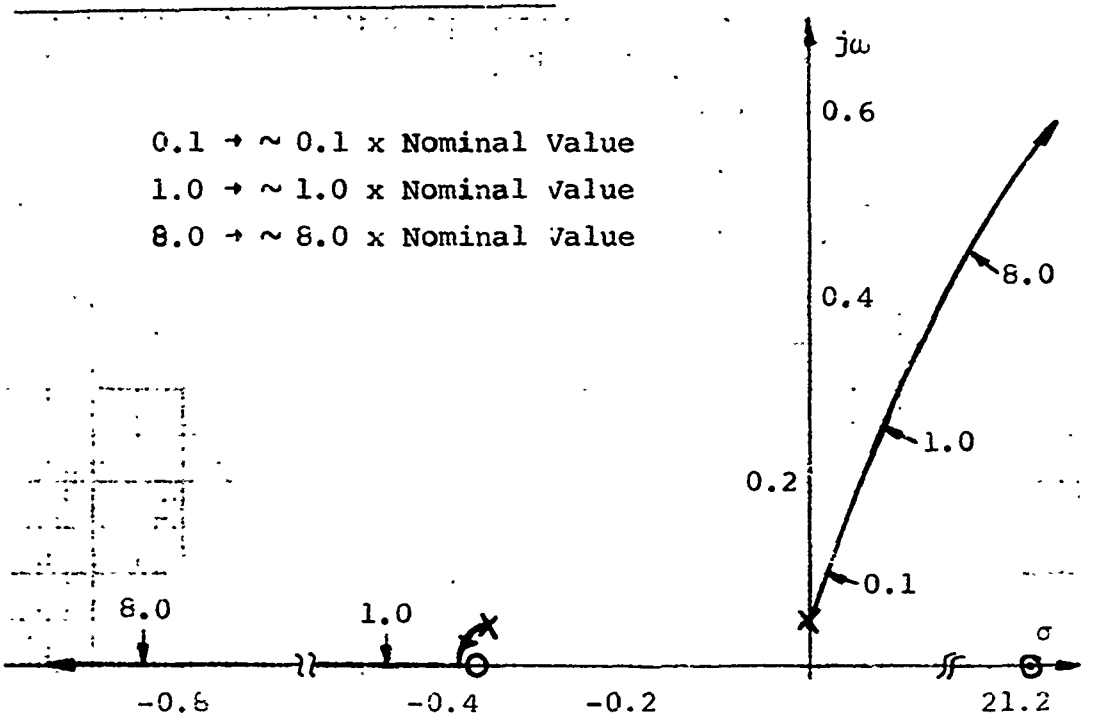

Z_w ROOT LOCUS LONG 1 (HOVER)

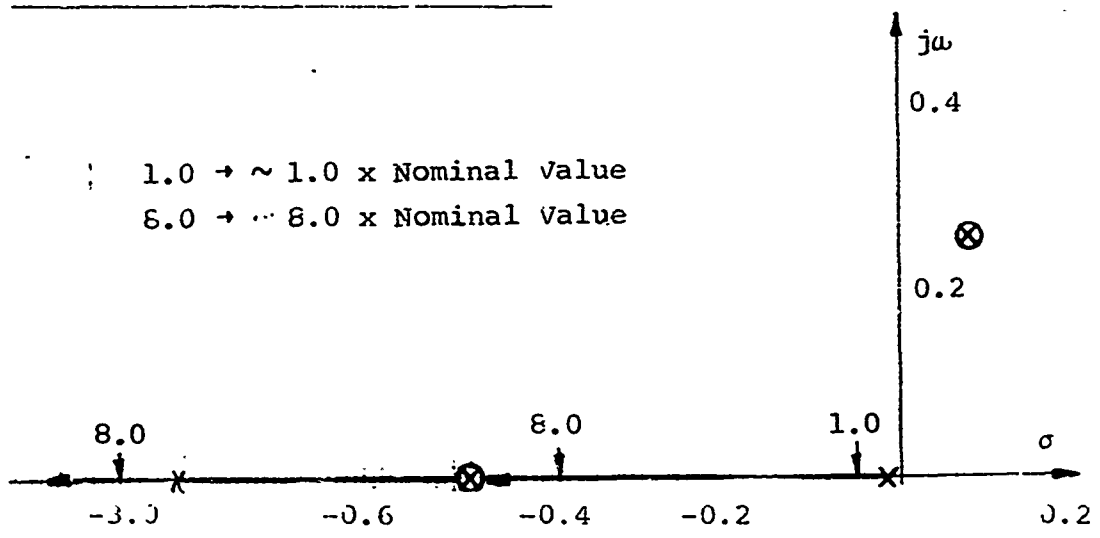

Figure 25. Hover Longitudinal M_u and Z_w Root Loci.

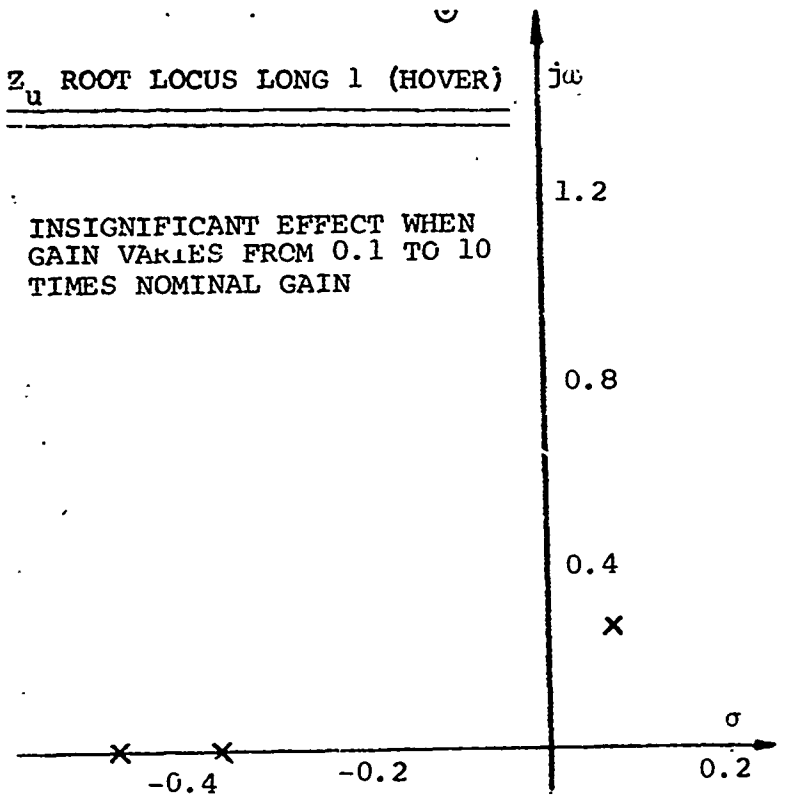

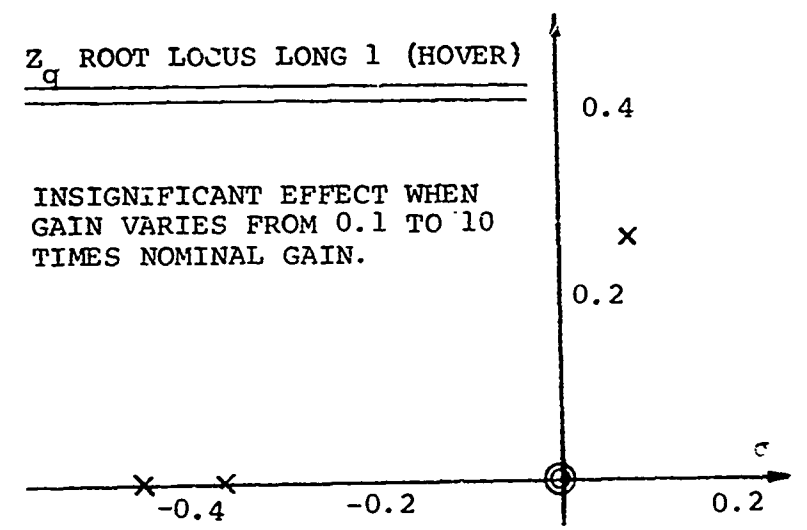

Figure 26. Hover Longitudinal Z_u and Z_q Root Loci.

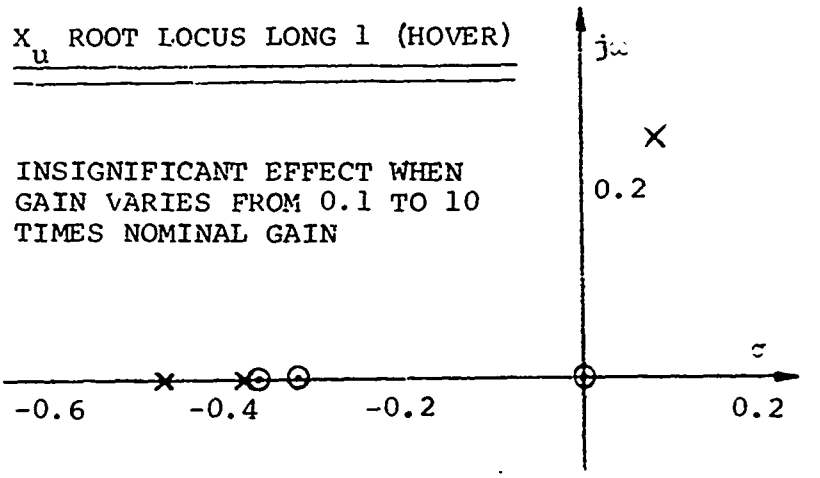

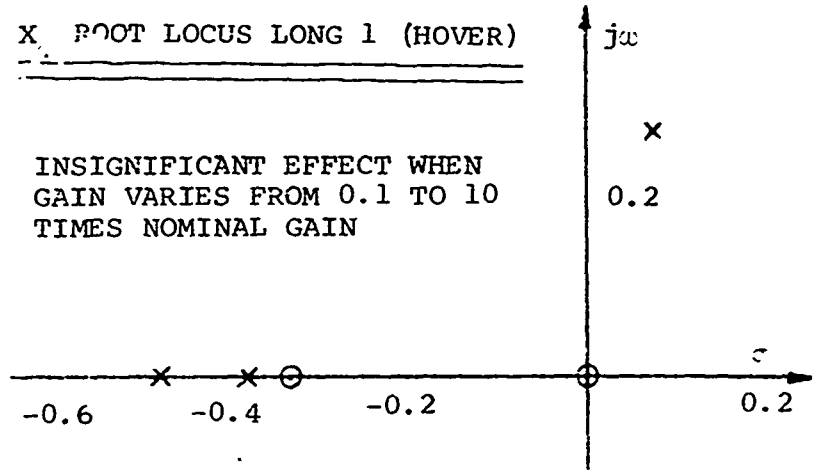

Figure 27. Hover Longitudinal X_u and X_w Root Loci.

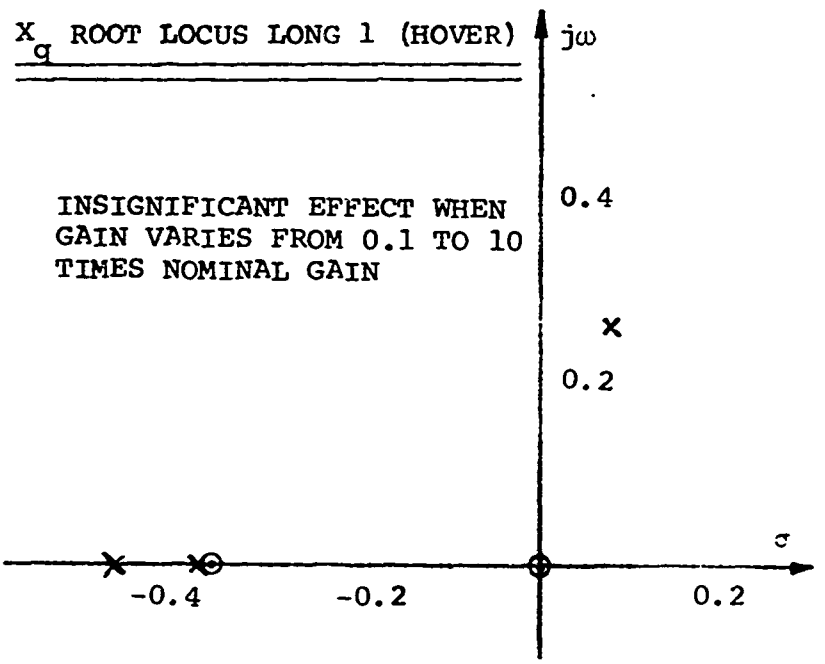

Figure 28. Hover Longitudinal X_q Root Locus.

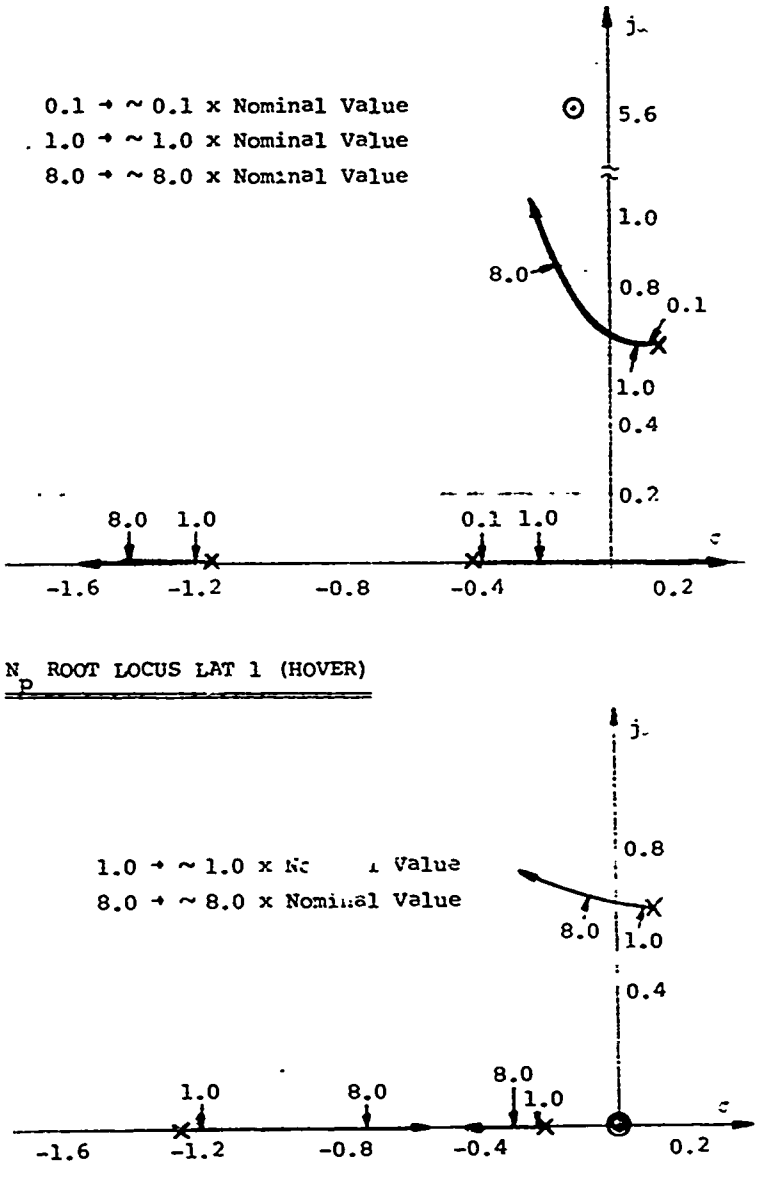

Figure 29. Hover Lateral N_v and N_p Root Loci.

N_r ROOT LOCUS LAT 1 (HOVER)

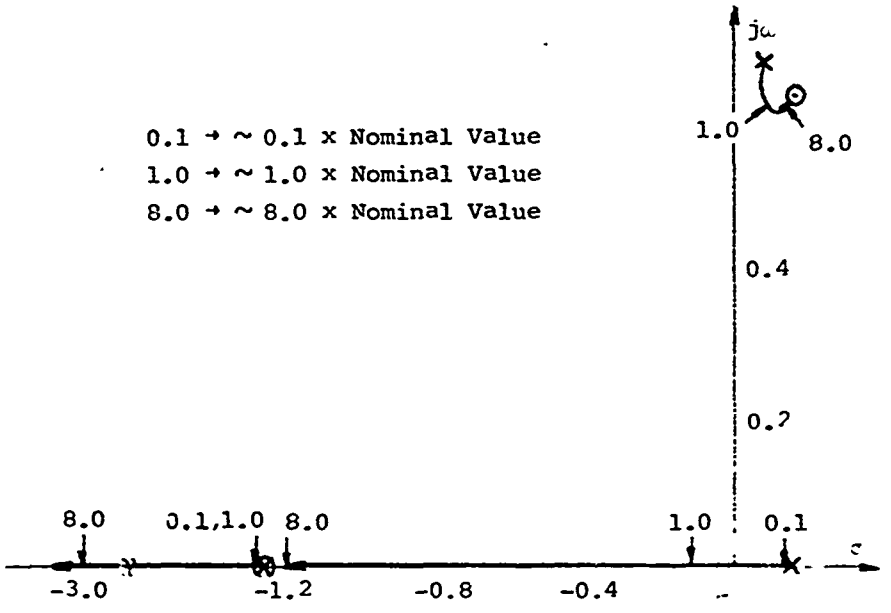

L_p ROOT LOCUS LAT 1 (HOVER)

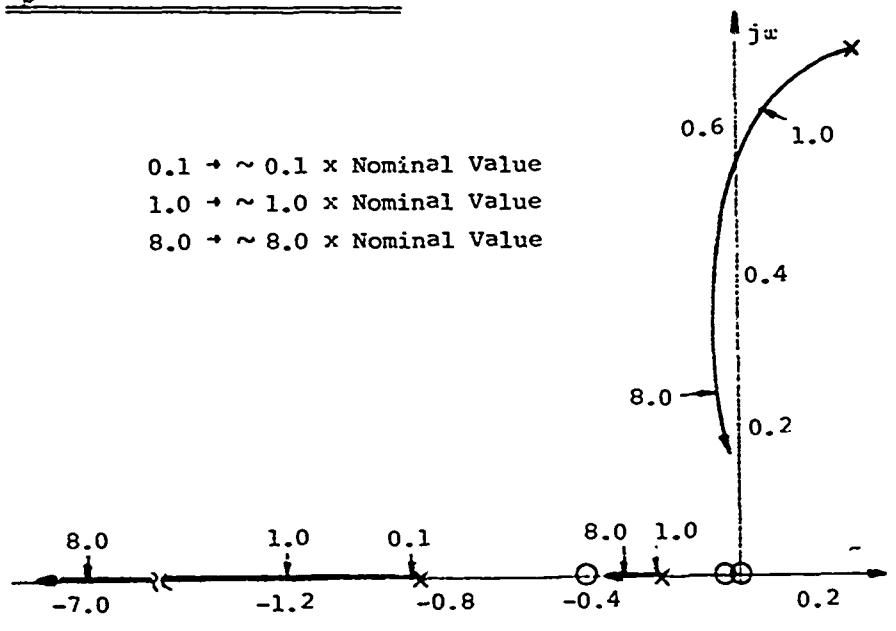

Figure 30. Hover Lateral N_r and L_p Root Loci.

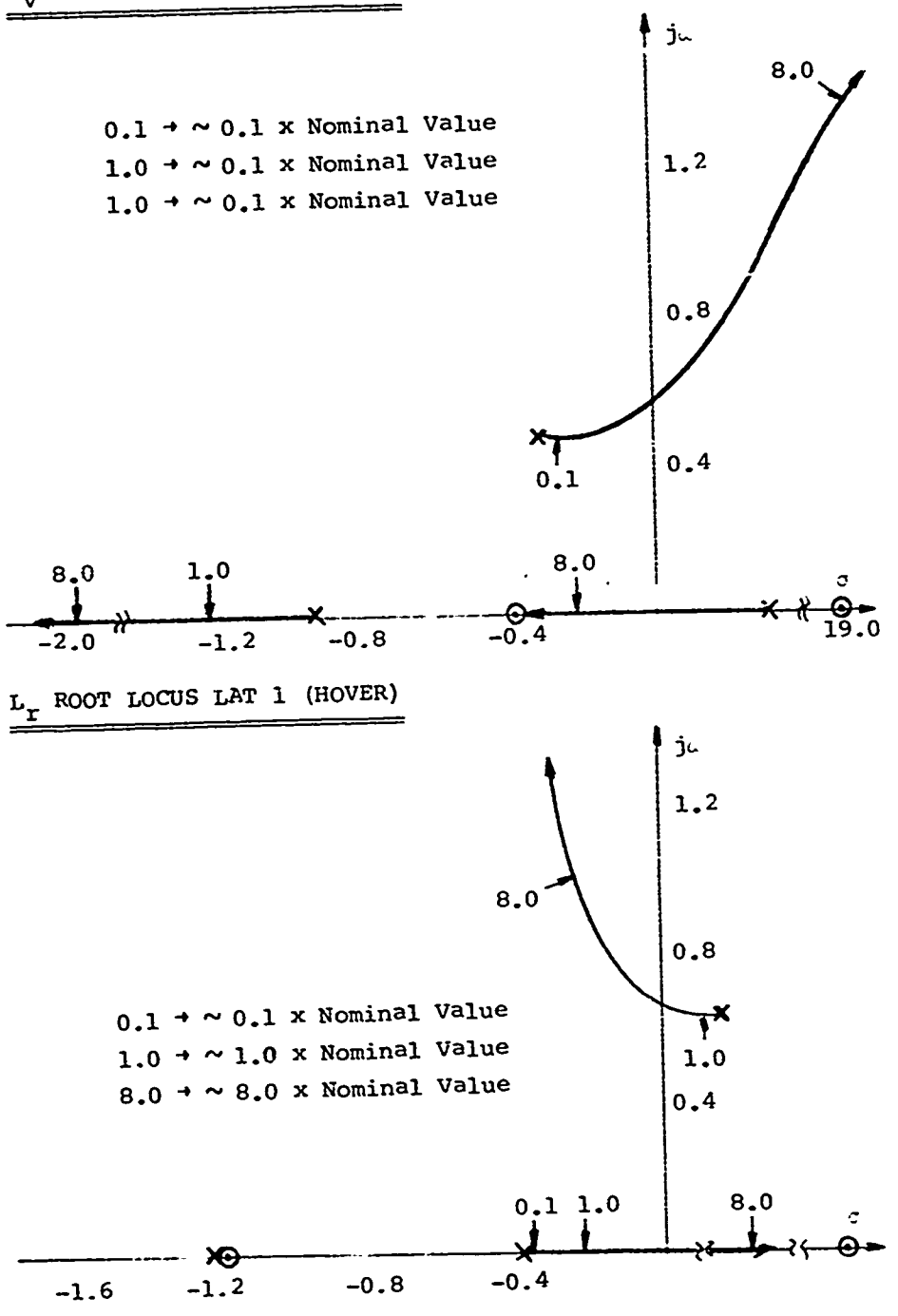

Figure 31. Hover Lateral L_v and L_r Root Loci.

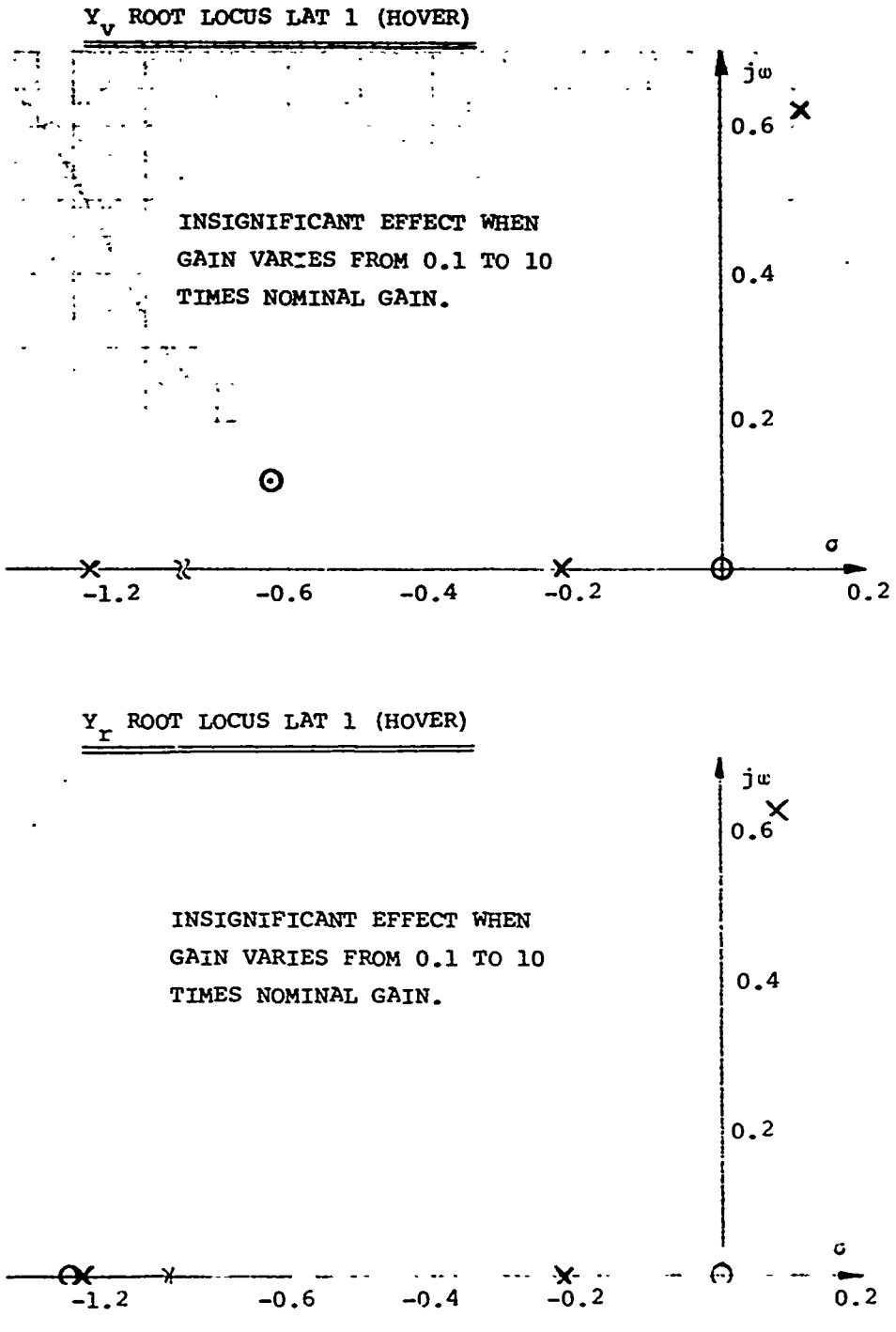

Figure 32. Hover Lateral Y_v and Y_r Root Loci.

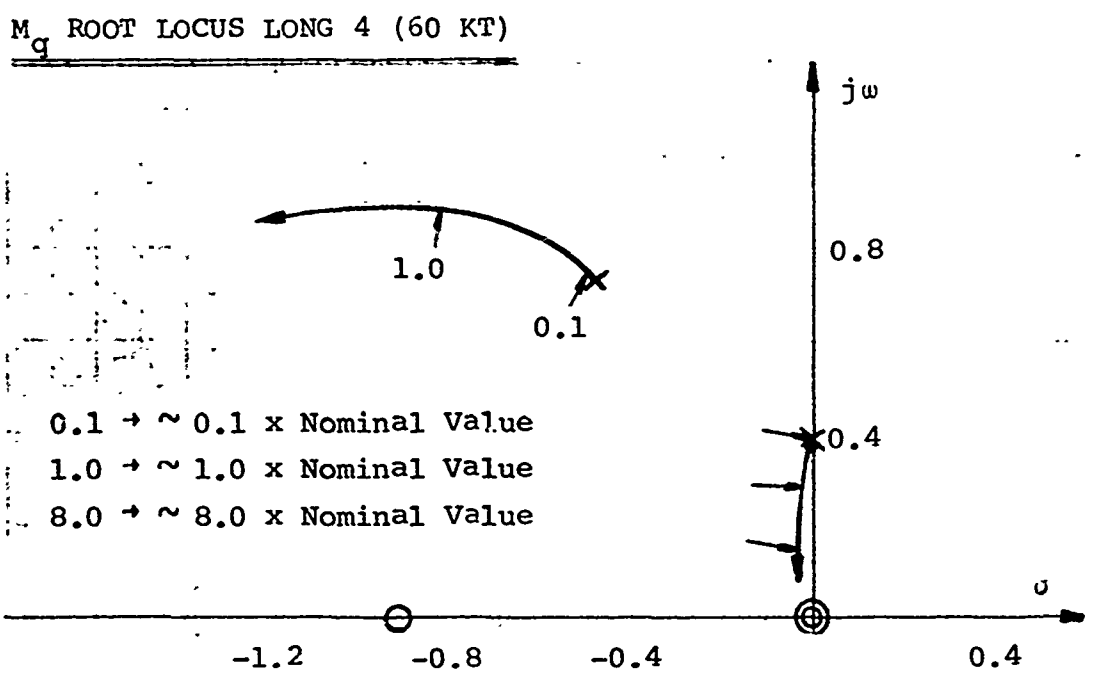

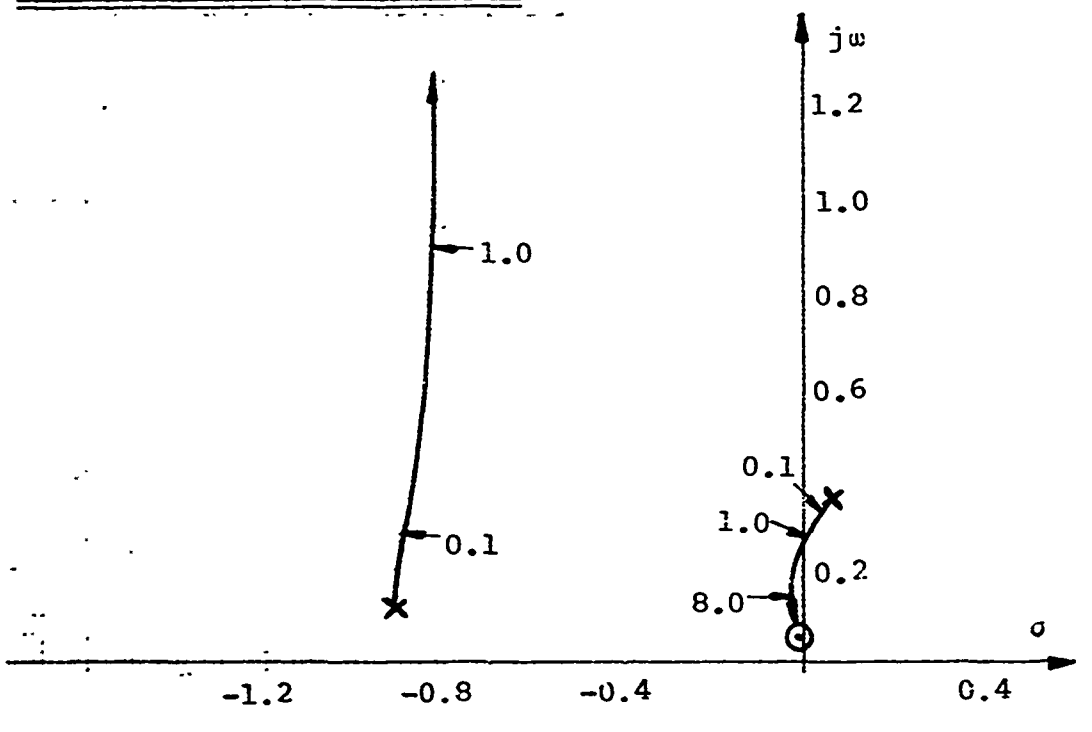

Figure 33. 60 Knots Longitudinal M_q and M_w Root Loci.

M_u ROOT LOCUS LONG 4 (60 KT)

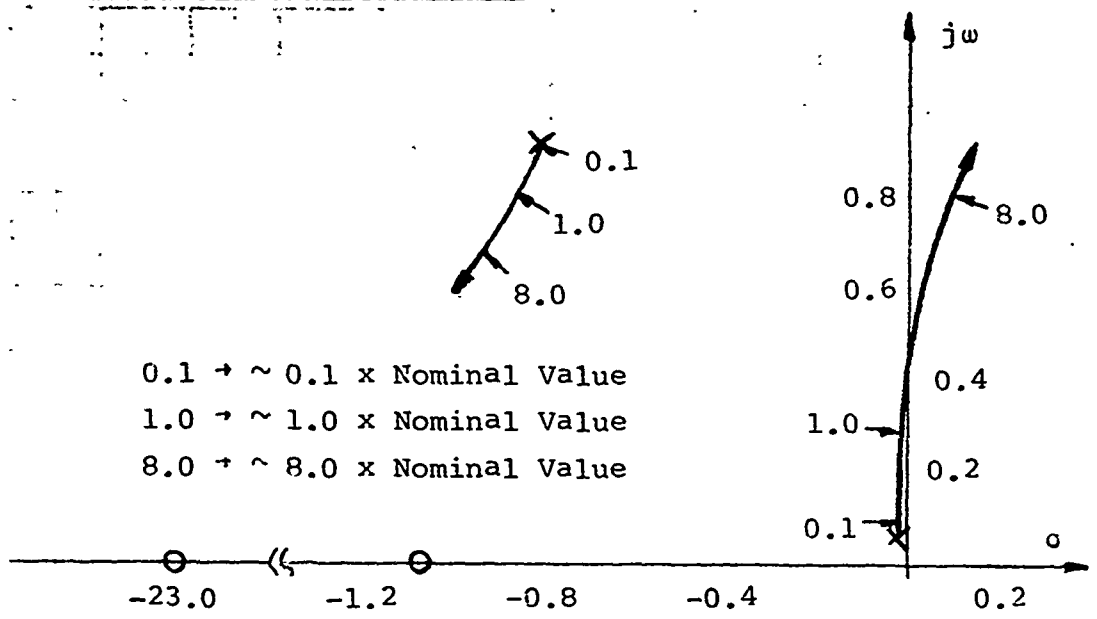

0.1 → ~ 0.1 x Nominal Value
1.0 → ~ 1.0 x Nominal Value
8.0 → ~ 8.0 x Nominal Value

Z_w ROOT LOCUS LONG 4 (60 KT)

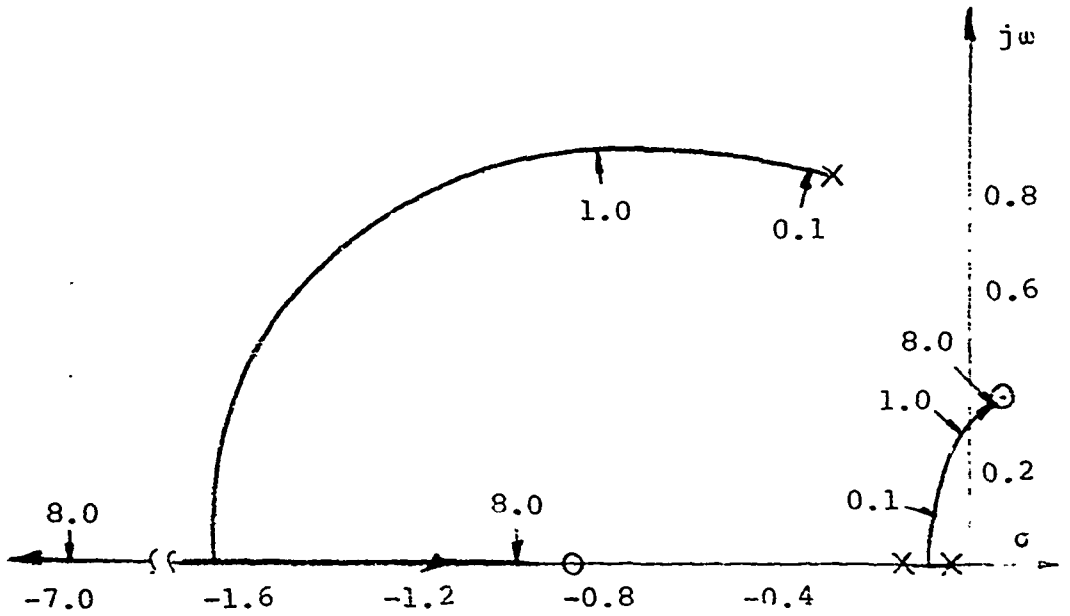

Figure 34. 60 Knots Longitudinal M_u and Z_w Root Loci.

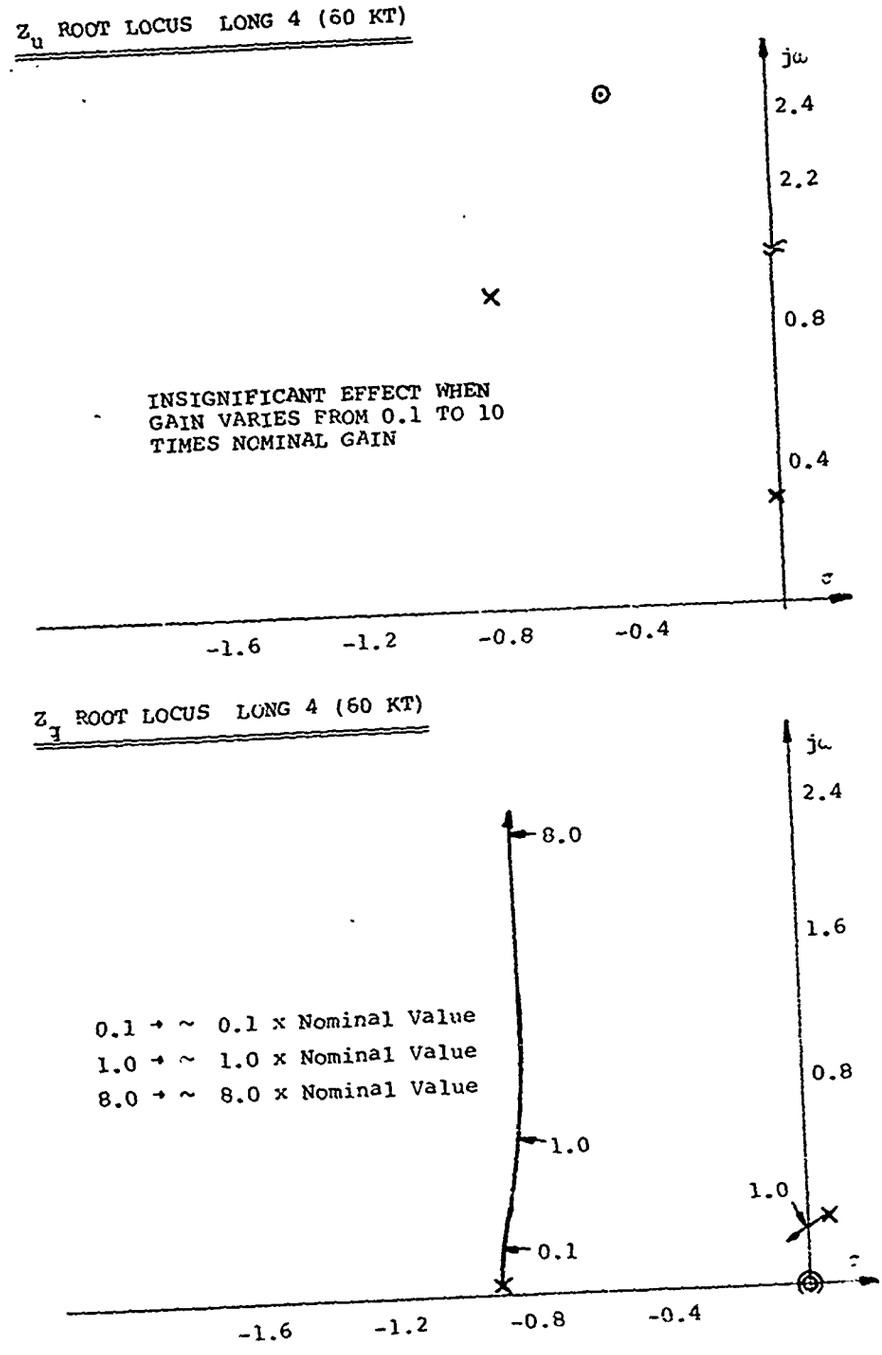

Figure 35. 60 Knots Longitudinal Z_u and Z_q Root Loci.

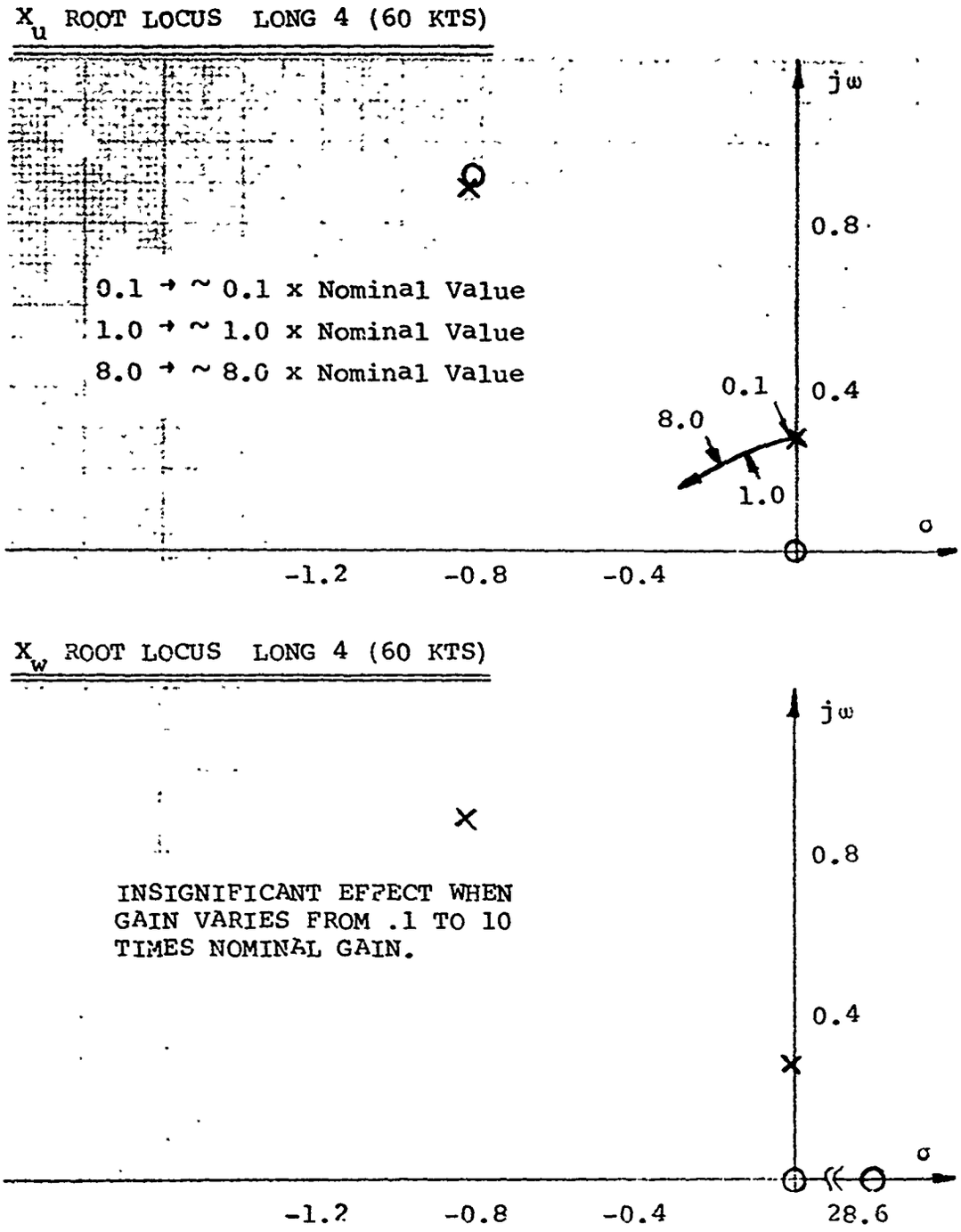

Figure 36. 60 Knots Longitudinal X_u and X_w Root Loci.

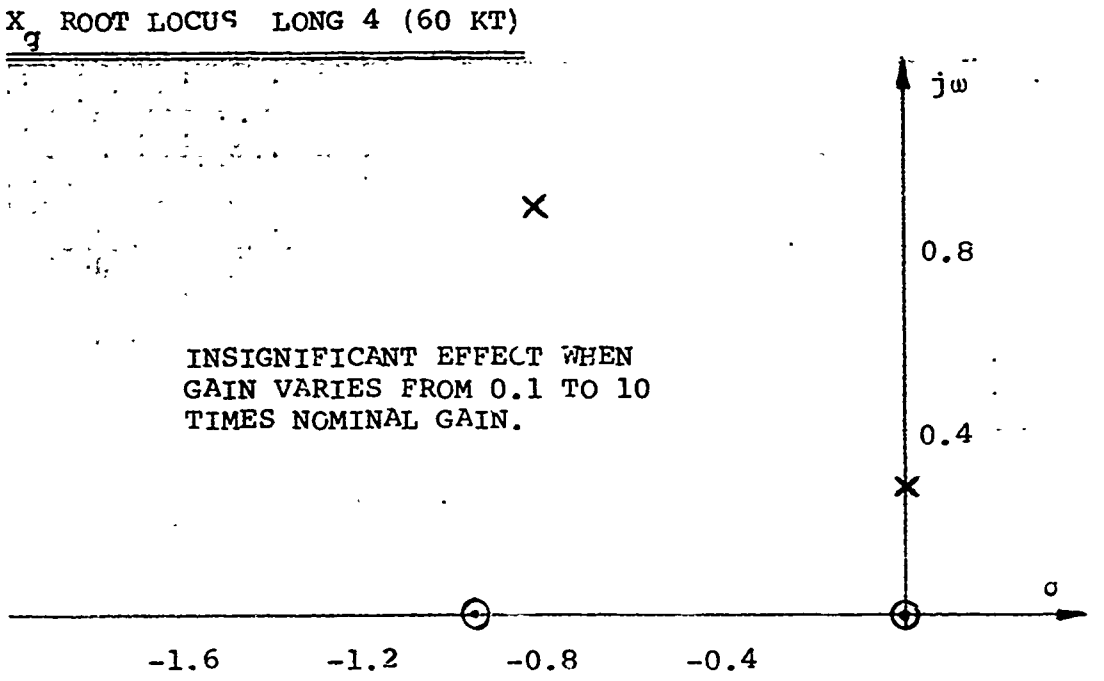

Figure 37. 60 Knots Longitudinal X_q Root Locus.

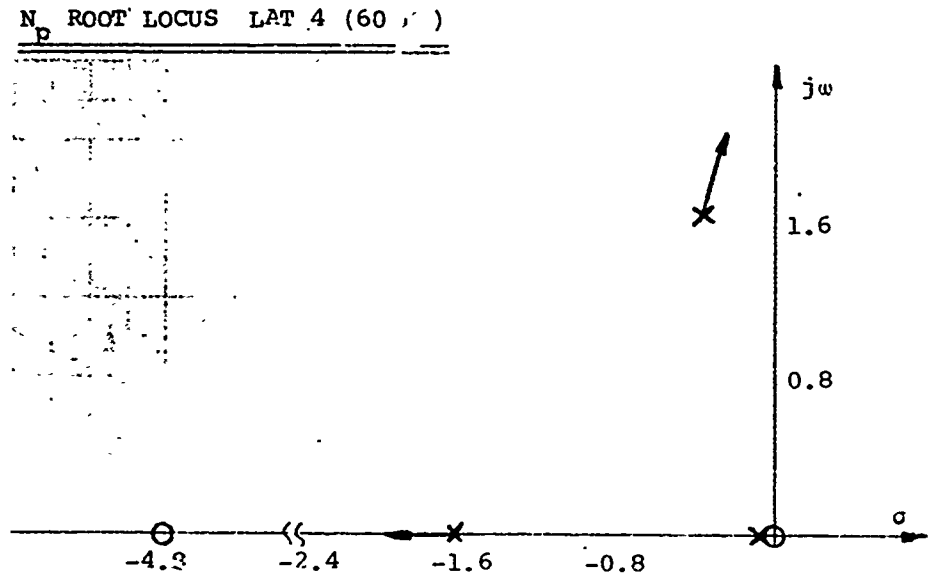

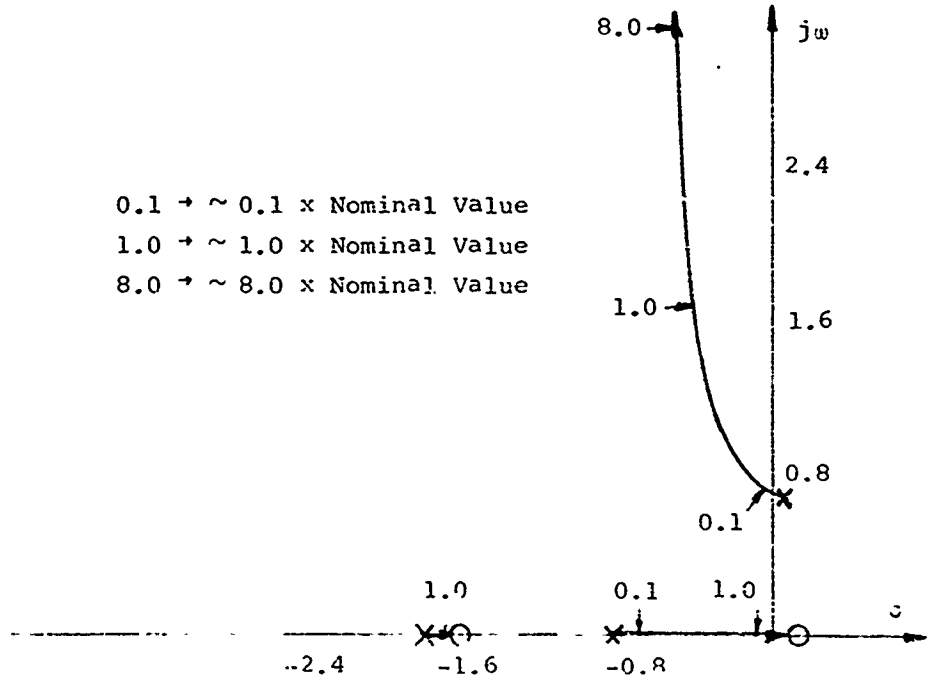

Figure 38. 60 Knots Lateral N_p and N_v Root Loci.

N_r ROOT LOCUS LAT 4 (60 KT)

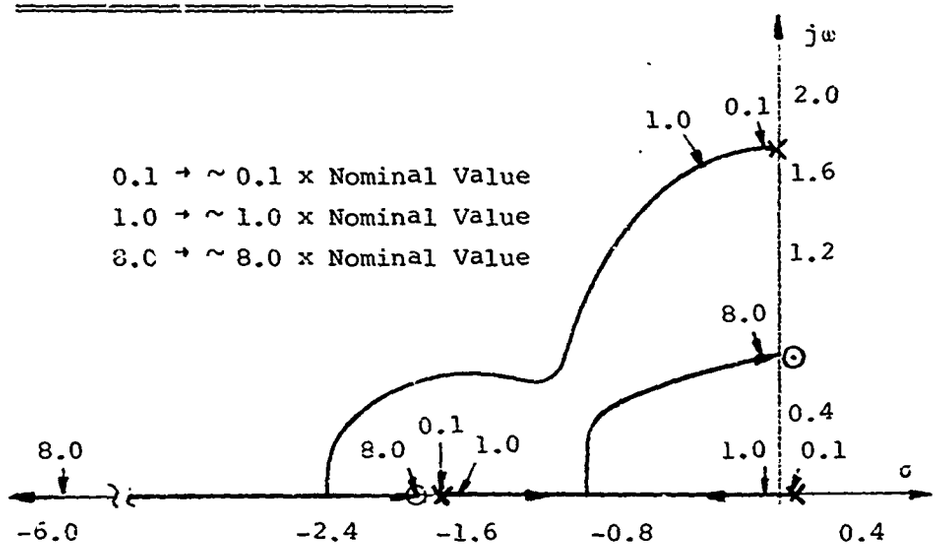

L_p ROOT LOCUS LAT 4 (60 KT)

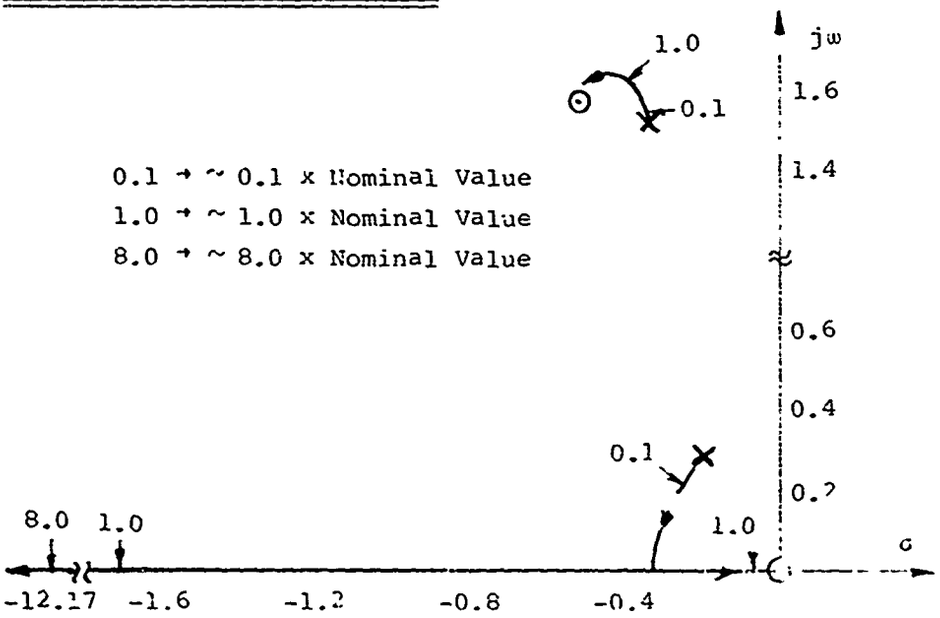

Figure 39. 60 Knots Lateral N_r and L_p Root Loci.

L_v ROOT LOCUS LAT 4 (60 KT)

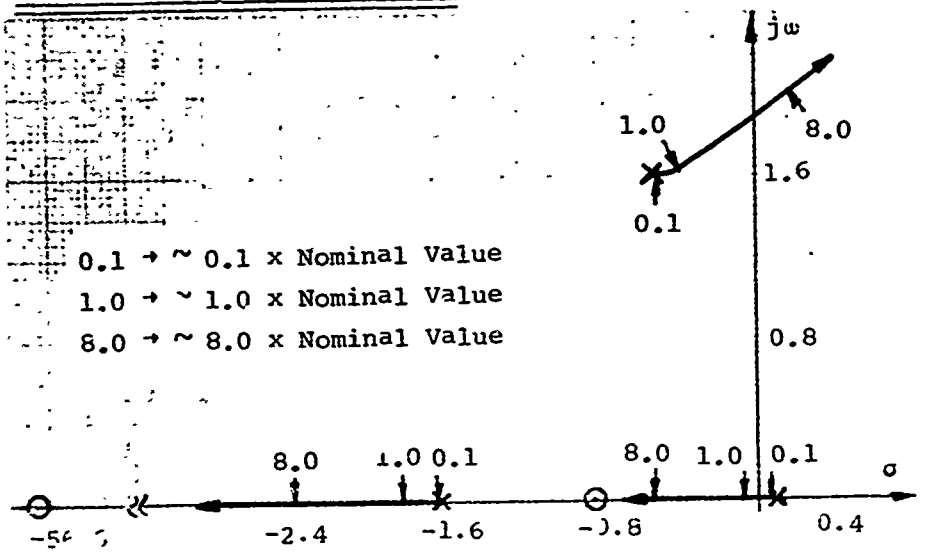

L_r ROOT LOCUS LAT 4 (60 KT)

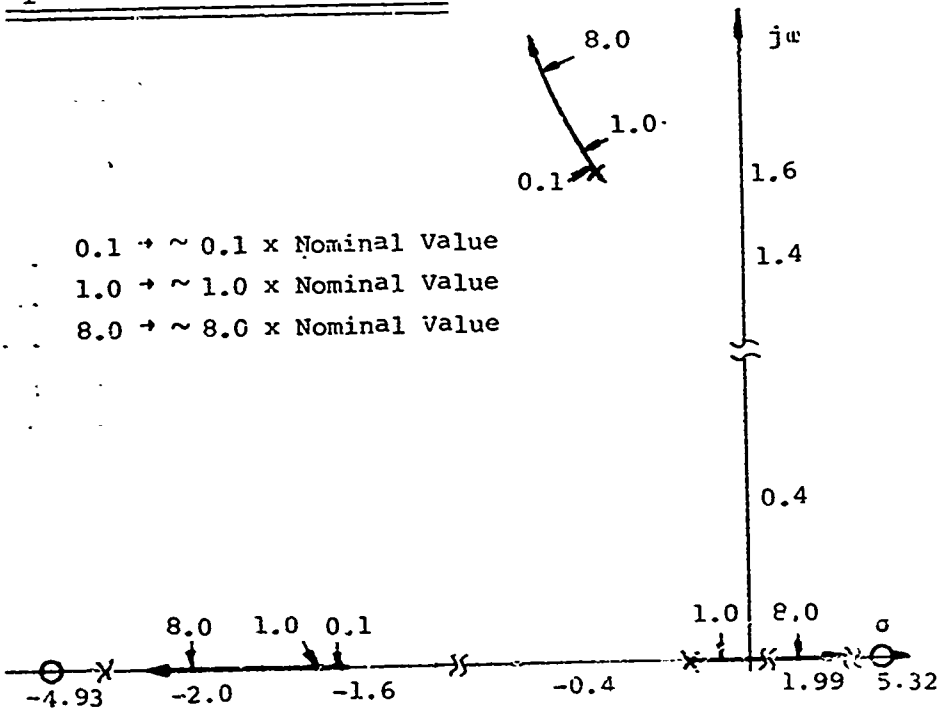

Figure 40. 60 Knots Lateral L_v and L_r Root Loci.

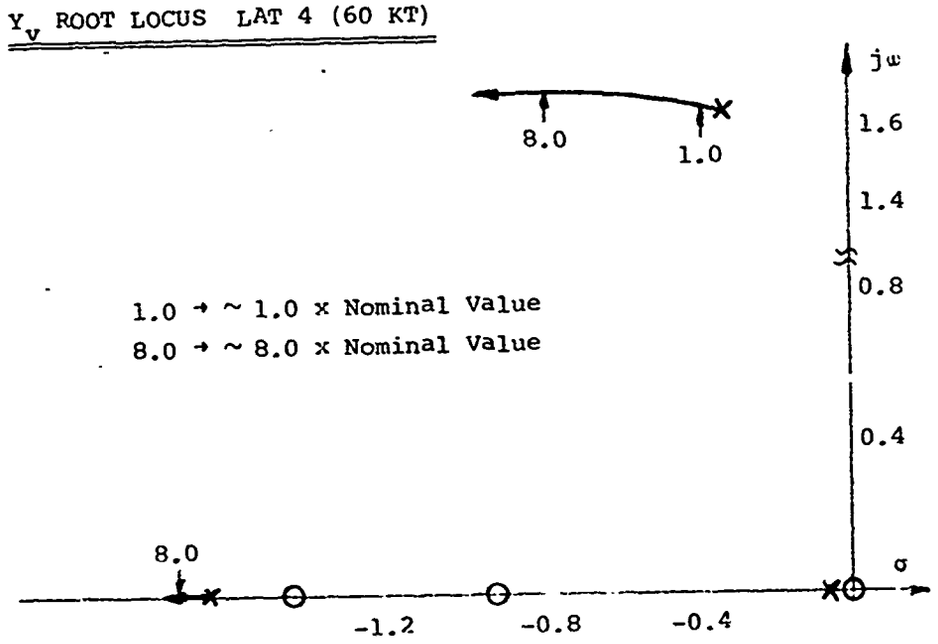

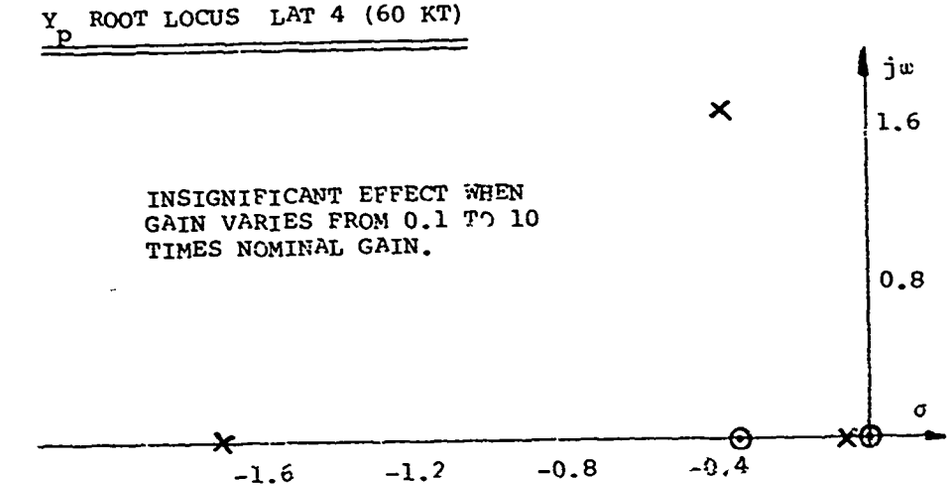

Figure 41. 60 Knots Lateral Y_v and Y_p Root Loci.

Y_r ROOT LOCUS LAT 4 (60 KT)

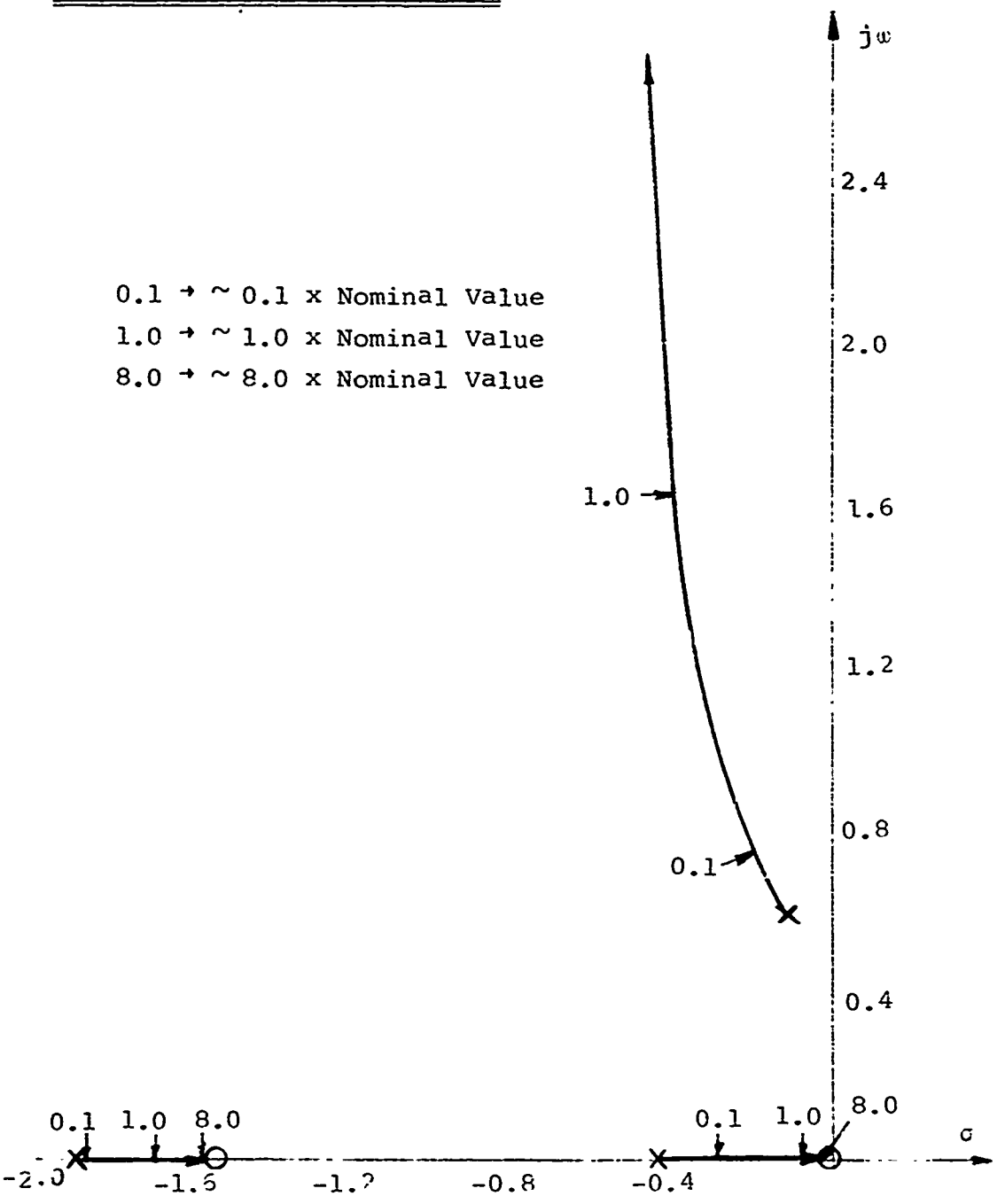

Figure 42. 60 Knots Lateral Y_r Root Locus.

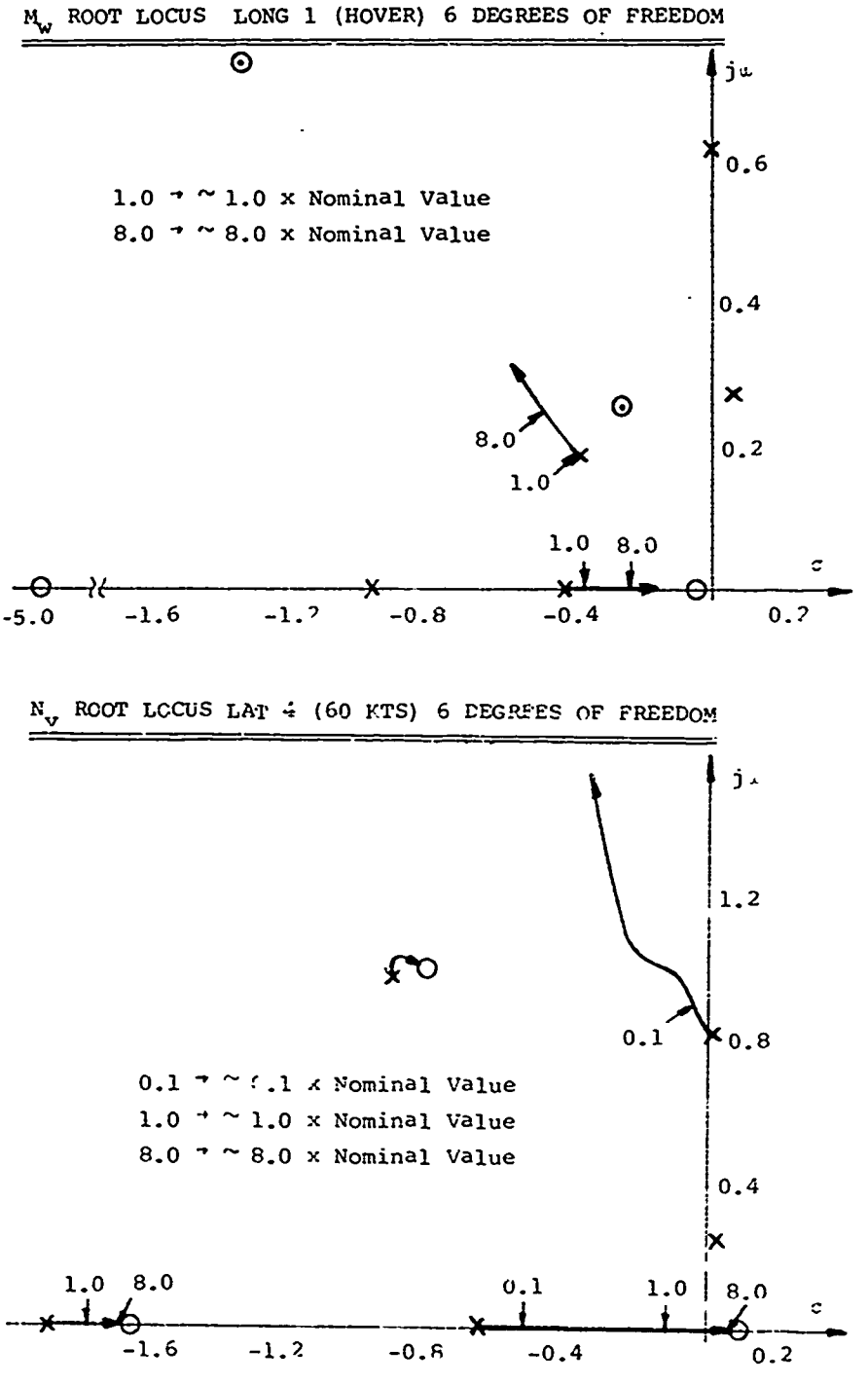

Figure 43. M_w Root Locus Hover 6 Degrees of Freedom and N_v Root Locus 60 Knots 6 Degrees of Freedom.

MODIFIED VEHICLE MODEL

MOSTAB-C derivatives were varied on the analog computer to obtain a closer match with flight test data. The technique used was to operate the analog in Rep-Op (i.e., switch between Compute and Reset) and ten times real time to have a response trace appear like it was stored (i.e., remain there) on a scope face. This stored display would then vary as a potentiometer (i.e., stability derivative) was varied. A translucent overlay representing a flight test response was placed in front of the scope so that an immediate comparison of the effect of changing a stability derivative was apparent. Figures 44 through 51 show some of the results of varying the "nominal" MOSTAB-C stability derivatives.

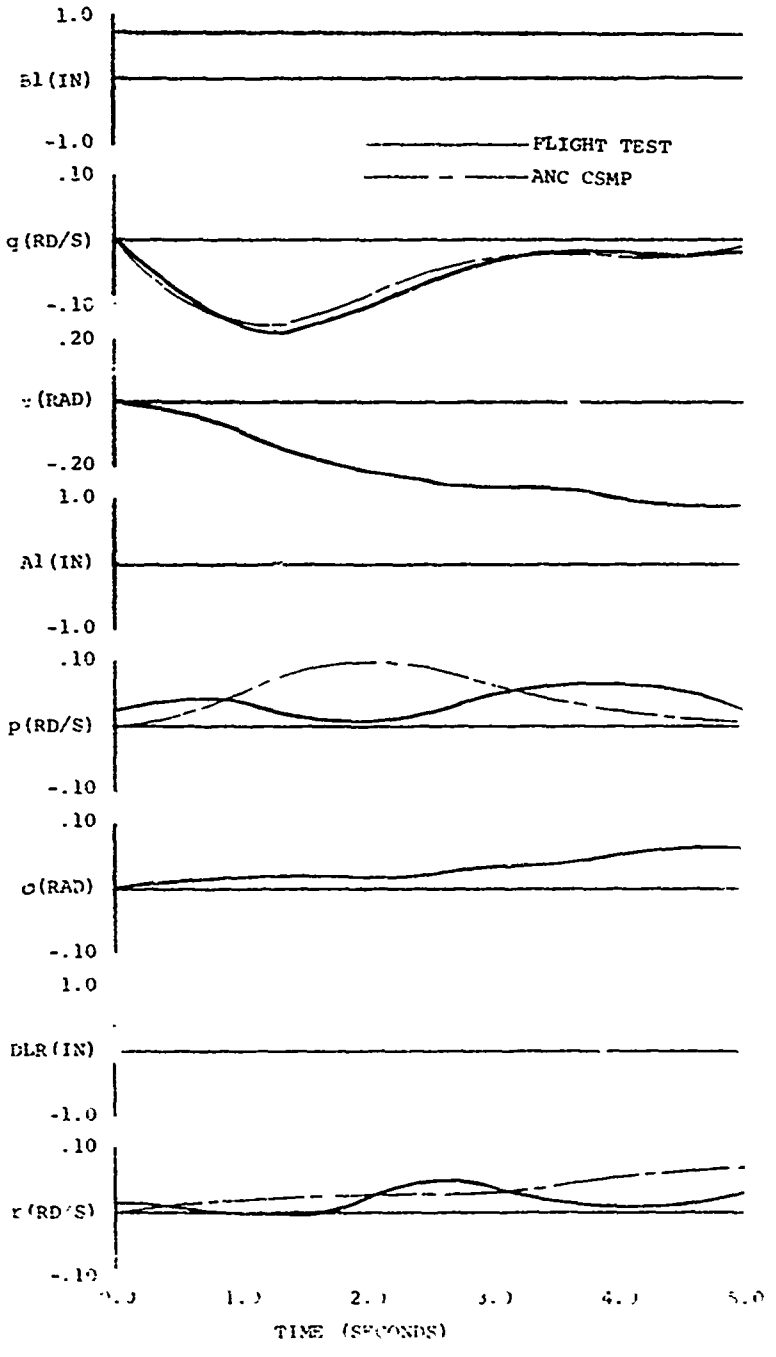

Figure 44. Flight Test vs. CSMP Simulation (60 Knots at 3000 Feet, Modified MOSTAB Pitch Step Response).

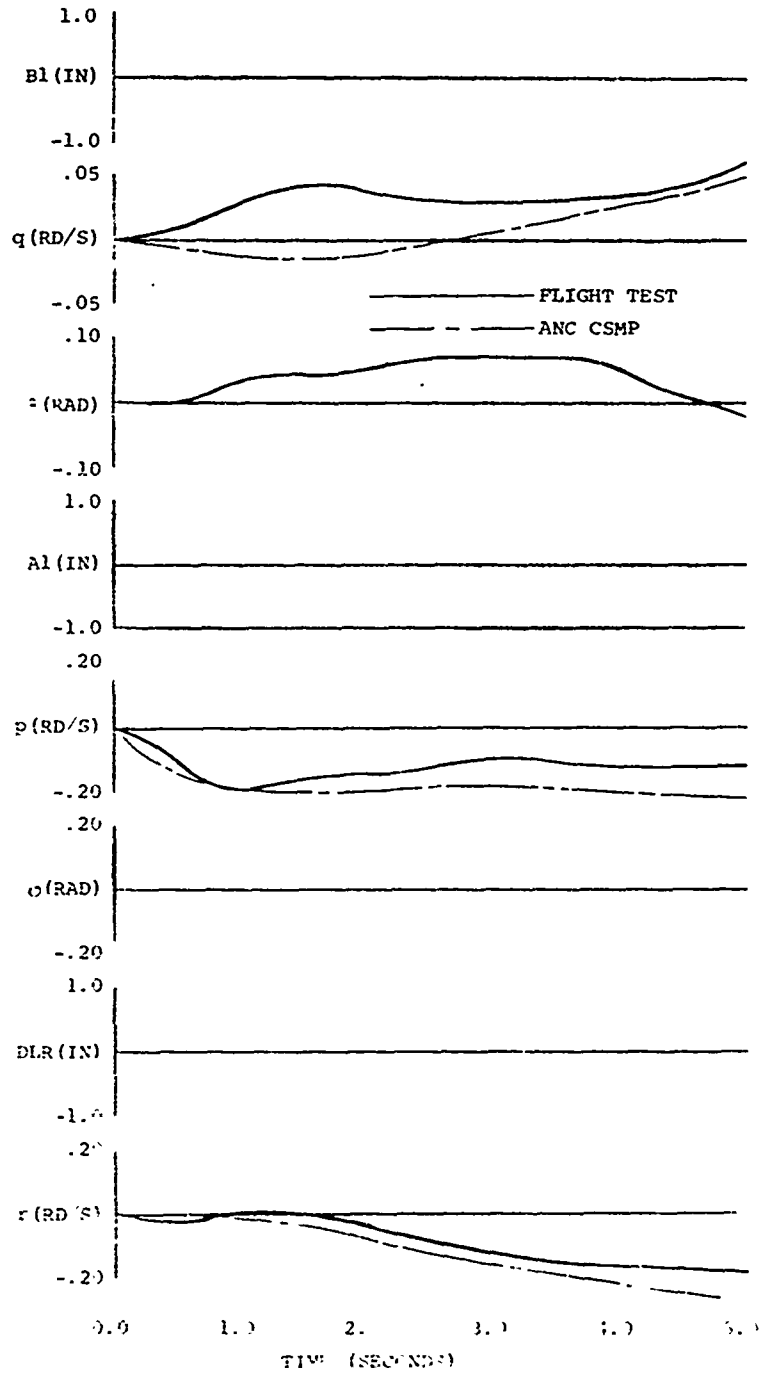

Figure 45. Flight Test vs. CSMP Simulation (60 Knots at 3000 Feet, Modified MOSTAB Roll Step Response).

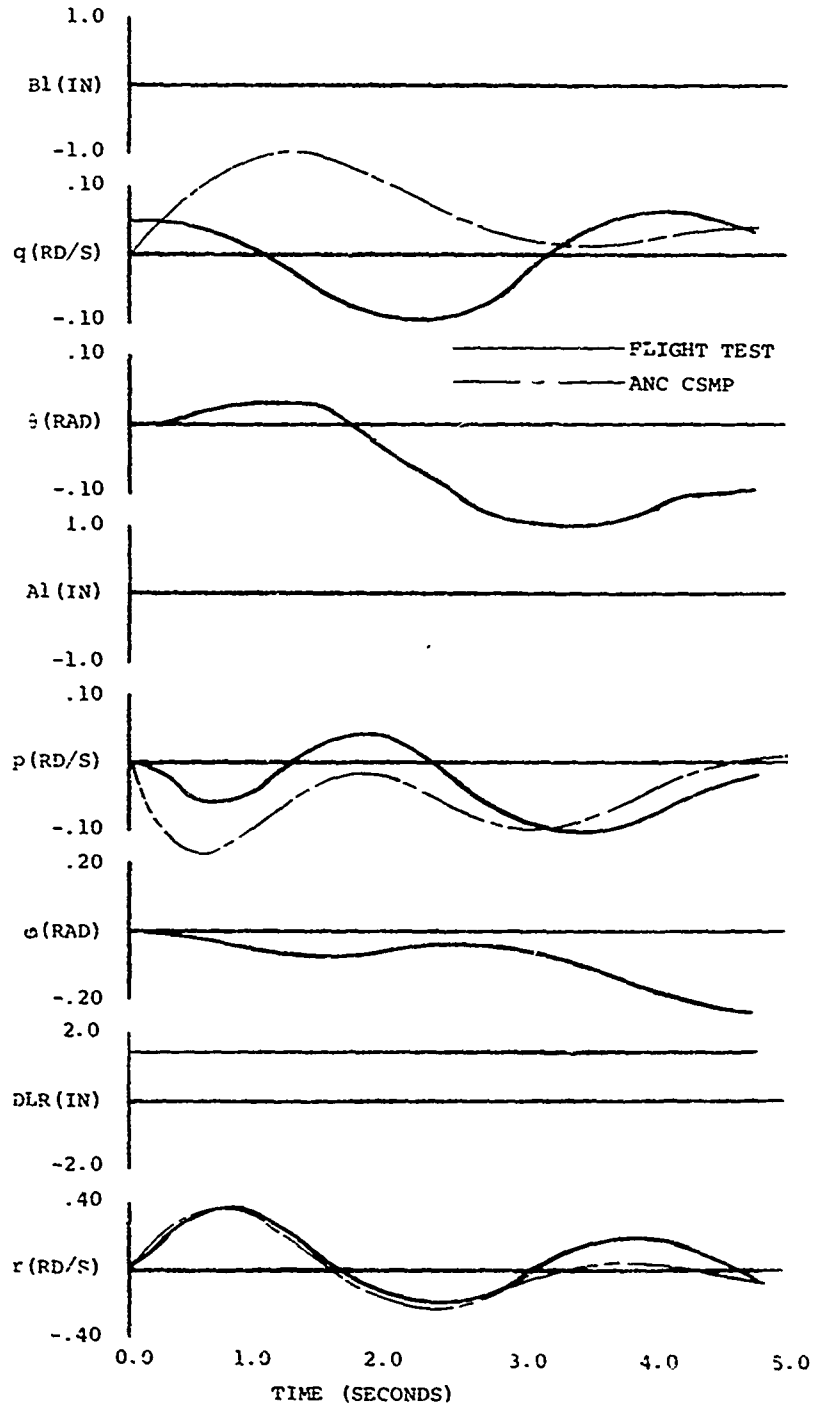

Figure 46. Flight Test vs. CSMP Simulation (60 Knots at 3000 Feet, Modified MOSTAB Yaw Step Response).

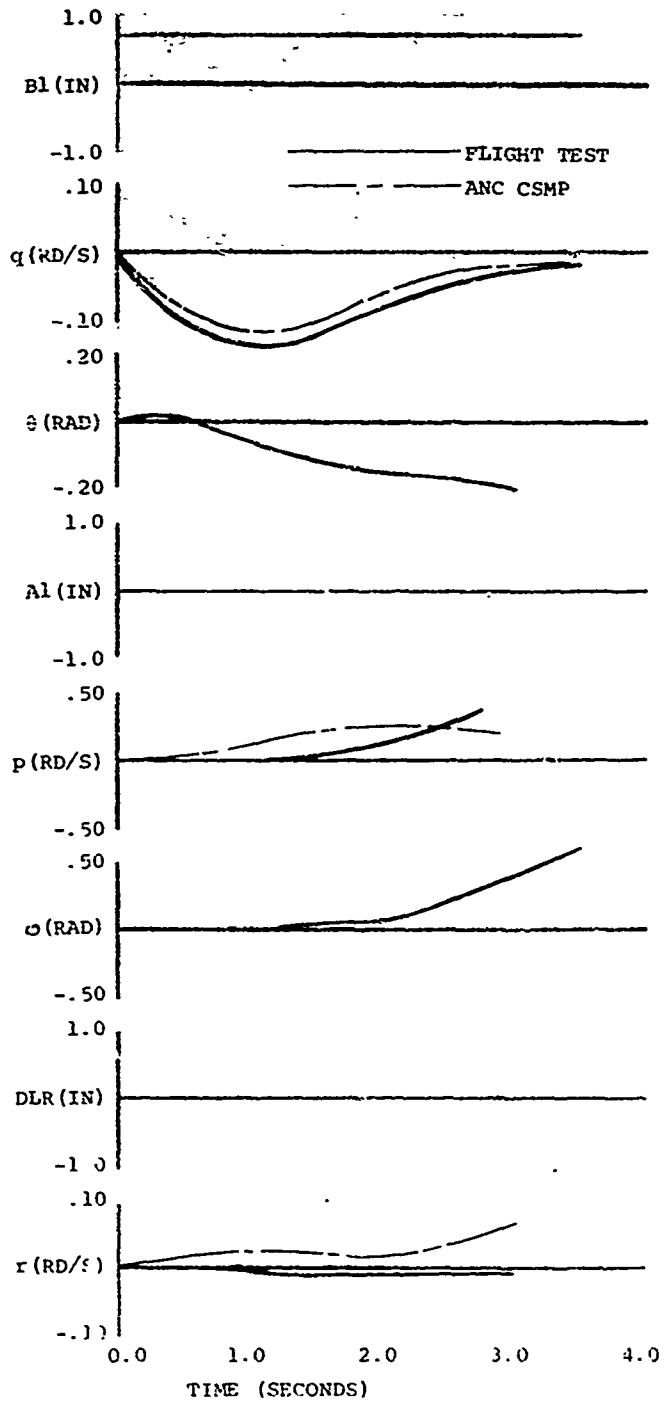

Figure 47. Flight Test vs. CSMP Simulation (110 Knots at 3000 Feet, Modified MOSTAB Pitch Step Response).

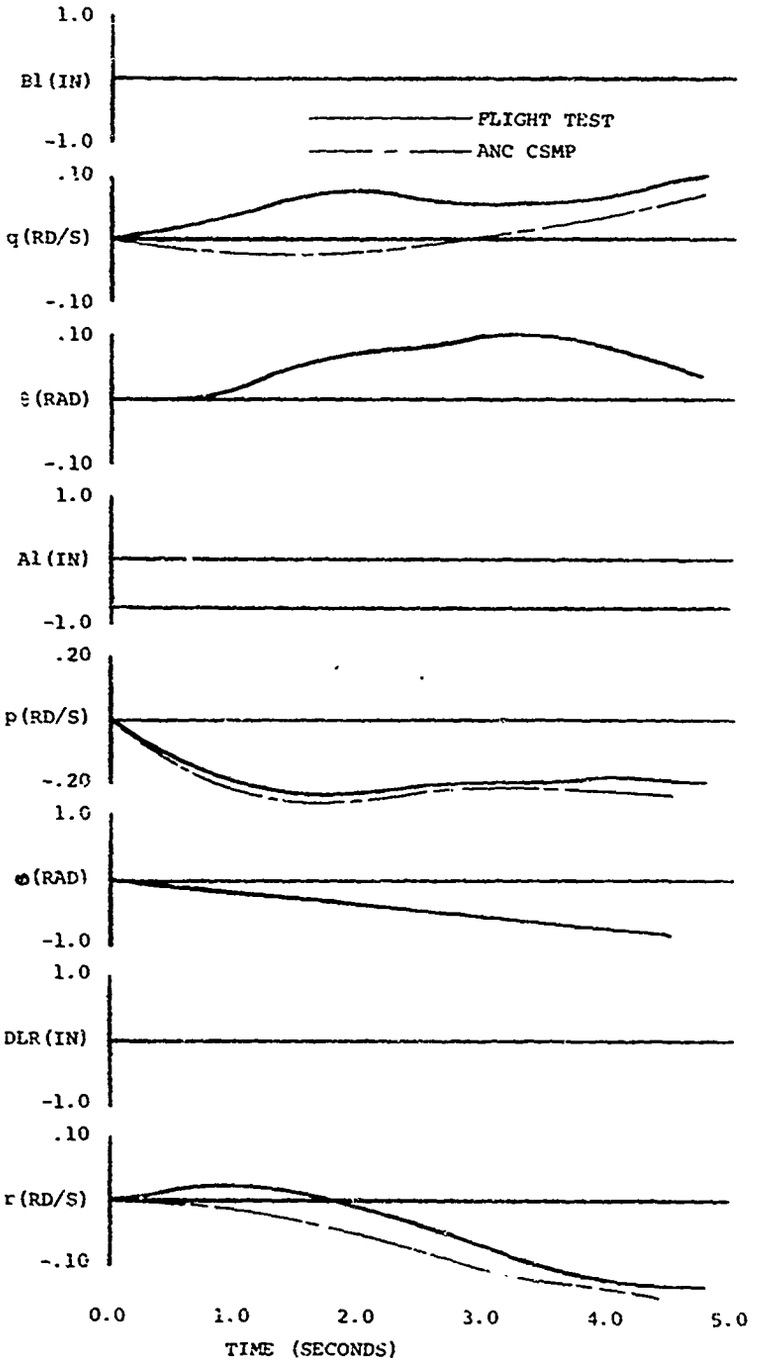

Figure 48. Flight Test vs. CSMP Simulation (110 Knots at 3000 Feet, Modified MOSTAB Roll Step Response).

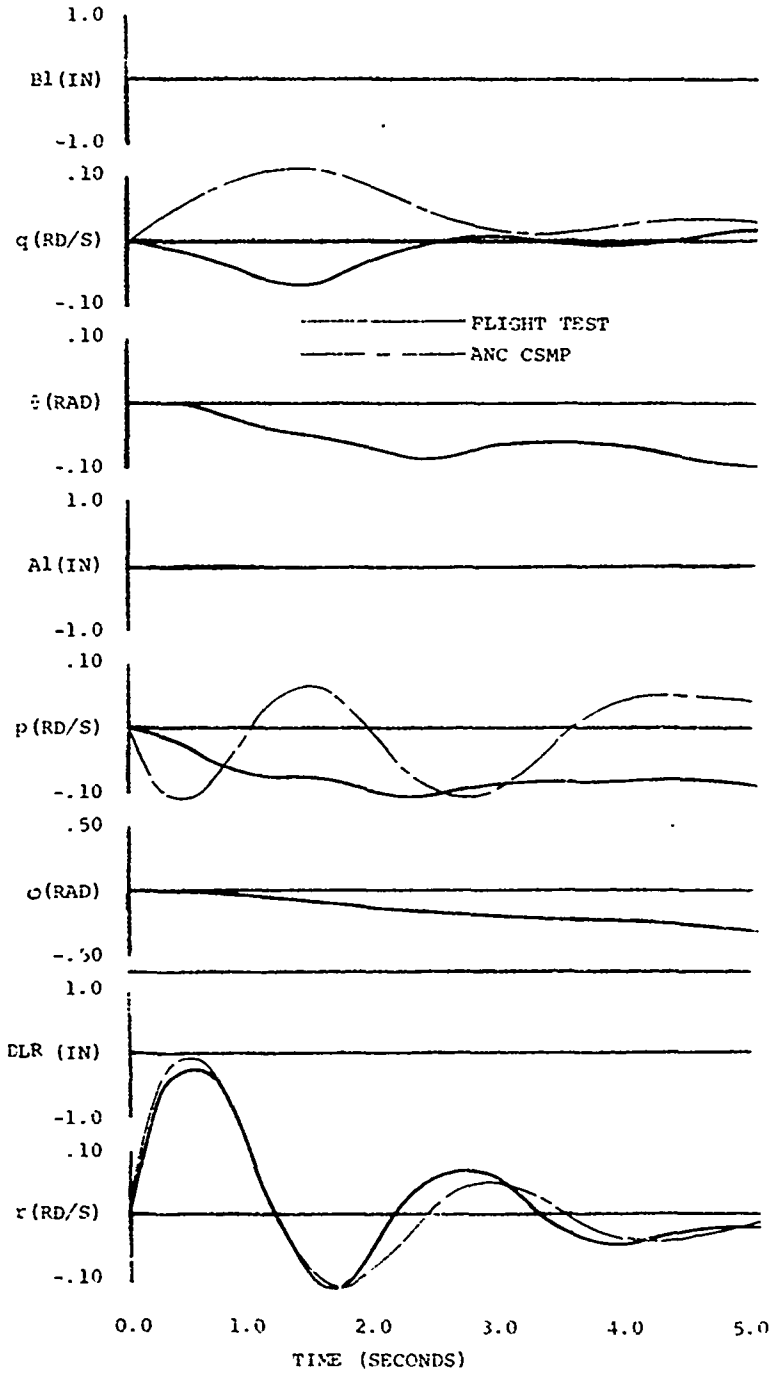

Figure 49. Flight Test vs. CSMP Simulation (110 Knots at 3000 Feet, Modified MOSTAB Yaw Step Response).

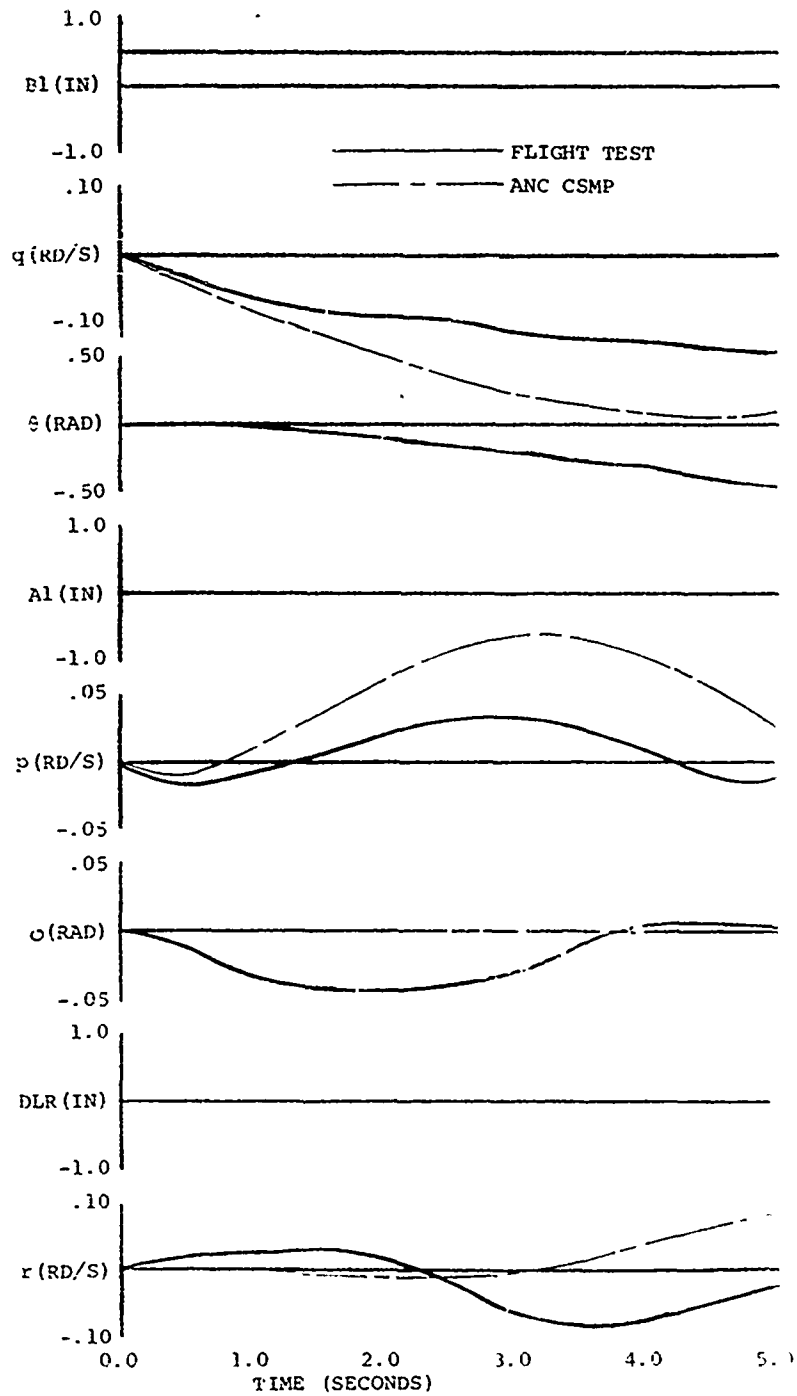

Figure 50. Flight Test vs. CSMP Simulation (Hover at 3000 Feet, Modified MOSTAB Pitch Step Response).

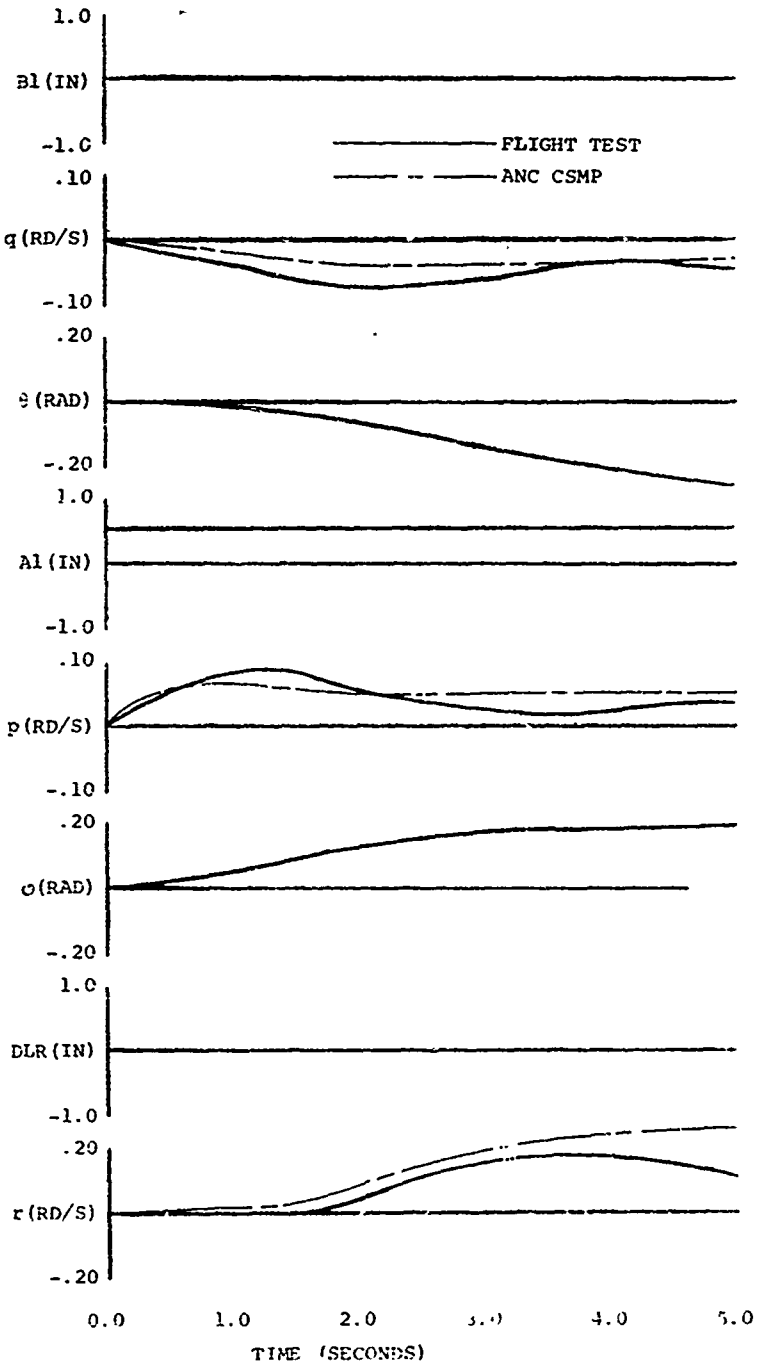

Figure 51. Flight Test vs. CSMP Simulation (Hover at 3000 Feet, Modified MOSTAB Roll Step Response).

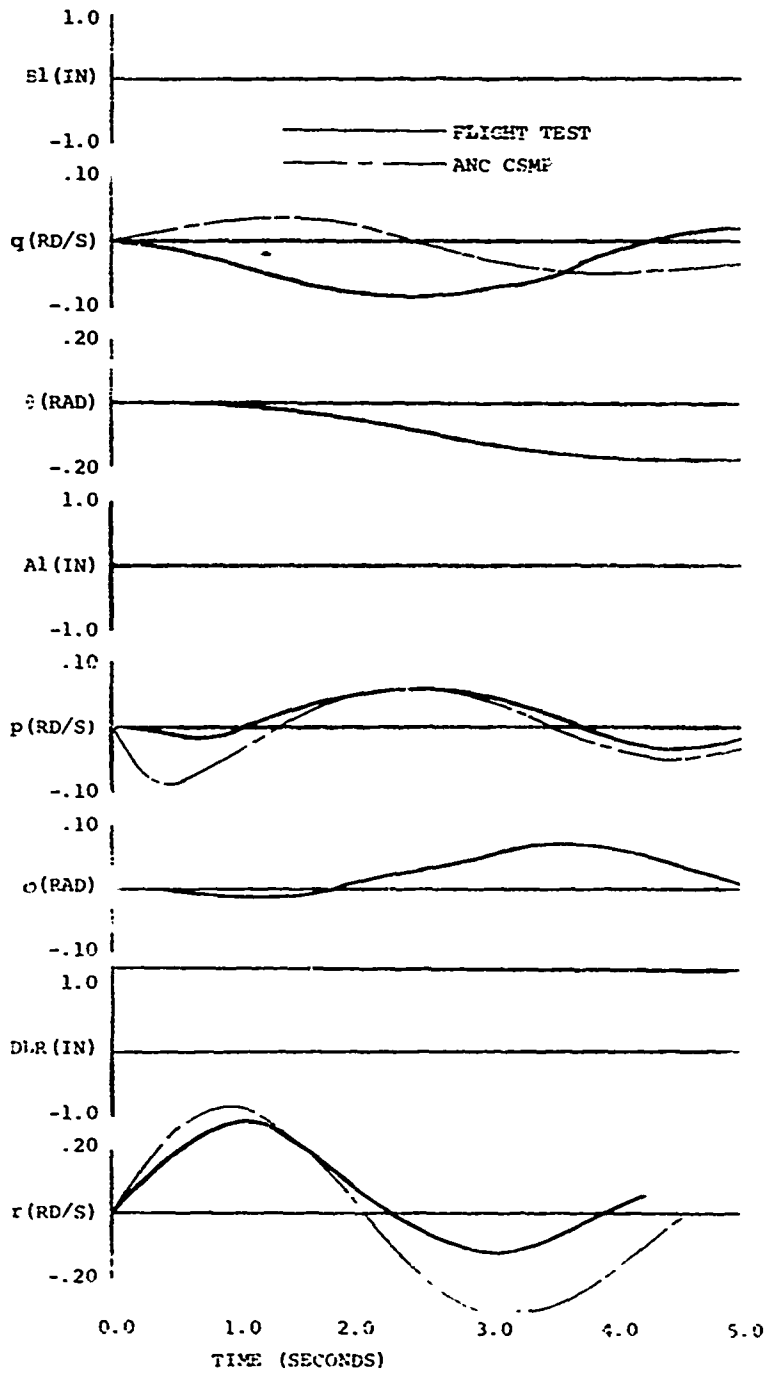

Figure 52. Flight Test vs. CSMP Simulation (Hover at 3000 Feet, Modified MOSTAB Yaw Step Response).

CURVE FIT MODEL

A curve fit program yields transfer characteristics of a system. The transfer characteristics are determined from the input and output data of the system. The nice feature of this program is that it yields a math model of the system from control inputs to used outputs (e.g., sensors that will be used for feedback control). Other modelling techniques have the following shortcomings:

1. Neglect mechanical control system characteristics;

2. Neglect defining sensor characteristics;

3. Are predictions which need at least subsequent test verification and possible iterations on the input data to improve the predictions.

A curve fit program can potentially be used to design a system (e.g., vehicle). All that needs to be done is to define desired outputs for given inputs. The resulting math model can then be related term by term to physical characteristics to define the desired physical characteristics.

The following sections illustrate comparison between UH-1C flight test data and simulation of curve fit program outputs.

MODEL OF SINGLE DATA SET

Figure 53 shows a comparison between UH-1C flight test data (3000 feet at 60 knots) for a longitudinal cyclic response and a CSMP simulation of the curve fit program output. The plots are very nearly identical. The input for the curve fit program was the eight aircraft parameters (in 0.25-second intervals) shown in Figure 53.

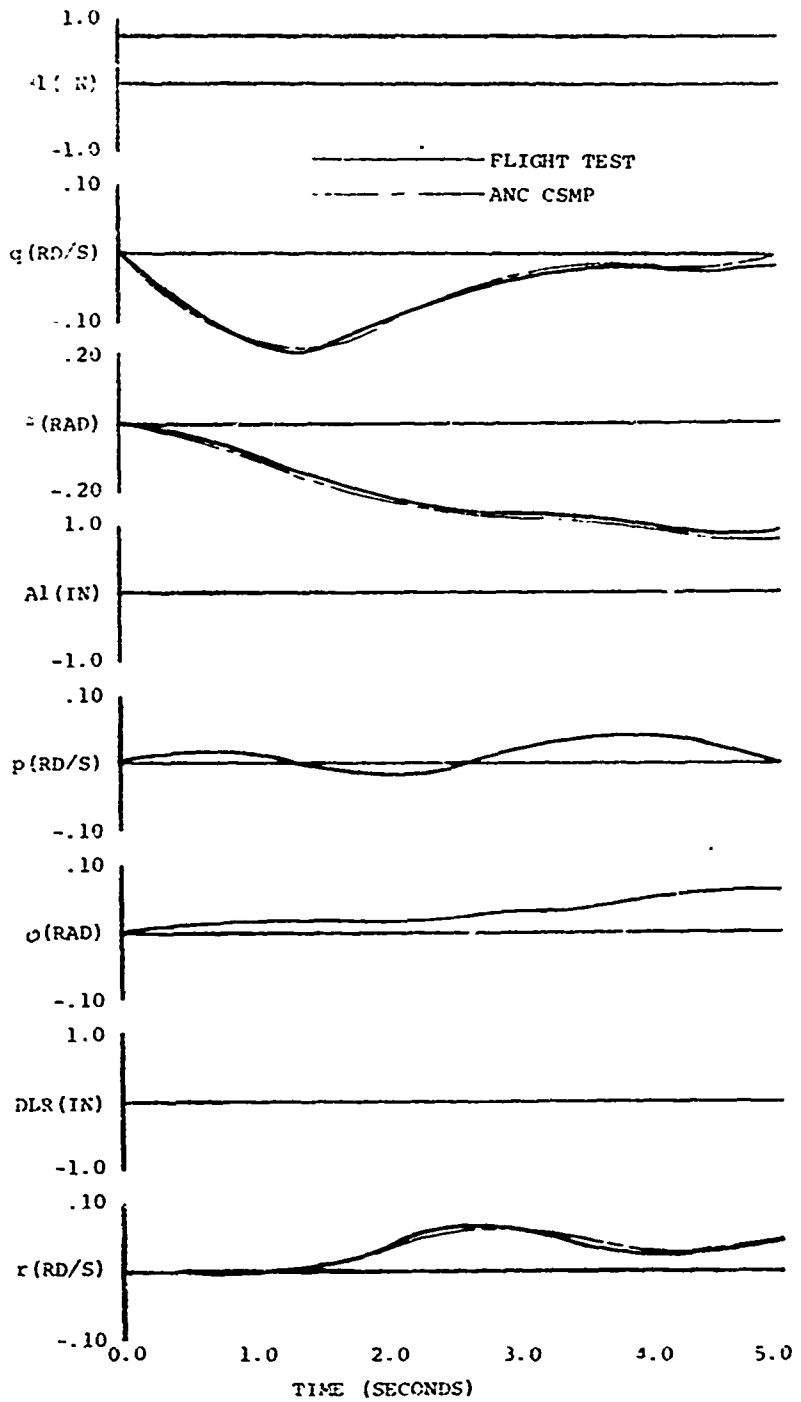

Figure 53. Pitch Response of a Single Data Set Model (60 Knots at 3000 Feet).

The resulting curve fit program output was given by:

$$\frac{d}{dt}\begin{bmatrix} q \\ \theta \\ p \\ \varphi \\ r \end{bmatrix} = \begin{bmatrix} -0.486 & -1.141 & -1.177 & -2.743 & 0.047 & -0.266 \\ 1.037 & -0.407 & -0.618 & -1.648 & -0.537 & -0.029 \\ 0.149 & 0.204 & 0.463 & -0.871 & 1.718 & 0.035 \\ -0.026 & -0.570 & 0.998 & -3.116 & -1.022 & -0.017 \\ 0.448 & -0.781 & -2.364 & -2.253 & -2.502 & 0.036 \end{bmatrix}$$

$$* \begin{bmatrix} q \\ \theta \\ p \\ \varphi \\ r \\ B1 \end{bmatrix}$$

The CSMP simulation of the curve fit program output is given by:

```
TITLE              MODEL   FC-60-3-P-DS
*     AIRCRAFT EQUATIONS
      QDT=-.486*Q-1.14*THETA-1.178*P-2.74*PHI+.048*R-.266*B1
      THEDT=1.04*Q-.407*THETA-.619*P-1.65*PHI-.573*R-.029*B1
      PDT=.149*Q+.205*THETA+.463*P-.872*PHI+1.72*R+.035*B1
      PHIDT=-.027*Q-.57*THETA+.998*P-3.12*PHI-1.02*R-.018*B1
      RDT=.449*Q-.782*THETA-2.36*P-2.25*PHI-2.50*R+.036*B1
      R=INTGRL(0.0,RDT)
      P=INTGRL(0.0,PDT)
      PHI=INTGRL(0.0,PHIDT)
      Q=INTGRL(0.0, QDT)
      THETA=INTGRL(0.0,THEDT)
*     SYSTEM INPUT
      B1=T1*STEP(0.0)
      A1=T2*STEP(0.0)
      DLR=T3*STEP(0.0)
PARAMETER    T1=+0.70,T2=-0.00,T3=0.00
TIMER DELT=.005,FINTIM=6.0,PRDEL=.25,OUTDEL=.25
PRINT      B1,Q,THETA,A1,P,PHI,DLR,R
METHOD     RECT
END
STOP
```

MODEL OF TWO DATA SETS

Figure 54 shows a comparison between UH-1C flight test data (3000 feet at 60 knots) for a longitudinal cyclic response and a CSMP simulation of the curve fit program output. Figure 55 shows a comparison between UH-1C flight test data (3000 feet at 60 knots) for a lateral cyclic response and a CSMP simulation of the curve fit program output.

Flight test data (in 0.25-second intervals) for the two responses (i.e., the flight test data shown in Figures 54 and 55) was fed into the curve fit program and a single model was obtained. The comparison is not quite as close as that shown in Figure 53, but is nevertheless quite good. A couple of possibilities exist for the model not being as close as shown in Figure 53; namely

1. The pitch attitude (vertical gyro) output was nonlinear (i.e., appeared to have approximately a 1.25-degree threshold) and a linear model was generated.

2. The two sets of test data may have been run under slightly different conditions (e.g., wind, different airspeed, etc.).

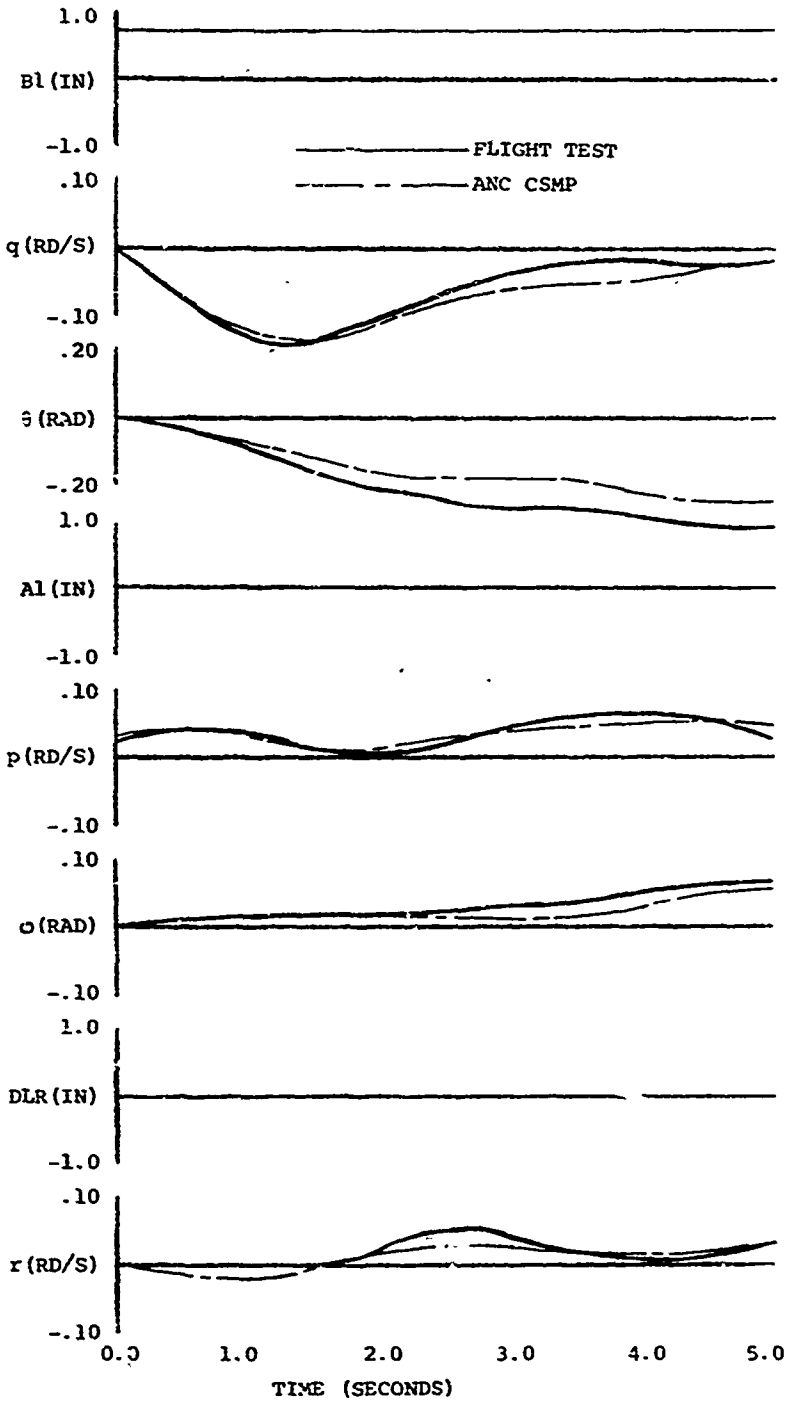

Figure 54. Pitch Response of Two-Data-Set Model (60 Knots at 3000 Feet).

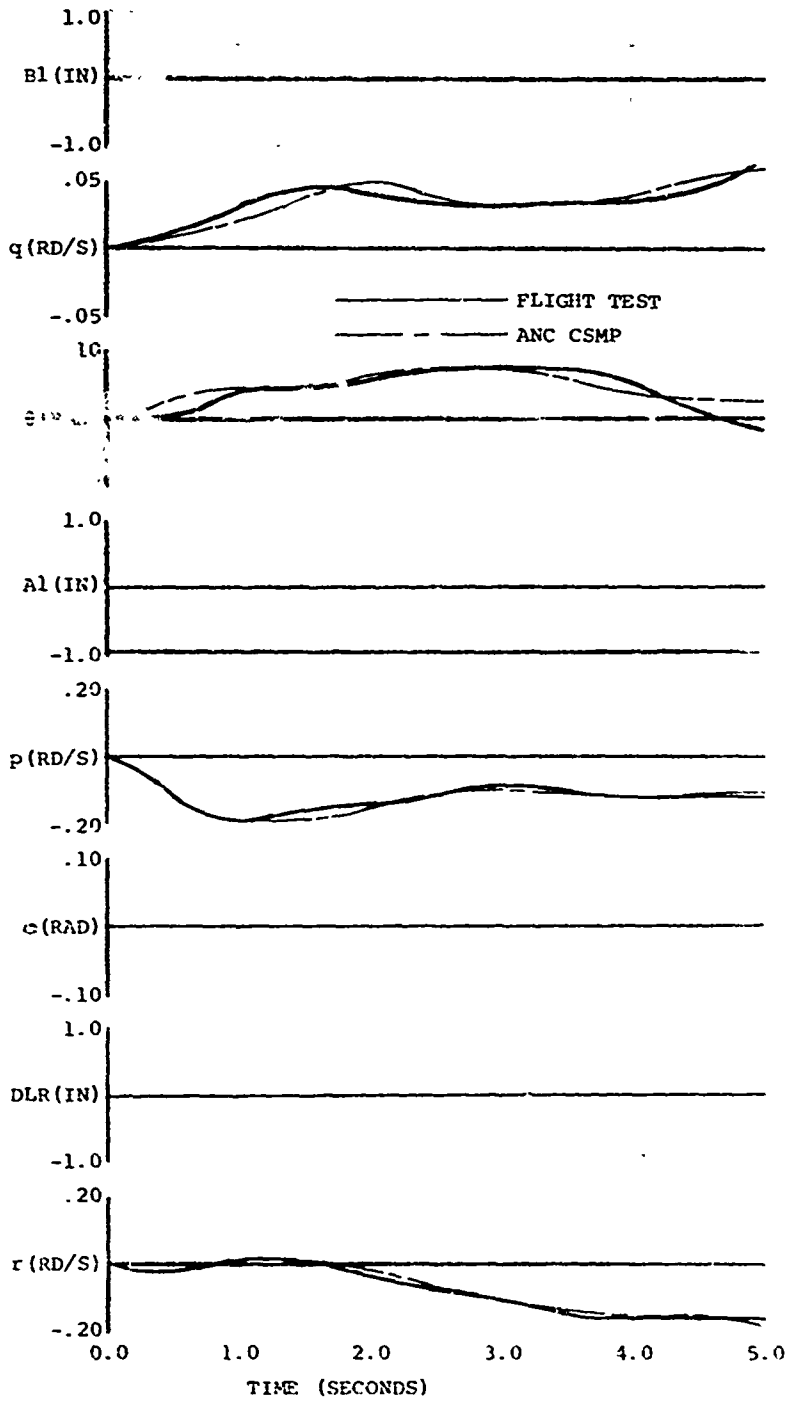

Figure 55. Roll Response of Two-Data-Set Model (60 Knots at 3000 Feet).

The resulting curve fit program output was given by:

$$\frac{d}{dt}\begin{bmatrix} q \\ \theta \\ p \\ \varphi \\ r \end{bmatrix} = \begin{bmatrix} -1.182 & -0.616 & -0.137 & -0.114 & 0.594 & -0.248 \\ 1.570 & -0.233 & -1.151 & 0.511 & 0.660 & 0.061 \\ 1.092 & 0.567 & -1.039 & -0.506 & 0.813 & 0.243 \\ -0.266 & 0.048 & 0.862 & -0.201 & 0.336 & -0.022 \\ -0.393 & -0.402 & -1.027 & 0.298 & -1.065 & -0.073 \end{bmatrix}$$

$$* \begin{bmatrix} q \\ \theta \\ p \\ \varphi \\ r \\ Bl \end{bmatrix} + \begin{bmatrix} -0.064 \\ 0.086 \\ 0.326 \\ 0.041 \\ 0.119 \end{bmatrix} * [Al]$$

The CSMP simulation of the curve fit output is given by:

```
TITLE       MODEL RESPONSES FOR FC-60-3-R,P-DS
*      AIRCRAFT EQUATIONS
       QDT   =AQ*Q+ATHET*THETA+AP*P+APHI*PHI+AR*R*AB1*B1+AA1*A1+ADLR*DLR
       THEDT=BQ*Q+BTHET*THETA+BP*P+BPHI*PHI+BR*R+BB1*B1+BA1*A1+BDLR*DLR
       PDT   =CQ*Q+CTHET*THETA+CP*P+CPHI*PHI+CR*R+CB1*B1+CA1*A1+CDLR*DLR
       PHIDT=DQ*Q+DTHET*THETA+DP*P+DPHI*PHI+DR*R+DB1*B1+DA1*A1+DDLR*DLR
       RDT   =EQ*Q+ETHET*THETA+EP*P+EPHI*PHI+ER*R+EB1*B1+EA1*A1+EDLR*DLR
       Q          =INTGRL(0.0,QDT)
       THETA      =INTGRL(0.0,THEDT)
       P          =INTGRL(0.0,PDT)
       PHI        =INTGRL(0.0,PHIDT)
       R          =INTGRL(0.0,RDT)
*           MODEL PARAMETERS
PARAMETER  AQ=-1.183   ,ATHET=-.6167,AP=-.1377    ,APHI=-.1145,AR=.5948
PARAMETER  BQ=1.57     ,BTHET=-.233 ,BP=-1.152    ,BPHI=.511   ,BR=-.6604
PARAMETER  CQ=1.093    ,CTHET=.567  ,CP=-1.039    ,CPHI=-.5067,CR=.813
PARAMETER  DQ=-.266    ,DTHET=.048  ,DP=.8626     ,DPHI=-.2020,DR=.3369
PARAMETER  EQ=-.3940   ,ETHET=-.4024,EP=-1.027    ,EPHI=.298   ,ER=-1.065
PARAMETER AB1=-.248    ,AA1=-.0645  ,ADLP=0.0
PARAMETER BB1=.0616    ,BA1=.0865   ,BDLR=0.0
PARAMETER CB1=.2439    ,CA1=.3268   ,CDLR=0.0
PARAMETER DB1=-.0222   ,DA1=.0419   ,DDLR=0.0
PARAMETER EB1=-.0733   ,EA1=.1192   ,EDLR=0.0
*      SYSTEM INPUTS
```

```
      B1   =AFGEN(CURVE1,TIME)
      A1   =AFGEN(CURVE2,TIME)
      DLR  =AFGEN(CURVE3,TIME)
*     SYSTEM INPUT PARAMETERS
TITLE        LONG CYCLIC STICK RESPONSE
*     B1 PARAMETERS
FUNCTION CURVE1=(0.0,0.0),(0.25,0.70),(10.0,0.70)
*     A1 PARAMETERS
FUNCTION CURVE2=(0.0,0.0),(10.0,0.0)
*     DLR PARAMETERS
FUNCTION CURVE3=(0.0,0.0),(10.0,0.0)
TIMER DELT=.005,FINTIM=5.0,PRDEL=.25,OUTDEL=.25
PRINT    Q,THETA,P,PHI,R,B1,A1,DLR
METHOD  RECT
END
STOP
```

MODEL OF THREE DATA SETS

Figure 56 shows a comparison between UH-1C flight test data (3000 feet at 60 knots) for a longitudinal cyclic response and a CSMP simulation of the curve fit program output. Figures 57 and 58 shows comparisons for roll and yaw responses, respectively.

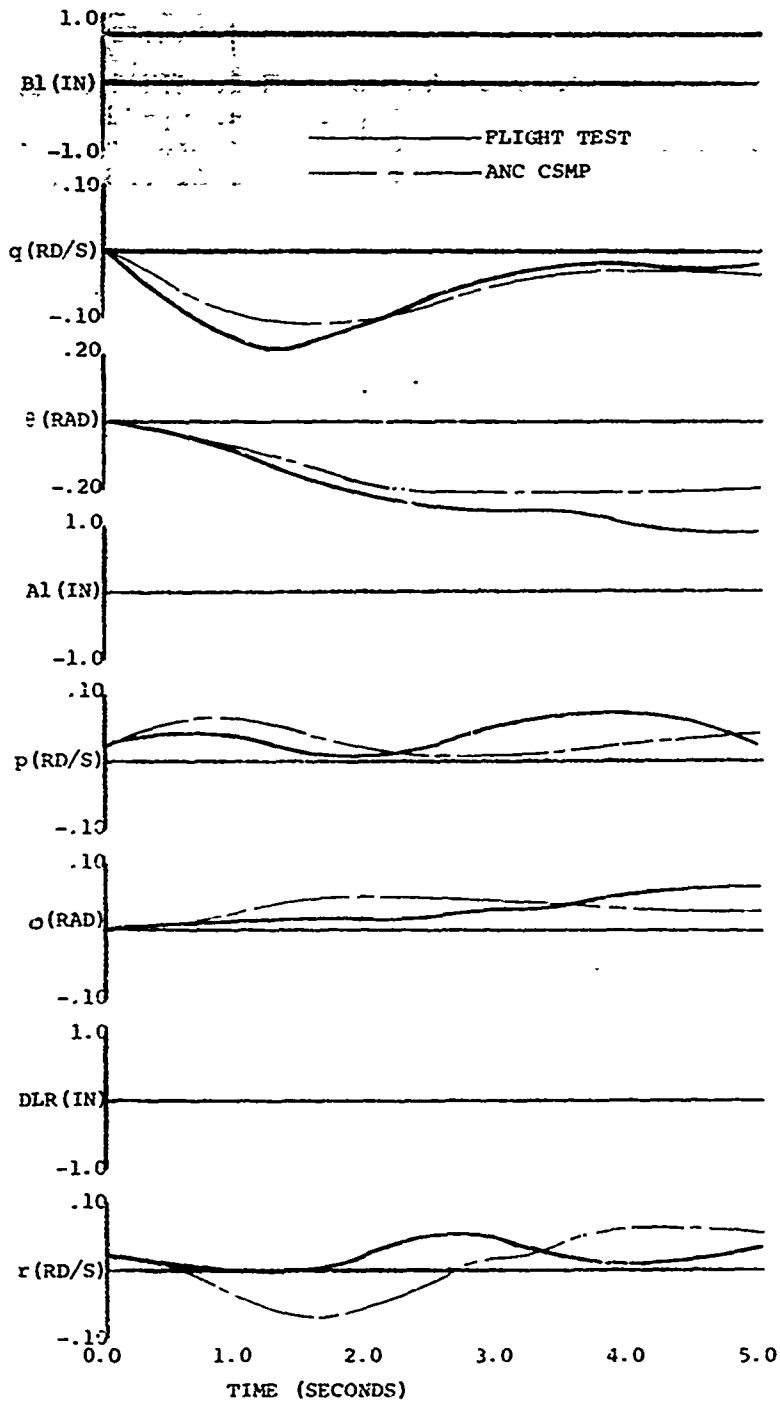

Figure 56. Pitch Response of Three-Data-Set Model (60 Knots at 3000 Feet).

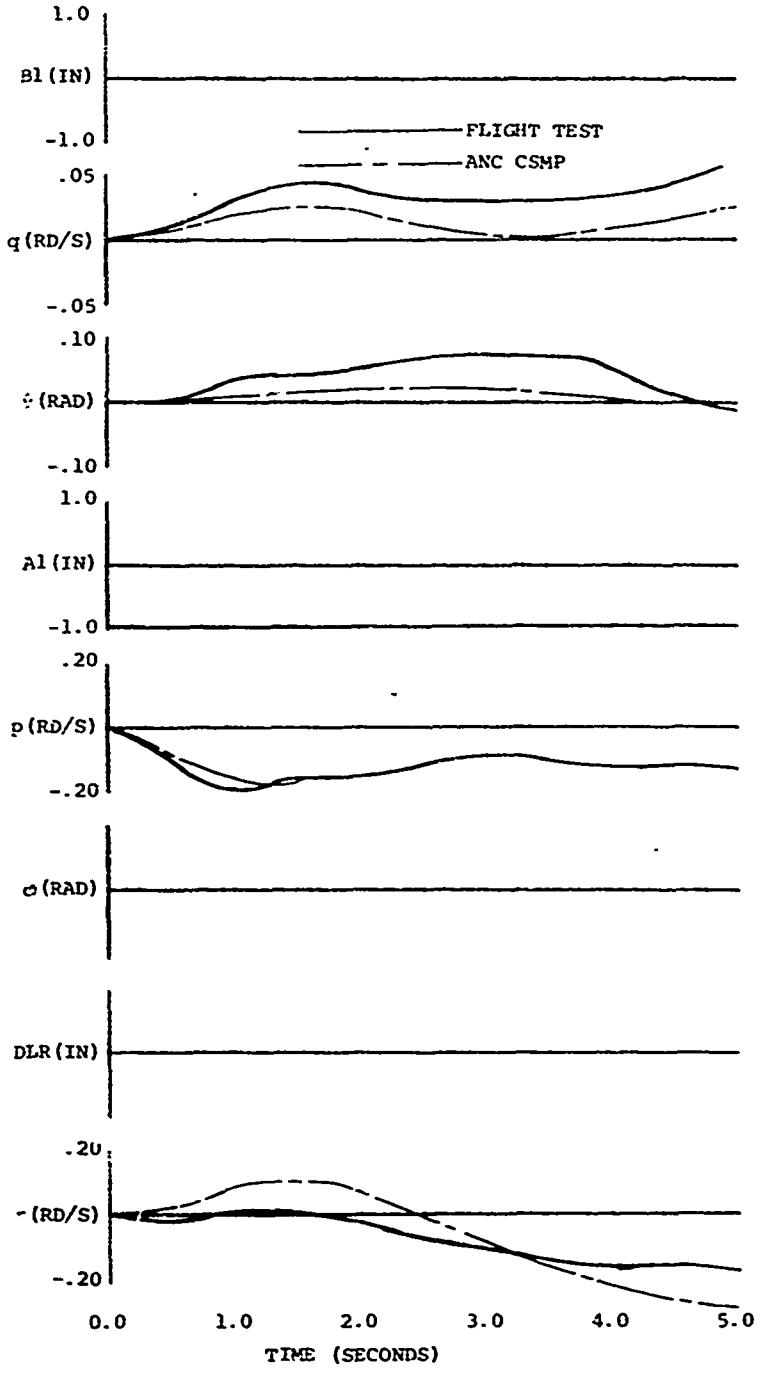

Figure 57. Roll Response of Three-Data-Set Model (60 Knots at 3000 Feet).

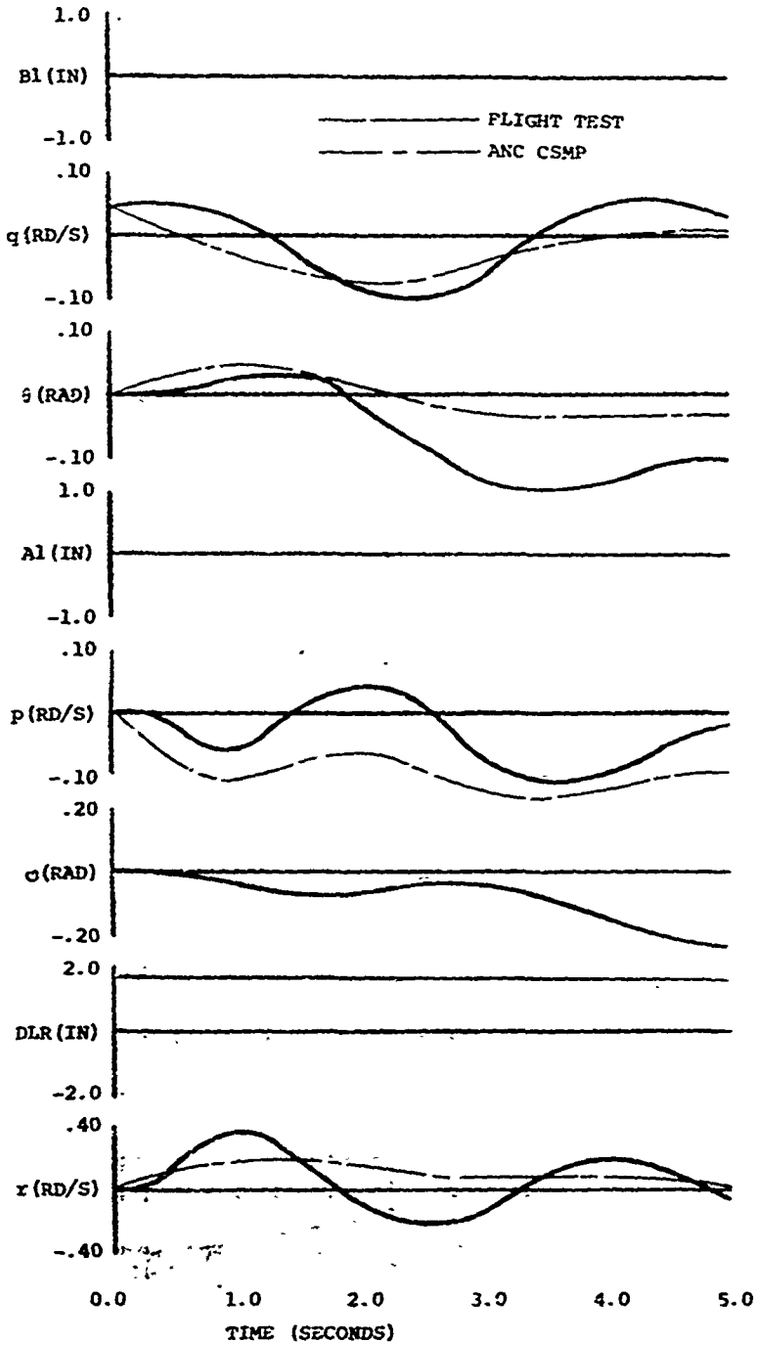

Figure 58. Yaw Response of Three-Data-Set Model (60 Knots at 3000 Feet).

The resulting curve fit program output was given by:

$$\frac{d}{dt}\begin{bmatrix} q \\ \theta \\ p \\ \varphi \\ r \end{bmatrix} = \begin{bmatrix} -0.745 & -0.651 & -0.490 & 0.033 & 0.044 & -0.184 \\ 0.811 & -0.322 & 0.295 & 0.146 & 0.368 & -0.080 \\ 0.996 & 0.389 & -1.417 & -0.480 & 0.104 & 0.286 \\ 0.175 & 0.111 & 0.618 & 0.053 & -0.214 & 0.014 \\ 2.093 & -0.154 & -1.890 & 1.160 & -1.382 & 0.182 \end{bmatrix} * \begin{bmatrix} q \\ \theta \\ p \\ \varphi \\ r \\ B1 \end{bmatrix}$$

$$+ \begin{bmatrix} -0.021 & -0.052 \\ -0.106 & 0.022 \\ 0.410 & -0.184 \\ 0.054 & 0.015 \\ 0.048 & 0.158 \end{bmatrix} * \begin{bmatrix} A1 \\ DLR \end{bmatrix}$$

CONCLUSIONS

Work performed under Contract DAAJ02-71-C-0023 revealed the following MOSTAB-C characteristics:

1. Comparison of the MOSTAB-C model for the UH-1C shows a fair agreement (aside from cross-coupling characteristics) with flight test data.

2. There is an error in the MOSTAB-C cross-coupling rate derivatives. The derivatives (primarily L_q and M_p) are apparently the wrong sign and approximately the right magnitude.

3. The "modified form stability derivative" output is an excellent summary of vehicle characteristics for use in subsequent simulations of the vehicle.

Generating an accurate vehicle math model using flight test data appears to be feasible for a vehicle like the UH-1C. Generating a model in this fashion provides a complete (i.e., from input to those outputs that might be used for feedback closures) and potentially more usable (i.e., when subsequently considering the vehicle as a subsystem) model than a basic vehicle model program.

RECOMMENDATION

Conduct a parallel flight test and ground-based simulation research program on a UH-1 configuration to evaluate the Pilot Assist System. This effort will provide an efficient evaluation and refinement of the Pilot Assist System designed during the work of Reference 5.

LITERATURE CITED

1. Hoffman, J.A., STABILITY DERIVATIVES AND OTHER DATA REQUIRED FOR SIMULATION OF THE BELL UH-1C HELICOPTER, Mechanics Research Inc. Report 2383-2, February 1970.

2. Hoffman, J.A., A DESCRIPTION OF THE MOSTAB COMPUTER PROGRAM OUTPUT DATA FORMAT, Mechanics Research Inc. Report 2414-1, July 1970.

3. Hoffman, J.A., and J. Wolkovitch, EQUATIONS FOR HELICOPTER SIMULATION, Mechanics Research Inc. Report R2383-1, December 1969.

4. Ebsen, M.E., H. Ogren, and D. Sotanski, THREE-AXIS FLUIDIC STABILITY AUGMENTATION SYSTEM FLIGHT TEST REPORT, Honeywell, Incorporated; USAAMRDL Technical Report 71-34 Eustis Directorate, U. S. Army Air Mobility Research and Development Laboratory, Fort Eustis, Virginia, August 1971.

5. Welch, A.J., and E. L. Warren, ANALYSIS AND DESIGN STUDY OF A PILOT ASSIST SYSTEM FOR HELICOPTERS, American Nucleonics Corporation; USAAVLABS Technical Report 71-11, U. S. Army Air Mobility Research and Development Laboratory, Fort Eustis, Virginia, April 1971, AD 725590.